Université de Montréal

Le rôle des formes périglaciaires dans l'hydrologie et l'évolution des pentes d'un désert polaire dans le Haut-Arctique canadien

par

Michel Paquette

Département de géographie

Faculté des arts et des sciences

Thèse présentée à la Faculté des études supérieures

en vue de l'obtention du grade de

Philosophiæ Doctor (Ph.D.)

en géographie

6 février 2018

RÉSUMÉ

Le contexte géomorphologique permet d'établir les liens de fonctionnalité d'un paysage avec ses composantes écosystémiques. Dans le cas des paysages périglaciaires, leurs mécanismes d'évolution demeurent peu étudiés, car leur historique de recherche est fortement empreint d'une impression d'exceptionnalité tirant son origine des conditions climatiques extrêmes qu'ils encourent. Il est cependant primordial de pouvoir identifier les mécanismes dominants de flux sédimentaires afin d'établir les liens entre les composantes du système géomorphologique. À l'échelle fondamentale d'une pente, les mécanismes issus du cryo-conditionnement du paysage vont dicter son évolution ainsi que ses fonctions écosystémiques. La thèse étudie ces mécanismes en examinant le rôle que tiennent les formes périglaciaires dans l'établissement d'un réseau de drainage sur une pente d'un désert polaire du Haut-Arctique. Elle cherche surtout à établir les liens entre les processus azonaux fondamentaux de transport sédimentaires par le ruissellement et les conditions dérivées des processus climatiques de redistribution de neige ainsi que de triage et de mouvements de masses associés à la formation des sols triés. Elle y parvient en s'attardant à la morphologie des dépôts de surface (ch. 2) ainsi qu'aux fonctions qu'occupent les patrons de triage face à l'hydrologie (ch. 3), à l'évolution de la pente (ch. 4) et aux impacts sur les conditions limnologiques d'un lac de tête (ch. 5).

L'organisation du réseau de drainage est issue de la combinaison des processus de triages ainsi que du pouvoir érosif des écoulements provenant de la fonte des combes à neige. La nature grossière des dépôts de surface permet un écoulement dans les vides entre les particules, formant un réseau de drainage souterrain possédant une conductivité hydraulique relativement élevée.

Ce réseau d'écoulement préférentiel est efficace afin d'évacuer les eaux de fonte de la neige, ce qui réduit la durée de leur interaction avec les sols se trouvant hors des zones d'écoulement préférentiels. Les eaux émergent en bas de pente, transportant parfois avec elles des sédiments en suspension dont les concentrations sont limitées par leur disponibilité. Ces concentrations demeurent comparables aux concentrations publiées pour les eaux de surface ailleurs dans l'Arctique. Le travail principal de dénudation de la pente s'effectue par le transport en solution, qui excède jusqu'à un ordre de grandeur les transports en suspension. Le ruissellement contribue à l'apport de chaleur au lac de tête qu'il nourrit, et la pente possédant cet écoulement préférentiel est le premier secteur de dégel du couvert de glace de lac, contribuant à sa disparition totale aux étés 2011 et 2012. Le réseau de drainage réagit également à la dégradation du pergélisol, transportant des eaux d'une salinité élevée. Ces apports de chaleur et de sels dissous ont le potentiel d'influencer les conditions limnologiques du littoral. La thèse souligne ainsi l'importance des processus azonaux dans l'établissement du modelé d'une région dominée par le gel. Elle démontre que l'évolution d'une pente en désert polaire s'est effectuée à travers la relation entre les processus périglaciaires de triages et le ruissellement, et que cette relation exerce un certain contrôle pour l'écosystème du lac de tête en aval.

Mots-clés : Dénudation du paysage, Écoulement préférentiel, Érosion, Évolution de pente, Géomorphologie, Hydrologie périglaciaire, Limnologie, Sols triés, Ward Hunt

ABSTRACT

Geomorphology exerts a fundamental control on ecosystems. In the case of periglacial landscapes, the mechanisms by which they evolve are not clearly defined, as research on the subject has often been excessively focused on the expressions of freeze-thaw processes as climatic control over landform development. It is however essential to identify and clarify what are the fundamental dynamics of sediment transport in periglacial regions to understand the evolution and the functions of these landscapes. At the scale of a unit slope, the mechanisms originating from cryo-conditioning are the main drivers of evolution. These include the effects of freeze-thaw processes on surface deposits and the production of large, periodic water supplies by snow redistribution and snowmelt. This thesis investigates the role played by periglacial landforms in the establishment of drainage pathways on a High Arctic polar desert landscape. It aims at establishing links between the azonal processes of runoff generation and sediment transport, and the climate-dependant processes of sorting and mass movement associated with the formation of patterned ground. It achieves this objective by focussing on surface deposit morphology (ch. 2), on the hydrological functions those patterned ground possess (ch. 3), on sediment transport on the slope (ch. 4) and on the impacts of those flowpaths on limnological conditions in a downstream headwater lake (ch. 5).

The organisation of the drainage pathways is dependant upon the combination of sorting processes with erosion from snowmelt of large snowdrifts. The coarse nature of the reworked glacial drift and gelifracted slope deposits allowed water to move through the large voids between the particles, creating underground flow pathways of a relatively high hydraulic conductivity.

These networks of preferential flow pathways similar to water tracks were efficient at transporting snowmelt, preventing the interaction of water with the rest of the soil outside of the flow paths. Some of the seeping water sources downslope from the snowdrifts yielded amounts of suspended sediments of similar amplitudes as other surface flow pathways in the Arctic. Solute transport was however the main driver of denudation, with concentrations exceeding suspended sediments by up to an order of magnitude. The presence of these flow paths influenced the timing of ice melting on the lake, contributing to the novel disappearance of perennial ice on the donwstream lake in 2011 and 2012. In addition, these flowpaths reacted to the degradation of the transient layer of permafrost in 2014, releasing solute rich waters in the soils and into the downstream lake. Further degradation of permafrost is expected to increase inputs of salt-rich waters to the littoral zone. The thesis effectively exemplifies how the evolution of a polar desert slope under severe periglacial conditions can be dependant upon the relation between sorting and water flow. This underlines the relevance of azonal processes for the geomorphology of a frost-dominated region, but maintains the importance of the periglacial control on soil morphology exerted by freeze-thaw processes.

Keywords: Geomorphology, Limnology, Patterned ground, Periglacial hydrology, Periglacial slope, Polar desert, Preferential flow, Sediment transport, Ward Hunt, Water tracks

Table des matières

Liste des tableaux

Table des figures

LISTE DES SYMBOLES ET DES ABRÉVIATIONS

SYMBOLES

α_{i-w}	Facteur de fractionnement isotopique entre la glace et l'eau / equilibrium isotope fractionation factor between ice and water
ϵ_{i-w}	Facteur de séparation isotopique entre la glace et l'eau / isotopic separation factor between ice and water
h_u	Niveau d'eau / water level
c_T	Concentration d'un traceur dans les eaux de ruissellement / tracer concentration in runoff
c_1	Concentration d'un traceur dans les eaux de fonte de neige / tracer concentrations in snowmelt
c_2	Concentration d'un traceur dans la glace de couche active / tracer concentrations in active layer ice
C_i	Concentration en sels dissous d'une solution / solute concentration of an injected solution
C_m	Concentration moyenne en sels dissous de l'eau dans un cours d'eau / mean solute concentration in running water
C_f	Coefficient d'écoulement libre / free flow coefficient
C_p	Capacité calorifique / heat capacity

ΔT	Différence de température / temperature difference
δ_o	Composition isotopique initiale de l'eau qui gèle dans un système ouvert / initial water isotopic composition freezing in an open system
δ_i	Composition isotopique de la glace qui gèle dans un système ouvert / isotopic composition of the ice freezing in an open system
δ_w	Composition isotopique des eaux résiduelles lors de l'engel dans un système ouvert / isotopic composition of residual water from freezing in an open system
f	Fraction d'eau résiduelle / residual fraction of water
F-value	Statistique F du test de Fisher / F statistic from an F-test
k	Conductivité thermique / thermal conductivity
k_s	Conductivité hydraulique saturée / Saturated hydraulic conductivity
K_f	Facteur de correction en écoulement libre / free flow correction factor
n	Nombre d'éléments d'un échantillon / number of elements in a sample
n_f	Exposant d'écoulement libre / free flow exponent
p	Probabilité d'accepter l'hypothèse nulle d'un test statistique / probability of accepting the null hypothesis in a statistical test
ρ	Densité de l'eau / water density
q	Flux de chaleur / heat flux
Q	Débit / discharge
Q_1	Contribution de la neige à l'écoulement / contribution from snowmelt
Q_f	Débit en écoulement libre / free flow discharge
Q_T	Ruissellement total / total runoff

r	Coefficient de corrélation de Pearson / Pearson coefficient of correlation
R^2	Coefficient de détermination / coefficient of determination
T	Temps / time
t	Statistique t de Student / Student's t statistic
V	Volume / volume
W	Statistique du test des rangs de Wilcoxon / Wilcoxon signed rank test statistic
W_{f_x}	Incertitude reliée au calcul de Q_x / Uncertainty in the calculation of Q_x
W_{c_x}	Incertitude de la valeur de c_x / Uncertainty for the value of c_x
nd	Absence de donnée / no data

ABBRÉVIATIONS

ASTM	American Section of the international association for Testing Materials
a.s.l.	Au-dessus du niveau marin / Above Sea Level
DSC	Concentration de solides dissous / Dissolved Solids Concentration
FDD	Degrés jours de gel / Freezing Degree Days
GMWL	Droite des eaux météoritiques globale / Global Meteoritic Water Line
GNIP	Global Network for Isotopes in Precipitation
GNSS	Système de positionnement par satellites / Global Navigation Satellite System
GPS	Système de positionnement global / Global Positioning System
GWC	Contenu en eau gravimétrique / Gravimetric Water Content

IT	Intertrack / intertrack
LMWL	Droite des eaux météoritiques locale / Local Meteoritic Water Line
MDD	Degrés jours de fonte / Melting Degree Days
NTU	Unité de turbidité néphélométrique / Nephelometric Turbidity Units
OM	Matière organique / Organic Matter
OLS	Moindres carrés ordinaires / Ordinary Least Square
PVDF	Polyfluorure de vinylidène / Polyvinylidene Fluoride
RMA	Axe majeur réduit / Reduced Major Axis
SAR	Radar à synthèse d'ouverture / Synthetic Aperture Radar
SD	Écart-type / Standard Deviation
SpC	Conductivité spécifique ou conductivité électrique à 25 °C / Specific Conductivity or electrical conductivity at 25 °C
SSC	Concentration de sédiments en suspension / Suspended Sediment Concentration
TDS	Somme des solides dissous / Total Dissolved Solids
TSS	Somme des sédiments en suspension / Total Suspended Sediments
VWC	Contenu en eau volumétrique / Volumetric Water Content
WHI	Île Ward Hunt / Ward Hunt Island

WHL Lac Ward Hunt / Ward Hunt Lake

WT Water track / water track

À Marc-André, qui voulait donc ben aller à l'école

REMERCIEMENTS

Un gros merci à « Danger » Dan, qui a su m'imposer (et non instaurer) avec brio l'importance de développer ma recherche moi-même. Blague à part, je crois fermement que j'ai pu développer une vision géomorphologique plus personnelle, plus large et plus accomplie avec lui que je n'aurais pu le faire ailleurs. Il a su stimuler mon sens des responsabilités face à mon travail, et en bon ami il a toujours tout fait en son pouvoir pour m'avoir à ses côtés lorsqu'il sentait que je pouvais en bénéficier. Il m'a également permis d'accumuler un nombre impressionnant d'anecdotes et de citations qui, de par leurs natures caustiques et débridées, m'assureront un ascendant à perpétuité grâce au chantage.

Je dois également remercier mon co-directeur Warwick Vincent, « le meilleur des meilleurs ». Toujours prêt à élargir l'envergure de notre travail, il a su m'encourager à voir le travail de scientifique comme davantage que la simple recherche. Nos contacts ont toujours été remplis d'apprentissages et de retours aux fondements. Il demeure source d'inspiration et d'admiration, ainsi que la raison première derrière mes débuts réussis en publications.

Merci à mes collègues du lab et partenaires de terrain, Sliger, Kat, Kate, Godin, Steph, Isa, Tchant, Manu, Sabine, Myriam, Gautier, Lin, Simon, Audrey et Karine. Merci également aux collègues, profs, anciens profs et employés du département de Géographie. Merci à tous mes collègues et collaborateurs hors UdeM, trop nombreux pour être nommés. Mention spéciale à Fred, Ashley, Denis, Marie, Derek, Scott et Melissa.

Merci à tous mes ami(e)s qui pensent que j'étudie les roches. Cette blague-là ne sera JAMAIS vieille. Un clin d'œil particulier aux membres de l'Anticintre^{TM}, LA référence. Merci à ma famille, qui me rappelle bien que c'est long un doc en me demandant quand est-ce que je termine.

Finalement, mille mercis à Mariane, qui est remplie de lumière. Tu es ma raison d'être le meilleur de moi-même. Asteure donne-moi mon cash.

INTRODUCTION

CONTEXTE HISTORIQUE ET CONTEMPORAIN DU PÉRIGLACIAIRE

L'utilisation du terme « périglaciaire » provient de Łoziński (1909, cité dans Tricart (1967)), et a vu le jour afin de désigner des phénomènes liés à l'action intense du froid qui opéraient en périphérie des Inlandsis lors de la dernière grande glaciation. Il était alors attribué à un faciès typique, représenté par des débris de gélifraction tel que dans les champs de blocs (Figure 0.1). La science périglaciaire s'intéressait beaucoup, dans ses débuts aux reconstitutions climatiques Pléistocènes et Quaternaires, notant les formes et dépôts issus des manifestations du froid. L'analyse des processus s'est ensuite amplifiée, grâce aux progrès méthodologiques et technologiques, permettant d'étudier l'action du froid sur la météorisation (la gélivation) et sur les mouvements du sol (la géliturbation) (Tricart, 1967).

Tricart (1967) suggèrera par la suite que le gel et dégel de l'eau représente le mécanisme essentiel du système morphogénétique des régions périglaciaires. Il n'accorde en général qu'une faible importance au délavage des pentes par l'eau, qui demeure loin derrière la solifluxion à titre d'agent de transport. Il soulève cependant le rôle parfois significatif de l'hydrologie lors du transport de débris fournis par la gélivation. Ce ruissellement est alors exclu des processus périglaciaires, car il vient réduire l'efficacité de la géliturbation et contribue à maintenir une pente abrupte, prévenant le développement d'un paysage périglaciaire. Son utilisation de la gélivation sous-entend également qu'il considère que les autres processus de modification du matériel parental sont négligeables.
Cette exclusion de la contribution des processus azonaux comme agent de développement du paysage périglaciaire demeurera centrale à la discipline de géomorphologie périglaciaire, et entache

FIGURE 0.1. Dépôt périglaciaire (débris de gel) tel que désigné par Łoziński (1909), développé dans la syénite au Mont Jacques-Cartier, Canada. Crédit photo : G. Davesne, 10/2012

encore de nos jours les raisonnements. Washburn (1979, p.4) propose une définition devenue classique du périglaciaire : « Les processus et éléments terrestres non-glaciaires des climats froids, caractérisés par une action du gel intense, peu importe l'âge ou la proximité aux glaciers ». Encore une fois, l'intensité du gel est centrale dans la définition, et suggère une géomorphologie périglaciaire centrée sur l'action du gel. L'ouvrage est d'ailleurs concentré sur les formes de gélivation et de géliturbation.

L'accumulation de preuves qui démontrent l'importance des processus azonaux dans la météorisation et le transport du matériel (Ballantyne, 1985 ; Dixon, Thorn et Darmody, 1984 ; Lewkowicz, 1981 ; Rapp, 1960) sera le contrecoup de l'augmentation de la quantité des études de processus, et viendra par la suite lancer le débat sur les considérations théoriques et académiques du terme périglaciaire. À ce titre, Barsch (1993) cite Karte (1979 p.7), qui énumère quatre sujets d'étude faisant partie de la géomorphologie périglaciaire :

1. Les zones enneigées ou à proximité des glaciers étant influencées par un climat froid significatif pour la géomorphologie
2. Les conditions – surtout climatiques – qui créent des formes de paysage autour de ces zones
3. Les processus géomorphologiques qui se produisent dans ces zones
4. Les formes et les sédiments produits par les processus géomorphologiques dans ces zones

De ces quatres sujets, aucun ne limite la géomorphologie périglaciaire à l'action spécifique du gel. En fait, la géomorphologie périglaciaire désigne ici essentiellement l'étude d'une zone morpho-climatique, ainsi que les processus et des formes qui s'y trouvent, peu importe leur origine. La discipline y est donc zonale, et au floue de sa caractérisation s'ajoute ainsi la difficulté de définir ses limites géographiques (French, 2007). Elle trouve à priori écho dans les considérations de French (1987, p.5), qui évoque que « Periglacial geomorphology seeks to explain the geomorphic processes and landforms of cold non glacial environments ». Cependant, bien que la définition semble s'accorder avec la précédente, le reste de l'article place l'emphase des considérations de recherche futures sur l'action du gel. Les mentions des processus azonaux y sont réduites à la section sur la météorisation, alors que les incertitudes y sont largement reconnues.

Au sujet de l'identification des régions périglaciaires, French (1987) suggère la présence de cycles de gel/dégel intenses et la formation de pergélisol. La vision centrée sur la glace et le gel fait également surface dans Thorn (1992, cité dans Barsch, 1993), qui appuie la géomorphologie périglaciaire sur l'impact de la glace (non-glaciaire) dans le développement des formes. Barsch (1993) déplore cette définition, qui est selon lui trop floue et pas suffisamment géographique, car l'action du gel peut s'étendre jusque dans les déserts chauds. Il rejette ainsi l'aspect basé sur un processus unique – le gel – et suggère une vision plus climatique de la géomorphologie périglaciaire. La discipline devrait ainsi étudier tous les processus liés à la formation du paysage des zones polaires ou alpines. Barsch (1993), dans son argumentation, ne précise cependant pas ce qu'il inclut (et surtout, exclut) comme processus périglaciaire. Les questions centrales de l'action du ruissellement et des glaces sont ainsi évitées. Il justifie cependant son raisonnement par soucis de ne pas exclure les régions qui ne sont pas purement « périglaciaire », par exemple la région boréale. Cet argument sous-entend l'existence d'un large domaine et d'un modelé purement périglaciaire, c'est-à-dire dominé par le gel. D'un côté, les définitions de la géomorphologie périglaciaire se buttent à l'arbitraire de la délimitation des régions périglaciaires, et de l'autre, elle se limite à n'étudier que les processus liés au gel.

Le rôle parfois dominant des processus autres que ceux liés au gel/dégel dans l'évolution des paysages périglaciaire n'est plus à prouver de nos jours (André, 2003 ; Dixon et Thorn, 2005 ; Hall, Thorn, Matsuoka et Prick, 2002 ; Seppälä, 2004). Face à la rareté de régions régies par des conditions et des processus purement périglaciaires (French, 2000), French (2007), dans ce qui est largement accepté comme manuel de base sur le sujet (Pissart, 2005), relève plusieurs problèmes de terminologie et soulève ainsi l'utilité limitée du concept de périglaciaire. Il étend alors le territoire périglaciaire à l'ensemble des milieux non-glaciaires affectés par le gel, et la géomorphologie périglaciaire aux formes froides et non-glaciaires (*cold, non-glacial landforms*). Il souligne également l'importance des processus azonaux, par exemple l'effet des eaux courantes. Ces spécificités n'incluent pas l'obligation de dominance des phénomènes liés aux froids sur le développement d'un paysage périglaciaire typique. Ce rejet est encouragé par French et Thorn (2006), qui définissent la région périglaciaire comme « zones de climat froid dans lesquels le gel saisonnier et permanent, la neige et les processus azonaux sont présent de manière plus ou moins importante ». On y distingue également la géomorphologie périglaciaire, qui se développe spécifiquement autour de la glace dans les sols comme agent géomorphologique, de la géomorphologie des régions froides, qui se soucie également des processus azonaux.

Cette discussion écarte ainsi toute vision zonale de la géomorphologie périglaciaire, et sous-entend que la compréhension et la modélisation des paysages des régions périglaciaires, où des processus autres que ceux liés à la glace se produisent et influencent le paysage, ne peut être atteinte que par la discipline englobante de la géomorphologie des régions froides. Il en ressort donc que, paradoxalement, la géomorphologie périglaciaire seule est insuffisante pour expliquer les paysages des régions périglaciaires.

Il est intéressant de noter que French (2015, p.1866) revient récemment sur ses pas lors d'une recherche d'un paysage purement périglaciaire. Il limite alors les environnements périglaciaires à « those in which cold, nonglacial processes dominate ». Ce recul témoigne de la résistance de la discipline de géomorphologie périglaciaire à abandonner les fondements climatiques associés au

développement d'un paysage dit « périglaciaire », et peut dans ce cas-ci être excusé par le sujet même de l'article. Cette résistance est néanmoins répandue. Elle témoigne autant de la force du concept introduit par Łoziński et soutenu pendant au moins un demi-siècle, que de l'ambiguïté qui émerge alors que les concepts de région, de géomorphologie et de processus périglaciaires ne s'accordent tout simplement pas.

En contrecoup à la popularité de cette limitation, Pissart (2005) dispute la réduction de la géomorphologie périglaciaire à ne considérer que l'action du gel, car elle néglige les caractéristiques distinctes que peuvent prendre les processus azonaux en milieu froid. Un exemple flagrant et désormais établi est la thermo-érosion, une forme d'érosion fluviale ou côtière qui dépend directement de l'interaction de l'eau avec les sols cryotiques (Fortier, Allard et Shur, 2007). Le délavage des pentes par le ruissellement peut également augmenter la sensibilité des sols au gel dans les zones de dépôt, créant des conditions favorables à la solifluxion (Verpaelst, Fortier, Kanevskiy, Paquette et Shur, 2017). Les processus de nivation sont d'ailleurs particulièrement propices à créer de telles conditions, car ils sont reconnus pour ne transporter leurs sédiments que sur de courtes distances (Ballantyne, 1985). Il est également important de prendre en compte les processus éoliens, dont l'action à long terme peut définir les propriétés du pergélisol (Fortier, Allard et Pivot, 2006) et former des *yedomas* (Murton et al., 2015), méritant amplement d'avoir son propre volume (Seppälä, 2004).

Berthling et Etzelmüller (2011) tentent de palier à cette contraction de la discipline en suggérant le concept de cryo-conditionnement comme condition unifiante. Le concept est attrayant car il permet aux formes et processus périglaciaires de demeurer sous le sujet des suites du gel, tout en considérant les formes et paysages comme étant issus de l'interaction de l'ensemble des processus avec un régime thermique cryotique. Le développement des paysages peut ainsi passer des effets d'un héritage glaciaire au périglaciaire sans influencer le cadre conceptuel de son développement, soit l'interaction entre le froid, les processus azonaux et le paysage. La cryo-géomorphologie n'est ainsi ni plus ni moins que l'application de l'expression « des régions froides » à l'étude du

développement des formes et paysages, et s'ajoute avec aisance à la vision suggérée par French et Thorn (2006). Le concept s'inscrit aussi dans le rejet prouvé d'un développement des paysages purement périglaciaires, sans influences glaciaires ou azonales.

LE DÉVELOPPEMENT DE LA PENTE PÉRIGLACIAIRE

Contrairement aux bassins et aux régions physiographiques, qui sont fortement influencés par des dynamiques fluviales, les pentes évoluent à travers les processus de mouvement de masse et de dénudation uniquement (Dylik, 1968). Il s'agit ainsi de l'élément de base de l'étude du paysage en géomorphologie, et la question d'évolution des pentes en milieu périglaciaire est loin d'être élucidée, entre autres à cause des paradigmes illustrés précédemment. Il existe plusieurs modèles, qui sont partiellement résumés par French (2015), lors d'une pénultième tentative de décrire un paysage purement périglaciaire (Figure 0.2). Dans le premier modèle, celui de Peltier (1950), les processus de météorisation et de transfert de sédiments sont ancrés dans le paradigme de dominance des processus périglaciaires typique de l'époque. Ils sont donc essentiellement l'affaire de gélivation et de géliturbation, dont les taux dictent les taux de recul et de mouvement de la pente. Le modèle de la cryoplanation, quant à lui, met de l'avant le rôle des combes à neige lors de la météorisation et de l'érosion du sol, sous une dynamique de nivation et de mouvements de masse (Demek, 1969).

Un troisième modèle est né de l'étude des environnements désertiques de l'Antarctique, et est basé sur une pente de Richter (Selby, 1971). Contrairement aux deux autres, ce modèle ne s'appuie pas nécessairement sur des processus, mais sur un rapport entre les taux de production et de transport de débris. Il s'ensuit une retraite parallèle dans le cas d'une falaise, puis la production d'une pente de plus en plus douce une fois la falaise éliminée, avec la possible formation de pédiments. L'auteur rompt du même coup avec le paradigme des processus périglaciaires prépondérants. Il justifie sa proposition de l'haloclastie comme processus dominant de production de débris par l'aridité du site, et suggère l'érosion éolienne pour justifier le transport lorsque la

solifluxion ou les mouvements de masse ne sont pas possibles (Selby, 1974). Plusieurs études viendront par la suite démontrer l'importance du ruissellement comme agent de modification des pentes périglaciaires (Beylich et al., 2004 ; Lewkowicz, 1981 ; Mercier, Marlin et Laffly, 1998 ; Thorn, Darmody, Dixon et Schlyter, 2001 ; Wilkinson et Bunting, 1975), questionnant davantage l'établissement de modèles uniquement basés sur des processus périglaciaires.

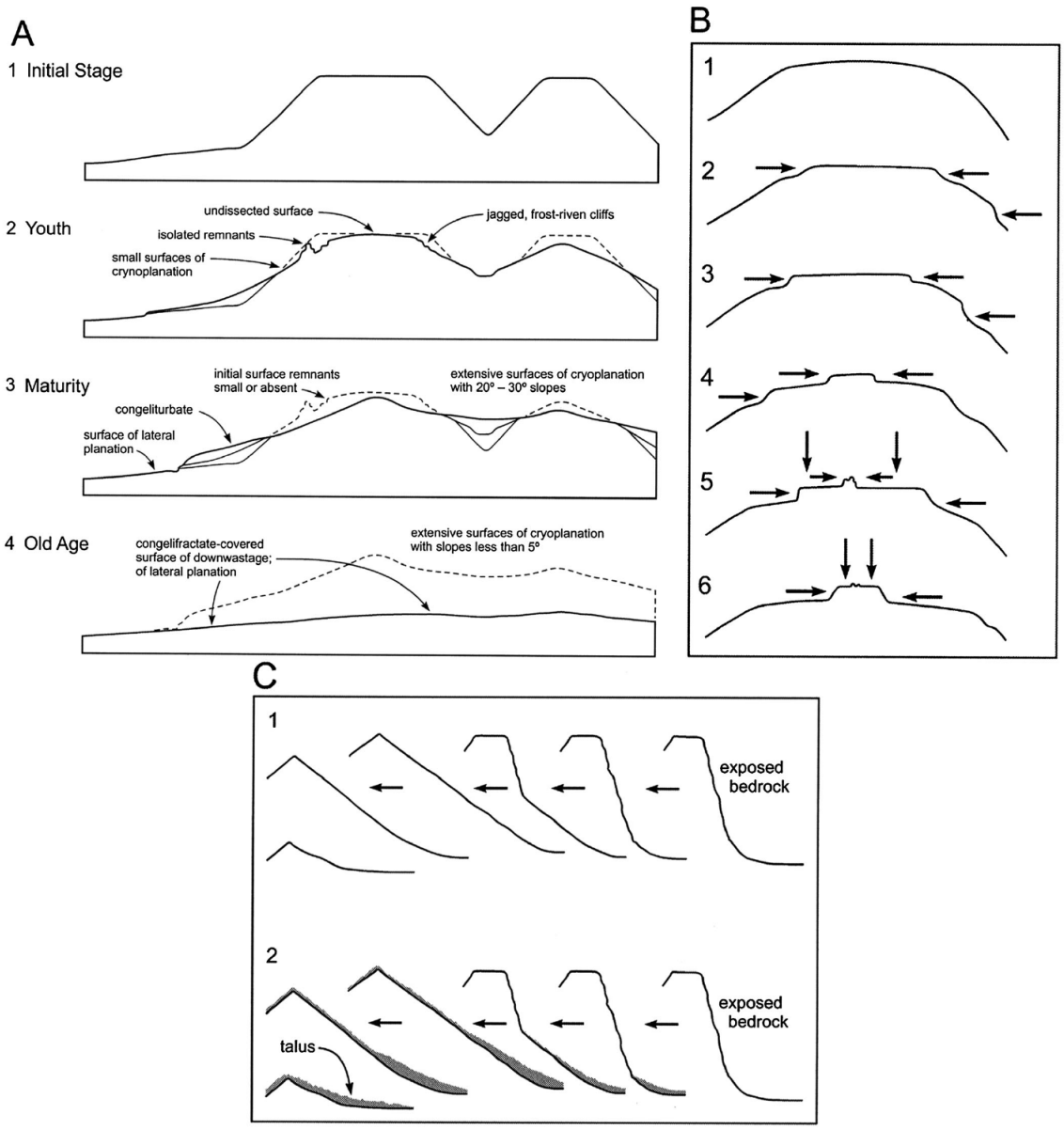

FIGURE 0.2. Modèles d'évolution des paysages périglaciaires, tel que présenté par French (2015). A) Le cycle d'évolution périglaciaire de Peltier (1950). B) Le cycle de cryoplanation de Demek (1969), basé sur les phénomènes de nivation. C) La dénudation d'une surface de roche exposée selon Selby (1974), formant une pente de Richter.

Le rejet progressif de la gélivation et de la géliturbation comme agents absolus de modification des pentes périglaciaires ne peut évidemment se faire sans heurts. Parmi les concepts pris à parti, la nivation, qui se base historiquement sur les processus de ces deux agents, semble occuper une place de choix. La définition classique de la nivation est celle de Washburn (1979, p. 236) :

« Nivation is the localized erosion of a hillside by frost action,
mass-wasting, and the sheetflow or rillwork of meltwater at the edges of,
and beneath, lingering snowdrifts. »

Cette définition inclue donc autant les processus de météorisation et de transport, dans la pluralité de leurs interactions, ce qui pousse Thorn (1988) à questionner la capacité du terme à réellement définir un processus quelconque. André (1999) est moins tendre envers les processus périglaciaires en général, soulignant l'effet parfois dominant des écoulements et réduisant même les formes typiquement périglaciaires à des « parures » peu fonctionnelles pour le paysage. L'auteure questionne abondamment l'efficacité de la cryoclastie et renie finalement le processus de nivation. Bien qu'elle ne nie pas le rôle de l'eau de fonte sur le transport de sédiment, elle remet en question l'aspect de météorisation, et soutient que les combes à neige ne possèderaient pas la caractéristique centrale d'agir sur la morphologie de leur propre niche. Elle s'inspire notamment de la suggestion d'abandon du terme par Thorn (1988) relayée par French (1997). Telle négation vient cependant sans mentionner et encore moins répondre aux observations des dernières études de l'époque de Christiansen (1998) ni de Berrisford (1991). La première démontre aisément le rôle de la présence de niche de nivation dans la retraite de la paroi arrière de dépôts de sédiments meubles, la seconde que les niches dans la roche en place progressent plutôt vers le bas de pente, suggérant la météorisation chimique comme agent de détérioration principal. En plaçant l'emphase sur le rôle des écoulements et de l'humidification des zones en aval des combes pour leur évolution, les deux auteurs rompent avec la théorie classique de gélifraction comme agent morphogénétique principal.

L'erreur d'André (1999) est de rejeter un agent évident de modification du paysage sur une faute sémantique, ignorant du coup l'historique de dévelopement de la discipline. Bien que la géliturbation ne soit pas reconnue comme un agent de transport de sédiments très efficace, elle

est, lorsque combinée à la gélivation, bien capable de réorganiser la roche et les sédiments pour créer des formes locales (Slaymaker, 2009), et est parfois le seul agent notable de remobilisation du matériel le long des pentes (Strömquist, 1983). Tel que mentionné plus tôt, les justifications de Thorn (1988) et de French (1997) sont plutôt liées à la confusion entourant le terme, ainsi qu'aux fondements souvent trompeurs présent dans la littérature. Bien que Christiansen (1996b) tente de sauver le terme en réduisant la spécificité de sa définition, Thorn et Hall (2002) soulèvent l'inutilité pratique et théorique d'une définition ratissant trop large, qui ne diffèrerait finalement pas de la terminologie de « nival ». À la place, les auteurs saluent les pivots conceptuels qui apparente maintenant la nivation à un assemblage de formes et de processus similaire au système glaciaire, (Christiansen, 1996a ; Nelson, 1989), ainsi qu'à l'emphase sur la météorisation chimique comme composante importante de la météorisation des milieux froids (Darmody, Thorn, Harder, Schlyter et Dixon, 2000 ; Hall et al., 2002 ; Thorn et al., 2001). Ils suggèrent d'emblée la poursuite du débat autour de la nivation jusqu'à pouvoir clarifier ses tenants propres.

Les débats entourant la nivation montrent un exemple flagrant de problèmes associés aux changements de paradigmes en géomorphologie périglaciaire. Longtemps considérés dominés par les processus spécifiques au froid, les environnements périglaciaires doivent maintenant être réévalués afin de déterminer les processus réellement dominants pour l'évolution du paysage.

La présente thèse s'attarde au **rôle que peut avoir la combinaison des formes périglaciaires avec un processus azonal – le ruissellement – dans la formation, le développement et l'évolution d'une pente périglaciaire, ainsi qu'aux fonctions issues de la morphologie obtenue**. L'hypothèse lancée est que le développement des pentes est influencé par les eaux de fonte, c'est-à-dire l'effet nival, couplé aux processus liés avec le gel et le dégel. La recherche adresse également la signification des processus d'évolution des pentes vis-à-vis d'autres composantes du système naturel, dans ce cas-ci un lac et son couvert de glace. Il s'agit d'une étude de processus qui consent à la vision de French et Thorn (2006) d'une géomorphologie des régions froides et à la cryo-géomorphologie de Berthling et Etzelmüller (2011), qui incluent les processus azonaux

comme essentiels à l'atteinte du but fondamental de la discipline : l'élaboration de modèles d'évolution du paysage. La recherche contribue à encourager cette vision de la géomorphologie périglaciaire englobante ainsi que l'abandon de la poursuite du modelé périglaciaire pur, en démontrant l'importance des liens entre les processus morphogénétiques périglaciaires et azonaux dans le développement d'un paysage périglaciaire.

STRUCTURE DE LA THÈSE

Le premier chapitre présente une revue de littérature permettant de présenter quelques concepts clés d'hydrologie en milieu de pergélisol, d'écoulements préférentiels et de transferts de matière en milieu périglaciaire. Il jette les bases théoriques permettant au lecteur de mieux saisir les particularités du système hydrologique du site d'étude, et est une base de références pour l'approfondissement des études sur les chemins d'écoulements préférentiels en milieu périglaciaire.

Le second chapitre s'articule autour de l'investigation d'un réseau hydrographique constitué de chemins d'écoulement préférentiels, water tracks en anglais, dont les caractéristiques connues sont essentiellement issues d'études publiées qui se situent dans deux endroits uniquement. Il s'agit de l'intégralité d'un article publié dans la revue Arctic Science, une contribution à l'édition spéciale du programme du conseil de recherche en science naturelles et en génie « Arctique en développement et adaptation au pergélisol en transition – ADAPT » (Paquette, Fortier et Vincent, 2017). Il examine la morphologie et l'organisation des chemins d'écoulement préférentiels, ainsi que leurs impacts sur les conditions physiques, thermiques et géochimiques dans les sols. Il s'agit de la première contribution sur ce type de réseau hydrographique dans le Haut Arctique Canadien, démontrant une morphologie particulière à l'interface entre le ruissellement et la cryoturbation, ainsi que plusieurs impacts sur les caractéristiques de la couche active. Il jette également les conditions générales de la morphologie et de l'hydrologie du site, conditions auxquelles le reste

de la thèse se réfère par la suite.

Le troisième chapitre porte sur l'hydrologie des chemins d'écoulement préférentiels. Il se base sur des mesures de débits, de géochimie isotopique et de conditions météorologiques afin de déterminer i) le régime hydrologique et les mécanismes de génération de ruissellement des chemins d'écoulement préférentiels ; ii) les conditions météorologiques qui déterminent la force des écoulements ; iii) la proportion d'interaction avec l'eau présente dans les sols. L'article a été publié dans la revue Hydrological Processes (Paquette, Fortier et Vincent, 2018), et démontre que les chemins d'écoulement préférentiels agissent comme lien relativement directs entre le dégel des combes à neige lors des cycles diurnes d'insolation et les bas de pente. On y voit également la distance relative des écoulements augmenter pendant la saison de dégel, et on y perçoit aussi la signature isotopique du dégel du pergélisol lors d'un été particulièrement chaud. Cet article démontre l'efficacité des chemins d'écoulements préférentiels pour l'évacuation de l'eau de fonte, soulignant l'adaptation du réseau de drainage à la redistribution de la neige par le vent.

Le quatrième chapitre lie les processus de transport de la matière à l'hydrologie et la morphologie des chemins d'écoulement préférentiels. Il cherche à i) mesurer les flux de sédiments et de matière en solution dans les chemins d'écoulement préférentiels ; ii) établir un modèle conceptuel de géomorphologie de pente le long des chemins d'écoulement préférentiels. Il émerge que la capacité de transport de sédiments en suspension dans les chemins d'écoulement préférentiels se compare au ruissellement de surface dans le reste de la littérature périglaciaire, et que les pentes sont adaptées aux conditions nivales, dont la présence représente la condition principale de transport. L'article établit le lien conceptuel entre le ruissellement en milieu périglaciaire et la cryo-géomorphologie. Il sera soumis à la revue Permafrost and Periglacial Processes suite aux commentaires du jury, avec Daniel Fortier, Mélissa Lafrenière et Warwick F. Vincent en tant que co-auteurs.

Le dernier chapitre (5^{e}) contextualise le rôle des écoulements dans la relation entre le bassin versant et le lac se trouvant au site d'étude. Publié dans la revue Geophysical Research Letters (Paquette, Fortier, Mueller, Sarrazin et Vincent, 2015), l'article se penche sur la primeur de la disparition du couvert de glace sur le lac, ainsi que sur les causes expliquant cette disparition. Il démontre que le couvert de glace s'est dégradé rapidement à la fin de la décennie 2000, avant de disparaître en 2011 et en 2012, une première en plus de 60 ans. La hausse des températures de l'air est mise de l'avant comme cause principale de la dégradation rapide, mais la morphologie du lac ainsi que les apports d'eau provenant des chemins d'écoulement préférentiels sont des facteurs accélérant le réchauffement de la colonne d'eau et la fonte de la glace.

Chaque article a été rédigé par l'auteur de cette thèse, qui est également responsable du développement de la méthodologie, de la collection et du traitement des données et de leur analyse. La contribution des co-auteurs s'est effectuée principalement par des commentaires et suggestions sur les manuscrits avant publication, excepté pour le dernier chapitre, où des images aériennes ont été fournies par Denis Sarrazin et des images satellites par Derek R. Mueller. Il est également important de mentionner que l'entretient de la station données météorologiques ainsi que la collecte de ses données ont depuis toujours été effectuées par Denis Sarrazin, professionnel de recherche au Centre d'études nordiques (CEN).

Chapitre 1

LES *WATER TRACKS* DANS LA LITTÉRATURE

1.1. HISTORIQUE DE LA RECHERCHE

L'hydrologie Arctique se différencie de ses équivalences en climats plus tempérés par la forte répartition de la neige, par la dominance de la période de dégel sur le régime hydrologique et par la présence de pergélisol (Woo, 2012). Les hydrographes sont dominés par le régime nival, et le processus le plus important pour la disponibilité en eau et les écoulements est l'accumulation de neige et sa redistribution par les vents (Woo, 1983). Le pergélisol et le front de dégel agissent comme une barrière pratiquement imperméable qui limite l'infiltration d'eau et favorise les écoulements de surface (Carey et al., 2010 ; Woo et Steer, 1986). Tôt dans la saison, la couche active est peu profonde, limitant sa capacité de stockage et favorisant l'émergence de la nappe phréatique et la mise en place de réseaux d'écoulements superficiels (Woo et Steer, 1982, 1983). Ce faisant, les distances et les chemins d'écoulement sont fortement affectés par la présence de pergélisol. Petrone, Jones, Hinzman et Boone (2006) ont démontré qu'un bassin versant avec plus de pergélisol entraîne une plus importante livraison des eaux de fontes vers l'exutoire, ainsi qu'une réponse plus rapide de l'hydrographe aux événements de pluie.

Au niveau des pentes, la présence d'un couvert continu de végétation empêche souvent le développement de ruisseaux incisés, et les écoulements se produisent de manière préférentielle dans l'épaisse couche de matière organique en surface (Hinzman, Kane et Everett, 1993 ; Quinton et Gray, 2003 ; Quinton, Gray et Marsh, 2000 ; Quinton et Marsh, 1998, 1999) ou dans la portion

grossière des sols triés (Hodgson et Young, 2001). Il s'agit donc d'une hydrologie dominée par de l'écoulements préférentiels (Hinzman et al., 1993 ; McNamara, Kane et Hinzman, 1998), un concept qui désigne de l'eau s'écoulant dans le sol en passant outre une portion du volume de la matrice poreuse de ce sol (Gerke, 2006). Or, les formes nées de cet écoulement préférentiel sont souvent appelées *water tracks* dans la littérature contemporaine. Ce chapitre présente quelques notions de base sur les *water tracks*, afin de jeter les assises et d'introduire la pertinence de la forme dans le cadre de la thèse.

Même si elles [1] sont habituellement associées aux régions périglaciaires, les premières mentions de *water tracks* proviennent plutôt des régions boréales et tempérées. Sjörs (1948) cité par Ingram (1967), les désigne comme des zones d'écoulement d'eau accru dans le sol, le long d'une pente dans les tourbières du Nord-Ouest Européen. Le terme décrit alors une zone d'écoulement qui ne comprend pas nécessairement l'émergence de la nappe phréatique, bien que cela puisse se produire suite aux précipitations. Ces zones sont visiblement marquées par une végétation différente, un effet attribuée aux conditions eutrophes des eaux qui y circulent. D'autres formes semblables furent par la suite répertoriées et étudiées dans les tourbières boréales de l'Amérique du Nord (Glaser, Wheeler, Gorham et Wright, 1981). Elles y sont omniprésentes, autant dans la région du lac glaciaire Agassiz que dans la région des basses-terres de la baie d'Hudson, du Grand Lac de l'Ours et du Grand lac des Esclaves. Elles sont retrouvées autant en milieu de pergélisol qu'en milieu tempéré, et leur formation ne semble pas dépendre de l'existence de conditions périglaciaires pendant l'Holocène (Glaser, 1987).

Un autre type de *water track* a commencé à être documenté sur des pentes périglaciaires à partir des années 1980. Elles furent tout d'abord décrites en tant que *shallow channels that conduct snow melt-water and subsurface water during the thaw season [...] giving the topography a ribbed appearance* (Walker et al., 1982). Ce sont les *water tracks* d'Imnavait Creek, un bassin

1. L'objet ne possédant pas de genre en anglais, l'article prend le genre de son nom équivalent en français. Étant donné que le terme *water track* se traduirait littéralement « piste d'eau », et parce que *water track* désigne une forme, le féminin est utilisé dans le texte.

versant fortement étudié dans le bassin de la rivière Kuparuk sur la plaine au pied de la chaîne des monts Brooks en Alaska. Elles sont développées sur des pentes non-incisées, et comme dans les tourbières, elles sont marquées par un changement de la végétation. À partir de ce moment, les mentions de *water tracks* ont fait apparition pour plusieurs paysages périglaciaires : près de Healy et de la rivière Toolik, en Alaska (Bowden et al., 2008 ; Osterkamp et al., 2009) ; dans le bassin versant de la rivière Kolyma (Curasi, Loranty et Natali, 2016) dans les planchers d'*alas* et les plateaux de *yedomas* en pente douce, en Sibérie (Morgenstern, 2012) ; en Antarctique dans les vallées sèches de McMurdo (Levy, Fountain, Gooseff, Welch et Lyons, 2011) ; ainsi que dans le désert polaire du Haut Arctique canadien à l'île Ward Hunt, au nord d'Ellesmere (Steven, Lionard, Kuske et Vincent, 2013). Chaque nouveau site y décrivait une morphologie différente, qui sont compilées dans le tableau 1. I.

Tableau 1. I. Caractéristiques morphologiques des *water tracks*

Site	Largeur	Longueur	Espacement	Référence
Imnavait Creek (Alaska)	5-20 m	250 m	10-20 m	Chapin et al. (1988), Stieglitz et al. (2003)
Antarctique	1-3 m	200-1900 m	nd	Levy et al. (2011)
Grand lac des Esclaves	50-250 m	Quelques km	nd	Glaser (1987)
Ward Hunt	20-300 cm	< 100 m	1-2 m	Cette étude

D'autres auteurs ont rapporté des formes similaires sans toutefois utiliser le terme. Des « seepage lines » existent dans certains terrains en pente faible du nord de l'Angleterre, provoquant une augmentation de la météorisation et le point de départ d'une érosion régressive (Bunting, 1961). Au Québec subarctique, des zones d'écoulement préférentiels le long de « wet lines » furent observés et décrites comme *an obvious and common feature of the permafrost affected areas*, qui pouvait également être la source de taliks (Nicholson, 1978). Dans les *yedomas* et *alas* de Sibérie, le terme *water tracks* fut également utilisé pour désigner les fonds humides de vallées en berceau (Morgenstern, 2012). Les même vallées en berceau sont répertoriées dans la vallée de Khorogor, en Sibérie (Grosse et al., 2007), bien que la description qu'en font les auteurs semble plutôt indiquer qu'il s'agit de *water tracks*. Enfin, d'autres études décrivent des rigoles en leur donnant quelques caractéristiques des *water tracks*, dont la présence d'écoulement préférentiel

sous la surface du sol (Wilkinson et Bunting, 1975 ; Woo et Xia, 1995). Une rigole est pourtant un « petit ruisseau, dû à l'érosion, dans lequel se concentre le ruissellement » (WMO, 2012) et ne possède pas la caractéristique non-incisée des *water tracks*.

La question de ce qui fait une *water track* n'a jamais vraiment été discutée dans la littérature, la plupart des auteurs s'en tenant à emprunter une définition ou à en créer une nouvelle. Ainsi, il existe plusieurs définitions, chacune en lien avec les intérêts de recherche des auteurs, c'est-à-dire basées soit sur la végétation, la topographie, la taille, les caractéristiques du sol, leur distribution, leur aspect et leur fonction. Le tableau 1. II montre une liste non-exhaustive de définitions pour le terme. Une des faiblesses de ces définitions réside dans la géographie limitée de chaque recherche, ce qui fait en sorte que les caractéristiques morphologiques, biologiques ainsi que les processus présentés dans une définition peuvent être fortement modifiés d'un endroit à l'autre, rendant les définitions obsolètes lorsque l'on s'éloigne du lieu de l'étude. La confusion et l'association avec d'autres termes (rigole, vallée en berceau) possédant quelques caractéristiques des *water tracks* soulève des questions sur la pertinence même de l'expression, et nécessite un effort de clarification. En premier lieu, malgré l'utilisation erronée et la comparaison avancée par Grosse et al. (2007), les rigoles et les vallées en berceau sont deux formes complètement différentes, d'un ordre de grandeur différent. Les rigoles ont déjà été décrites, tandis que les vallées en berceau sont des vallées sèches en pente douce, d'origine fluviale, d'une longueur pouvant atteindre 300 m et formé principalement par ruissellement (Klatkowa, 1965). En second lieu, les deux formes sont issues de l'érosion ou l'incision par ruissellement de surface, tandis que l'une des caractéristiques centrales des *water tracks* est l'absence d'incision dans le matériel, ainsi qu'un écoulement se produisant principalement sous la surface. Par contre, même ces caractéristiques ne sont pas infaillibles, car les *water tracks* peuvent parfois produire du ruissellement de surface et être incisées sur de courtes distances (McNamara et al., 1998). La définition de Gooseff, Barrett et Levy (2013) semble être la plus englobante, bien qu'elle se limite aux régions polaires à pergélisol.

Tableau 1. II. Liste de définitions de *water tracks*

Définition	Référence
"Zones of usually several meters in width where water drained from a portion of the slope runs down-slope to feed into a permanent water course at the valley bottom."	Matthes-Sears et al. (1988)
"*water tracks* are distinct bands of vegetation 5-15 m wide and with a soil surface 10-20 cm lower than adjacent tundra. They collect water from their surroundings and serve as subsurface drainage channels down slope."	Chapin et al. (1988)
"*water tracks* are subtle features on the slopes and convey flow downslope perpendicular to the elevation contours."	Kane et al. (1991)
"*water tracks* are small channels which are formed on slopes as permafrost features. They can be quite subtle and are often distinguished more by changes in vegetation than topography. A visible channel is not always obvious. "	Hinzman et al. (1993)
"*water tracks* are surface drainage features which act to quickly route excess water off hillsides to the valley bottom"	Hinzman et al. (1993)
"[. . .] essentially a linear channel that flows directly down a slope draining an enhanced soil moisture zone, and is best detected by a change in vegetation from the surrounding hillslope."	McNamara et al. (1998)
"Regions of enhanced soil moisture that run down the hillslope at a spacing of 10–20 m."	Stieglitz et al. (2003)
"*water tracks* are shallow, linear, parallel depressions that form on gently sloping hillsides in areas with continuous permafrost or on toe slopes with retransported deposits in the discontinuous zone."	Jorgenson et al. (2008)
"Poorly defined shallow linear depressions with high soil moisture that allow richer vegetation growth than elsewhere on the slopes."	Woo (2012)
"*water tracks* are narrow bands of high soil moisture that route water downslope, in the absence of overland flow, through permafrost dominated soils in polar regions".	Gooseff et al. (2013)

À la lumière de la discussion et des différentes sources présentées ici, les *water tracks* peuvent être définies selon leurs caractéristiques physiques. Ce sont des zones d'humidité et d'écoulement accru dans les sols, organisées de manières subparallèles et quasi linéaires, pouvant entrainer le développement de patrons de végétations. Les écoulements sont habituellement dominés par les

écoulements hypodermiques, bien que des écoulements en surface et des résurgences peuvent se produire lors de périodes de forts débits. Elles peuvent nicher dans de faibles dépressions topographiques ou être indissociables du reste de la pente. Bien qu'elles soient essentiellement non-incisées, elles peuvent posséder des sections incisées là où les écoulements de surface se produisent. La largeur des *water tracks* dépend fortement de leur environnement, et leur espacement n'est pas toujours régulier. Il ne semble pas exister de raison à ce moment de suivre la suggestion de Walker et al. (1989) qui veut différencier les *water tracks* de basses-terres de celles des pentes, car elles partagent plusieurs éléments en commun. De cette manière, elles deviennent un élément azonal plutôt qu'un terme d'hydrologie en milieu de pergélisol.

1.2. HYDROLOGIE DES *water tracks*

Comme l'ont dénoté plusieurs auteurs dans leur définition de *water tracks*, ce sont avant tout des zones d'écoulement préférentiels. En ce sens, elles agissent comme voie de transfert de matière vers le bas de pente. Les études d'hydrologie les plus complètes proviennent du bassin versant de 2.2 km^2 chargé de *water tracks* d'Imnavait Creek (plus de 130 comptées), au nord de l'Alaska. Elles ont montré que les *water tracks* réagissaient rapidement aux événements de pluie et de fonte des neiges, diminuant le temps de réponse de l'hydrographe en bas de pente (Kane, Hinzman, Benson et Liston, 1991). Deux raisons expliquent cette réponse : Premièrement, l'humidité accrue dans les *water tracks* nécessite moins d'eau, donc moins de temps lors des événements de précipitation avant d'atteindre la saturation, et les valeurs de conductivité hydraulique saturées (Kane et al., 1991). Ce faisant, il n'est pas nécessaire de remplir un large bassin de stockage avant que le débit ne réponde aux événements (McNamara et al., 1998). Deuxièmement, les dépressions végétalisées d'arbustes où se trouvent les *water tracks* récoltent davantage de neige que les *intertracks* (zones qui séparent les *water tracks*). Cette variation spatiale positionne ainsi la source du ruissellement plus près du canal, réduisant le temps de transit et les possibilités d'évaporation (Kane et al., 1991). L'étude des sources d'eau d'Imnavait Creek a démontré que, pendant la période de fonte des neiges, les *water tracks* transportent essentiellement de la « nouvelle » eau

provenant de la fonte, dans une proportion de 90-93% du débit total. Cette proportion est renversée lors d'événements de pluie, alors que la « vieille » eau devient le contributeur principal à l'écoulement. Ceci indique que, lors des pluies, l'eau déjà présente dans les *water tracks* est déplacée par écoulement translatoire (McNamara, Kane et Hinzman, 1997). La relation positive entre la quantité relative de « vieille » eau et la profondeur de la couche active démontre l'importance de la capacité du stockage dans les sols (Woo et Steer, 1983). Les conditions antécédentes sont de plus en plus importantes lorsque la couche active dégèle, mais le ratio d'écoulement / précipitations est généralement important lorsque les *water tracks* sont omniprésentes (McNamara et al., 1998).

Une des incertitudes face aux *water tracks* d'Imnavait est leur rôle comme distributeur ou collecteurs d'eau dans les pentes, c'est-à-dire s'il s'agit d'écoulements en perte ou en gain d'eau. Il existe des mentions de liens entre *water tracks* et drainage des sols (Chapin, Fetcher, Kielland, Everett et Linkins, 1988), mais les preuves démontrent que l'eau qui s'y écoule ne provient pas nécessairement des sols environnants. Étant donné qu'il n'est pas nécessaire de remplir le bassin de stockage dans les sols avant que l'écoulement se produise, la connectivité entre les pentes et les zones d'écoulement n'est pas nécessairement grande, et il apparait que l'eau s'écoule le long de la pente sans drainer les sols des *intertracks* (McNamara et al., 1997). L'écoulement provient alors d'une faible portion du bassin versant seulement (3% à Imnavait). L'écoulement entre les tussocks a déjà été mentionné comme source d'eau pour les *water tracks* (Hinzman et al., 1993), mais ceci impliquerait une saturation de la surface dans les *intertracks*, ce qui est contraire aux données d'humidité démontrant une forte humidité des sols uniquement dans les *water tracks* (Kane et al., 1991). Il semble que la survenance de l'écoulement entre les *tussocks* se produirait surtout lorsque la couche active est très mince, ou lors de ruissellement hortonien (Hinzman, Kane, Gieck et Everett, 1991). Ces événements créeraient de la connectivité avec le surface tôt en saison, mais les sols resteraient déconnectés plus tard dans l'été. Cette conclusion est également épaulée par la modélisation du bassin versant à l'aide de TOPMODEL, qui démontre que les sols minces des sommets et les basses terres humides sont rapidement saturées lors des événements de précipitation, mais que le reste des pentes est rarement connecté avec ces deux zones (Stieglitz

et al., 2003). Les *water tracks* agissent alors comme connecteurs entre les sommets et le fond de vallée, augmentant leur connectivité pendant que les pentes demeurent non-saturées (Figure 1.1).

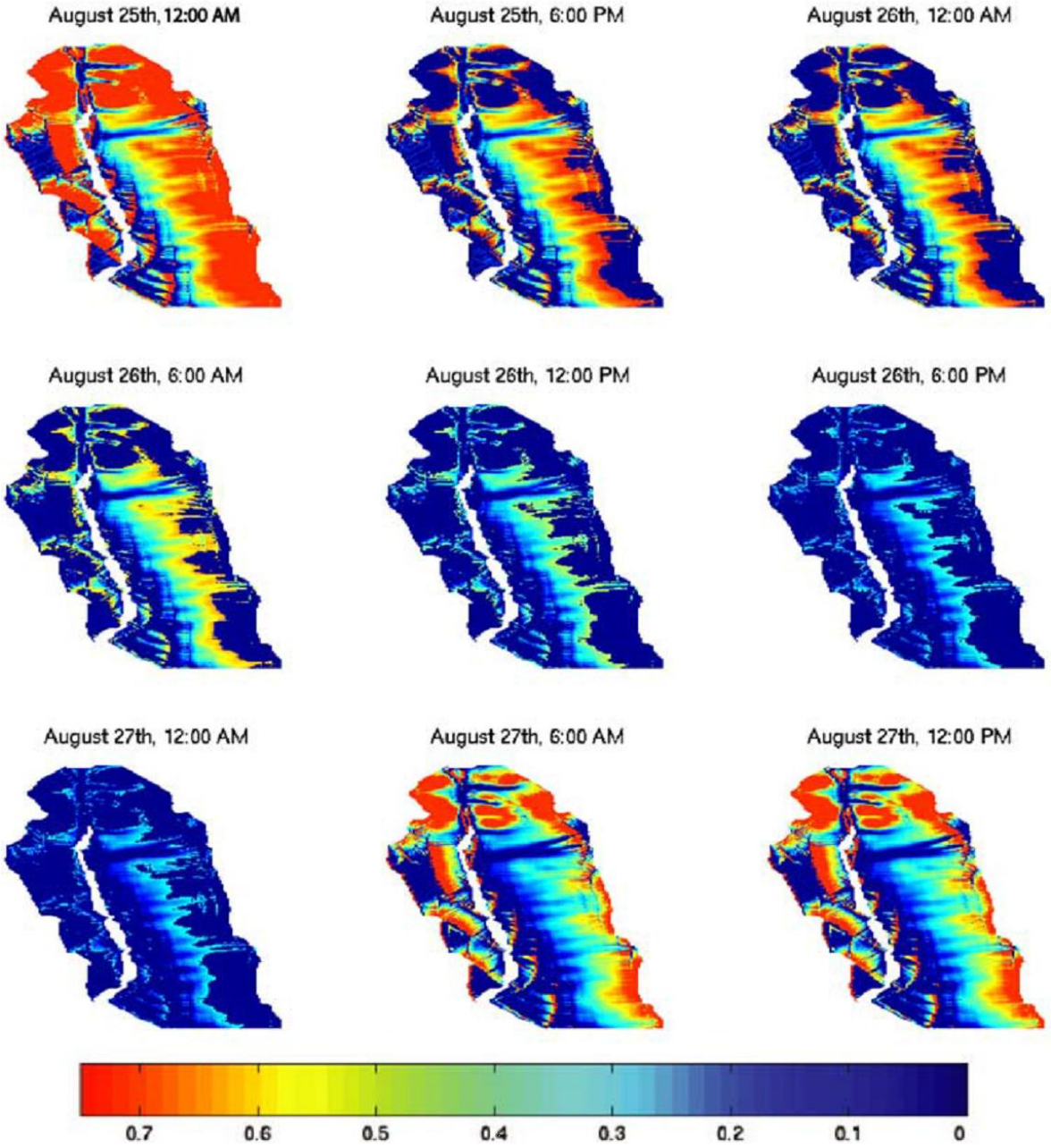

FIGURE 1.1. Résultat des simulations distribuées de TOPMODEL montrant les cartes de la profondeur de la nappe phréatique par rapport à la surface du sol, dans le bassin versant de Imnavait Creek. On y perçoit l'influence des *water tracks*, qui connectent les hauts de pente avec les bas de versant. (Stieglitz et al., 2003)

Les *water tracks* en Antarctique n'ont pas la même morphologie qu'en Alaska, et leur fonction est également différente. Elles possèdent une relation longueur / aire de drainage similaire aux ruisseaux environnants et agissent comme collecteurs pour les eaux des sols (Levy et al., 2011). Dans les vallées sèches, ce ne sont pas des contributeurs importants pour les eaux des lacs et rivières en talweg (qui sont plutôt alimentés par la fonte glaciaire), mais fournissent une source d'eau locale importante pour les écosystèmes (Ball, Barrett, Gooseff, Virginia et Wall, 2011 ; Gooseff, McKnight, Runkel et Vaughn, 2003).

1.3. Origine et rôle pour l'évolution géomorphologique

L'origine et le mode de formation des *water tracks* demeure essentiellement hypothétique à ce jour. Jorgenson, Shur et Osterkamp (2008) ont suggéré que la subsidence des sols riches en glace lors de leur dégel peut être à l'origine de la formation des dépressions formant des *water tracks*. Les échanges de chaleur convectifs lors de l'écoulement souterrain causeraient ces tassements différentiels, et ces *water tracks* seraient alors des formes de thermokarst. D'autres spéculations antérieures suggèrent que les chemins furent créés par une augmentation des écoulements, un produit de l'accumulation de glace dans la couche active suivant la végétalisation des pentes (Jorgenson, 1984). McNamara, Kane et Hinzman (1999) ont plutôt suggéré une origine fluviatile aux *water tracks*. En modélisant les paramètres du bassin versant d'Imnavait, ils ont démontré que les *water tracks* étaient situées aux endroits où des ruisseaux devraient se trouver. Ils suggèrent que ce sont des canaux immatures, dont le développement fut inhibé par le pergélisol. Dans ce cas, les *water tracks* seraient une réponse de la pente aux écoulements plutôt qu'un produit du dégel du pergélisol. Il est également possible de combiner les deux causes, car l'apparition de canaux rudimentaires aurait eu comme conséquence le dégel différentiel de la couche active sous les proto *water tracks*, dégel qui se produit toujours et qui peut excéder de 50% les valeurs des *intertracks* (Chapin et al., 1988 ; Hastings, Luchessa, Oechel et Tenhunen, 1989 ; Oberbauer, Hastings, Beyers et Oechel, 1989). Ce faisant, l'effet d'affaissement par la fonte de la glace entrainerait les

dépressions qui caractérisent les *water tracks*.

Il existe peu de savoir sur le rôle des *water tracks* dans la dynamique sédimentaire des bassins et dans l'évolution du paysage, bien que ces informations pourraient être directement liées à leur formation et à leur évolution. L'intensification d'un réseau de drainage est habituellement lié à une augmentation de la charge sédimentaire (Graf, 1977 ; Schumm et Rea, 1995), mais ce cas-ci a le potentiel de représenter une exception, car le réseau n'est pas constitué de canaux à proprement parler, et qu'il ne s'y produit pas vraiment d'écoulements en surface. La classification de Frickel, Shown et Patton (1975) dans Walling (1983) indique que les bassins versants possédant des canaux non-incisés vont généralement générer moins de sédiments. Dans un désert polaire, des rigoles non végétalisées au front de combes à neige peuvent transporter jusqu'à 120 g de sédiments par jour en charge de fond et des concentrations de plus de 1.6 g L^{-1}, tandis que celles végétalisées demeurent habituellement claires (Wilkinson et Bunting, 1975) et que les pentes végétalisées en milieu périglaciaire vont habituellement fournir moins de sédiment (Jahn, 1961 ; Strömquist, 1983). Le fait que les *water tracks* soient rarement incisées laisse croire que la quantité d'érosion et de transport qui s'y produit est plutôt faible. Par contre, le transport en solution y demeure actif, avec ou sans végétation, mais son effet sur la morphologie n'est pas pris en compte.

Étant donné le rôle que joue la végétation sur la prévention de l'érosion, on peut s'attendre à ce que les *water tracks* des déserts polaires possèdent une dynamique sédimentaire différente que celles de la toundra. En réalité, il n'existe pas d'étude sur cet aspect en désert polaire, mais certains auteurs ont noté que les *water tracks* transportaient une concentration élevée d'ions en solution (Gooseff et al., 2013 ; Levy et al., 2013 ; Levy et al., 2011). De plus, des mesures de conductivité hydraulique ont suggéré que les *water tracks* peuvent modifier leur propriété hydraulique en éliminant les sédiments fins (Schmidt et Levy, 2017). La rareté des écoulements de surface dans cet environnement pourrait y être un facteur limitant, car une grande portion de leur eau provient du dégel de la glace dans les sols (Levy et al., 2011).

La formation de ravins de thermo-érosion est sans doute l'un des rôles les plus significatifs et les plus d'actualité des *water tracks* dans l'évolution du paysage. La hausse des températures et la modification du couvert de neige ont mené à une augmentation de la formation de thermokarst dans l'Arctique (Osterkamp, 2005, 2007). Les ravins de thermokarst, ou ravins de thermo-érosion, ont récemment été liés à l'incision des *water tracks* dans le plafond riche en glace du pergélisol (Bowden et al., 2008). En 2003, l'approfondissement de la couche active ou le changement de direction d'une *water track* a mené au développement d'un tunnel de thermo-érosion et de son effondrement dans un ravins de 10 m de largeur et de 400 m de longeur. Plus de 4000 t de sédiments furent déplacés en 3 ans, soit 18 fois la quantité qui est transportée à travers la rivière Kuparuk, dont le bassin abrite le ravin (Bowden et al., 2008). Les ravins de thermo-érosion peuvent également se former de manière rétrogressive le long de *water tracks*, accumulant de la neige en hiver et modifiant le régime thermique du pergélisol (Osterkamp et al., 2009). Des décrochements de couche active ont également été signalés dans des *water tracks*, mobilisant des sédiments et des solides dissous vers le bas de pente (Kokelj, Smith et Burn, 2002). Bien que les ravins de thermo-érosion et les décrochements de couche active ne soient pas aussi gigantesques que les glissements rétrogressifs, une étude dans la région du lac Feniak en Alaska a démontré que ces petits thermokarsts sont beaucoup plus nombreux que les glissements rétrogressifs, mobilisant autant de sédiment mais affectant le double de la superficie (Balser, Gooseff, Jones et Bowden, 2009). Les *water tracks* risquent ainsi de continuer à être un élément important de modification du paysage, alors que les approfondissements de couche active se poursuivront.

1.4. CONSIDÉRATIONS ÉCOLOGIQUES

Le développement de patrons de végétation est l'un des traits les plus importants des *water tracks*. Selon Hastings et al. (1989), la production primaire dans *water tracks* serait de 40% plus élevée, avec une biomasse de 1.5 à 1.7 fois celle du reste du paysage, une affirmation par la suite démentie par Hope, Kimball et Stow (1993), qui y mesuraient plutôt une diminution de la biomasse. Dans tous les cas, la végétation y est différente, avec une augmentation des plantes

vasculaires et décidues dans les *water tracks* d'Alaska, au dépend des bryophytes du reste du paysage (Hastings et al., 1989 ; Walker, 1983 ; Walker et al., 1989). Ces sites sont également moins affectés par les sécheresses, et peuvent maintenir leurs taux de photosynthèse pendant ces périodes (Matthes-Sears, Matthes-Sears, Hastings et Oechel, 1988) et ainsi influencer les bilans de carbone à l'échelle du paysage (Curasi et al., 2016 ; Oberbauer, Tenhunen et Reynolds, 1991). En général, les *water tracks* y seraient des écosystèmes plus actifs, avec une plus forte biomasse microbienne, un meilleur index de disponibilité en carbone et un statut nutritif plus intéressant que dans les sols des *intertracks*, où la décomposition est plus lente (Cheng et al., 1998). Dans le haut Arctique, Steven et al. (2013) ont mesuré des abondances relatives différentes de bactéries dans les *water tracks* et les *intertracks*, tandis que Ball et Levy (2015) ont démontré que certaines *water tracks* en Antarctique sont simplement trop salines pour les communautés de nématodes, qui sont habituellement dominantes à Taylor Valley.

En tant que chemin d'écoulement principal sur les pentes, les *water tracks* jouent un rôle fondamental sur les transferts de matière en solution et de nutriments vers les base de pente. Levy et al. (2011) ont démontré que les *water tracks* peuvent parfois agir comme véritables convoyeurs de sels en transportant Ca^{2+}, Cl^-, Na^+, SO_4^{2-}, NO_3^- et F^- à des taux excédants de deux ordres de grandeur les taux retrouvés dans les ruisseaux des vallées sèches. Elles deviennent ainsi des chemins de lixiviation vers les bas de pente, accélérant les transferts de matière en concentrant leur écoulement. Les conditions plus anoxiques des écoulements dans les *water tracks* peuvent également empêcher la nitrification, permettant de transférer de plus grandes concentrations d'ammonium vers les bas de pente (McNamara, Kane, Hobbie et Kling, 2008). À Ward Hunt, dans le haut Arctique, les écoulements vers les bas de pentes et le lac de tête Ward Hunt se produisent surtout à travers les sols triés, répondant aux caractéristiques des *water tracks* (Vincent et al., 2011). Le lac Ward Hunt est ultra-oligotrophe, et est peuplé de tapis microbiens, dominé par les cyanobactéries, le long des berges (Villeneuve, Vincent et Komárek, 2001). Ces tapis sont particulièrement présents le long des pentes où se retrouvent les *water tracks*, et ne semblent pas affectées par le manque de nutriments dans la colonne d'eau (Bonilla, Villeneuve et Vincent, 2005). Étant donné

le lien fondamental entre la géomorphologie d'un bassin versant et les conditions limnologiques dans un lac (Quesada et al., 2006), il est fort probable que les *water tracks* aient un effet positif sur l'établissement de ces organismes benthiques.

Chapitre 2

WATER TRACKS IN THE HIGH ARCTIC : A HYDROLOGICAL NETWORK DOMINATED BY RAPID SUBSURFACE FLOW THROUGH PATTERNED GROUND

Abstract

Water tracks play a major role in the headwater basin hydrology of permafrost landscapes in Alaska and Antarctica, but less is known about these features in the High Arctic. We examined the physical and hydrological properties of water tracks on Ward Hunt Island, a polar desert site in the Canadian High Arctic, to evaluate their formation process and to compare with water tracks reported elsewhere. These High Arctic water tracks flowed through soils that possessed higher near-surface organic carbon concentrations, higher water content, and coarser material than the surrounding soils. The water track morphology suggested they were initiated by a combination of sorting, differential frost heaving, and eluviation. The resultant network of soil conduits, comparable to soil pipes, dominated the hydrology of the slope. The flow of cold water through these conduits slowed down the progression of the thawing front during summer, making the active layer consistently shallower relative to adjacent soils. Water tracks on Ward Hunt Island, and in polar desert catchments with these features elsewhere in the High Arctic, strongly influence

Paquette, M., Fortier, D. et Vincent, W. F. (2017). Water tracks in the High Arctic: a hydrological network dominated by rapid subsurface flow through patterned ground. *Arctic Science, 3*(2), 334-353. doi: 10.1139/as-2016-0014

slope hydrology and active layer properties while also affecting vegetation distribution and the quality of runoff to the downstream lake.

2.1. INTRODUCTION

Water tracks are widespread features of high-latitude watersheds (Kane et al. 1991). As preferential subsurface flow paths, they are often the only surface indicators of drainage patterns on non incised permafrost slopes, yet the periglacial literature makes little mention of water tracks as an important feature of high-latitude landscapes. The term itself is relatively recent and is not defined in permafrost glossaries (Harris et al., 1988, Van Everdingen, 2005). Overall, there is no consensus on the specific characteristics of this landform feature, and authors have adapted their definition according to their specific research interest or study site (Walker et al., 1982, Chapin et al., 1988, Kane et al., 1991, Hinzman et al., 1993, McNamara et al., 1998, Stieglitz et al., 2003, Jorgenson et al., 2008, Levy et al., 2011). An encompassing definition is provided by Gooseff et al. (2013) who defined water tracks as a regional feature of permafrost areas, forming "narrow bands of high soil moisture that route water downslope, in the absence of overland flow, through permafrost dominated soils in polar regions".

Water tracks in periglacial regions have been the subject of research in two contrasting polar environments: the foothills of the Brooks Range, northern Alaska, and the Taylor Valley, Antarctica. The Brooks Range Arctic tundra water tracks are broad, highly vegetated hillslope depressions fed by a mix of snowmelt and rainfall, while the water tracks in Antarctica are narrower and located on polar desert soils, devoid of vegetation and of organic matter accumulation (Levy et al., 2011, Chapin et al., 1988). Mainly by comparison with intertracks (areas between water tracks), studies have shown that water tracks have multiple physical, chemical, and biological effects on landscape slope properties. In Alaska, primary production was 40% higher in water tracks than in intertrack soils (Hastings et al., 1989). The superior soil moisture conditions in water tracks reduced water stress on plants, allowing higher photosynthetic rates during periods of

drought (Matthes-Sears et al., 1988) and influencing CO2 efflux in late summer (Oberbauer et al., 1991). Nutrient supplies may increase in water tracks (Cheng et al., 1998), partly as a result of the deeper active layer beneath them (Oberbauer et al., 1989, Gooseff et al., 2013). Vegetation, microfauna, and bacterial assemblages are also modified by the presence of water tracks (Walker, 1983, Walker et al., 1989, Steven et al., 2013, Levy et al., 2013). The greatest effect of water tracks is on the hydrology of their watersheds, where they decrease the delivery time and increase the outflow response of catchment basins (Kane et al., 1991). They achieve this by remaining at levels close to soil water saturation and by acting as potential contributing areas that extend considerable distances upslope; this reduces the need for basin storage pools to fill up before initiating their input to storm runoff events (McNamara et al., 1998).

The studies in Alaska and Antarctica showed pronounced contrasts in morphologies and other physical properties of the water tracks between the two sites, underscoring the need for wider geographical coverage to understand the full diversity of these features. In the present study, we focused on water tracks in the High Arctic to determine their morphological and flow characteristics in a polar desert landscape. We undertook this study on Ward Hunt Island at the northern limit of the Canadian Arctic Archipelago, which is a slightly wetter polar desert landscape than in the McMurdo Dry Valleys of Antarctica but that still sits far from the widespread vegetation cover of Arctic tundra water tracks. The aims of our study were to identify the geomorphological context and properties of water tracks and the role of these features in slope hydrology.

2.2. METHODS

2.2.1. Study site

Ward Hunt Island (83.08°N, 74.14°W) is located 6 km off the north coast of Ellesmere Island near the northern limit of the Canadian High Arctic (Fig. 2.1). A description of the physiography, geomorphology, and ecology of the island and the surrounding areas is given in Vincent et al. (2011). Our study focused on the slopes of Ward Hunt Lake watershed, a headwater catchment

of 1.82 km^2 feeding the 0.35 km^2 lake, which is located 26 m above sea level (a.s.l.). The lake drains to the south and its watershed is delineated by a beach ridge to the north (40 m a.s.l.) and by two hills to the east (Ward Hunt Hills, unofficial name; 165 and 245 m a.s.l.) and one to the west (Walker Hill, 436 m a.s.l.). The geology of the island includes mostly limestone to the west (Walker Hill) and some igneous and volcanic rocks to the east (Trettin, 1991). Surficial deposits on the island are a mix of glacial drift and gelifracted parental material that probably pre-date the last glacial maximum (Lemmen, 1988), along with some sandy gravel beaches below the Holocene marine limit. The mean annual air temperature is -17.9 °C (1995-2015), with average air temperature of -33.4 °C in February and 1.5 °C in July (CEN, 2016). The freeze-thaw regime at this location is sensitive to slight changes in temperatures, and year-to-year variation can cause a threefold increase in the number of thawing degree-days as measured by air temperatures (Paquette et al., 2015). Hourly snowmelt was measured using a Sonic SR50 sensor connected to a CR10X data logger (Campbell Scientific, Edmonton, Alberta) and precipitation was measured using a metric rain gauge read twice a day (0700 and 1900 local time zone). Total precipitation has not been measured but is likely to be slightly lower than the average of 158 mm $year^{-1}$ measured at Alert, located 170 km to the south east (Environment Canada, 2016), as rainfall events are rarer. The study site is an eastward-facing slope located at the base of Walker Hill; water tracks are the final component of a succession of coarse gelifracts (angular rock fragments produced by frost action), nivation hollows (depressions created by snowpatch erosion), and solifluction landforms (produced by the downslope deformation of saturated or thawing soils) down the slope.

2.2.2. Morphology and soil properties of water tracks

Water tracks on Ward Hunt Island most commonly take the form of regularly spaced, linear vegetated depressions similar to non-sorted stripes. They expand upslope into a network of elongated patterned ground (polygons and stripes) that becomes increasingly bare farther up the slope. In a few cases, water tracks seep to the surface as return flow and become rills. In order to cover the widest range of conditions, measurements were performed at multiple sites in contrasting morphologies. General slope topography and profiles were first measured using a GNSS station

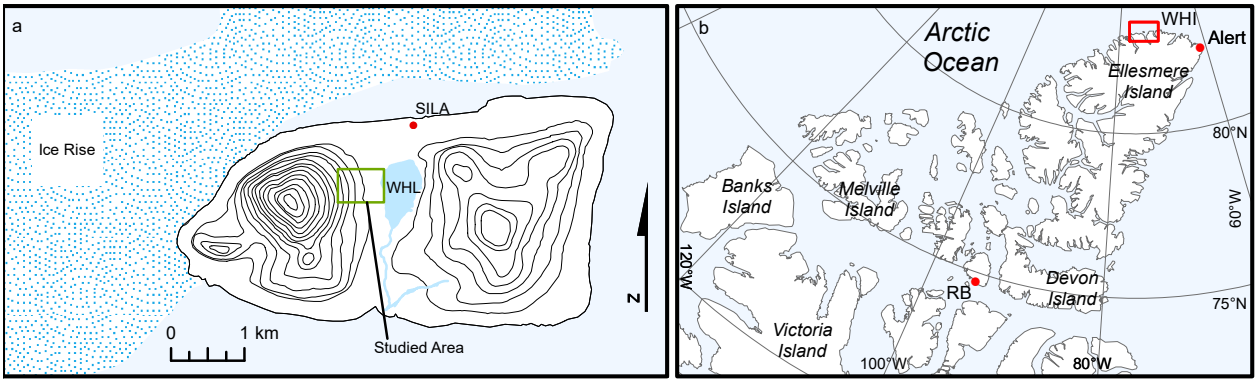

Figure 2.1. Topographic map of Ward Hunt Island (a) and location at the northern tip of the Queen Elizabeth Islands (b). Isolines are 30 m apart. RB: Resolute Bay; SILA: Weather station; WHI: Ward Hunt Island; WHL: Ward Hunt Lake.

and a VX station (Trimble, Sunnyvale, California), geo-positioned by a survey-quality geodesic point (x, y, z precision of 5, 5, and 18 mm). Microtopographic profiles transverse to the water tracks were measured at six locations along the slope using a clinometer (1° precision) and measuring tape. A point-transect survey of vegetation was conducted along a 100 m transect (10 cm intervals), perpendicular to the water tracks, 20 m up from (and parallel to) the edge of the lake. To describe the fine-scale morphology of the soil, five soil pits were excavated in contrasting positions across the sorting pattern and water tracks. Pit Sp-1 was in the vegetated water track near the lakeshore, pits Sp-2 and Sp-3 were in the patterned ground network, with Sp-2 slightly upslope, in a mostly bare section of the network, and pit Sp-4 was under a seeping stream emerging from a water track. A final pit, "Backslope", was also dug upslope from the patterned ground area of Sp-2 and Sp-3, outside the water track network, where a small snowdrift laid until mid summer. All pits were along a transect perpendicular to the slope, covering both a water track and an intertrack and down to the frost table. Identification and delimitation of organic matter, soil morphology, and gravel concentrations were performed in the field. Each profile was photographed and then its morphology was digitized over a mosaic of the pictures. Sediments were sampled using a 250 cm^3 sampling ring in Sp-1, allowing the measurement of volumetric soil parameters, but the high gravel concentration in other pits prevented the use of the rings, and grab samples were collected instead.

A total of 17 pairs of water tracks and intertracks were probed for active layer depth (depth to refusal) using a manual earth auger. Triplicate measurements were performed each time. In addition to samples from the soil pits, soil from these pairs was sampled at the surface (0-5 cm depth) and subsurface (5-10 cm depth) by grab sampling. Each sample collected in the field was analyzed for water content by oven drying at 105 °C until stable mass was reached. The samples were then crushed and dry sieved for grain size analysis, following a modified ASTM D6913 standard to include subsampling. Fractions of the sediments <2 mm were subsampled and were processed by lost on ignition for organic matter and carbonate content (Dean Jr, 1974, Heiri et al., 2001). Electrical conductivity and pH measurements were also conducted in the laboratory using a 2:1 water to sediment ratio for mineral soils and 5:1 ratio for organic-rich soils.

2.2.3. Water track hydrology

The flow and hydraulic conductivity characteristics of the water tracks were determined with in situ monitoring, point measurements, and laboratory tests. The hydrological regime of water tracks was compared to that of a rill located 20 m from a multi annual snowdrift in order to evaluate its similarity with an open channel flow regime. A cut-throat flume (length, width, and throat width of 91, 26 and 5.25 cm, respectively) was installed in the seeping area just downslope of a water track, and a second one was installed in the rill. The flumes were secured by excavation and fitting them into the soil so that no water flowed underneath them. They were each equipped with a Hobo U20 pressure sensor (accuracy of ±0.14 cm) (Onset, Bourne, Massachusetts) to measure water levels (h_u, cm), which were converted to free flow discharge (Q_f, $cm^3\ s^{-1}$) with the equation

$$Q_f = K_f\ C_f\ h_u^{n_f} \tag{2.1}$$

where K_f is a free flow correction factor calculated from the specific dimensions of the flume, C_f is the free flow coefficient, and n_f is the free flow exponent, both of which can be extracted from tables according to flume standard dimensions (Siddiqui et al., 1996). These measurements

were performed for 30 days in 2013, covering the early melt season until after peak discharge.

Hydraulic conductivity of the soil as well as flow velocity in vegetated water tracks were also evaluated in 2014 for comparison. Four flow velocity tests were performed using a salt tracer and a conductivity probe, using the slug centroid method described in Whiting (2005). To measure hydraulic conductivity (k_s) of the sediments, undisturbed material in the first 15 cm of soil in the water tracks and intertracks was sampled by inserting 250 cm^3 sampling rings horizontally; the samples were then analyzed using a KSAT apparatus (UMS, München, Germany) and a laboratory permeameter. Hydraulic conductivity tests in the field usually measure downward conductivity of the soil material, but by inserting the sampling rings horizontally in the soil, these tests provided the downslope hydraulic conductivity, in the direction of water flow.

All statistical analyses were performed using R 3.1.1 (R Core Team, 2014). Paired t-tests with 95% interval of confidence were used when comparing specific water tracks with their intertracks, while unpaired t-tests were performed when comparing undifferentiated sets of measurements. The Shapiro-Wilkes test was used to verify normality of distribution or of paired differences, and if the data failed to pass this test even after transformation, the non parametric Wilcoxon test was used to evaluate differences.

2.3. RESULTS

2.3.1. General slope morphology

Below its rounded top, the eastern slope of Walker Hill could be differentiated into three sections with distinct geomorphic features. The upper section (>150 m a.s.l.) was characterized as a steep, 22.5°-29.5° angled slope covered with coarse glacial debris and gelifracts. This section showed little slope variation except for the occasional poorly developed nivation niches and also contained isolated fractured bedrock exposures. The middle section (150-65 m a.s.l.) had a concave morphology, with slopes irregularly decreasing downslope from 21.6° to 11°. Its uneven topography retained multiple annual and semi permanent snowdrifts. The latter had the typical

characteristics of well-developed nivation hollows: coarse and bouldery backslopes followed by a small field of sorted material often overlain by snow and solifluction lobes a few tens of metres downslope of the snowdrifts. These snowdrifts (>1 m depth) were usually the only remaining snow patches a few days after snowmelt had begun and were likely to be the main contributors of freshwater to Ward Hunt Lake (Paquette et al., 2015). This section of the slope was also mainly covered by coarse glacial debris and gelifracted colluviums, but without clear bedrock exposures. The third, lowermost section was demarcated by the upper limit of the toe of the slope (65-26 m a.s.l.) corresponding to around the upper limit of the marine transgression for the sector ($\geq$ 62 m a.s.l.) (Lemmen, 1988). This lower section contained the patterned ground formations and water tracks observed in the present study (Fig. 2.2a). It had low, steady angles between 3.5° and 9.7° and was covered with muddy gravel and sand. Snowdrifts in this section were sparse, <70 cm deep, and usually underlain by coarser material than the rest of the slope toe.

2.3.2. Water track physical characteristics

The water tracks stretched from 20 m to nearly 100 m long, with their length increasing toward the northern edge of their zone of occurrence. They were readily discernable from the rest of the soil because of their organic cover, which contrasted with the dominantly bare or darkened appearance of the intertrack soil (Fig. 2.2c). The survey of vegetation showed that the water tracks, as demarcated by thick moss-coated ground, covered 19.8% of the surface of the slope near the lake. The rest of the slope section was mostly dominated by black cryptogamic crust (61.5% of total cover), with rocks (5.3%), white crusts (3.4%), *Saxifraga oppositifolia* L. (2.9%), or bare ground (2.7%) as other recurrent types of soil surface. The spacing between the moss-covered water tracks averaged (±SD) 1.5 (±0.9) m along the transect. Whenever water tracks ended with a seeping section, the above ground water flowed along a rill containing pink and orange cyanobacterial mats, mosses, *Phippsia algida* (Sol.) R. Br., gravel, and cobbles (Fig. 2.2d). These seeping rills were short, and the water usually dissipated into the ground within <50 m. Other water tracks terminated by discharge into the lake, and some could be seen extending across the

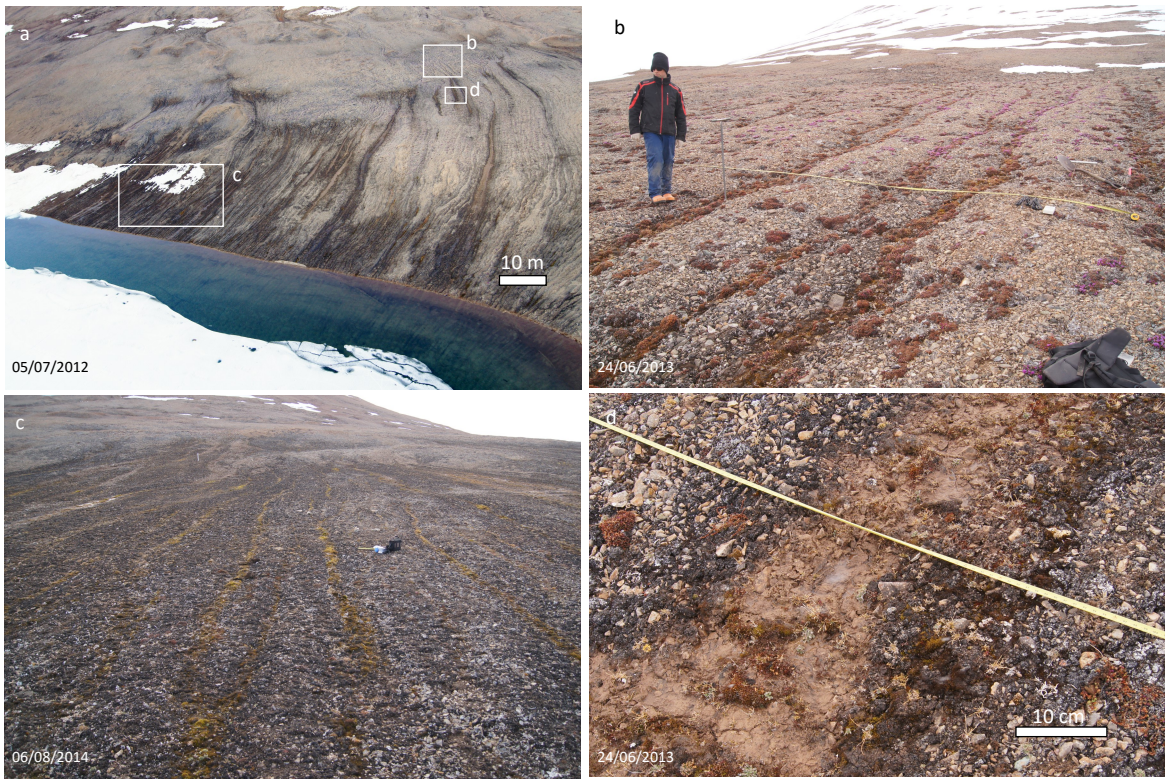

Figure 2.2. Photographs of water tracks and intertracks. a) Lower slope of Walker Hill and water tracks flowing and extending into Ward Hunt Lake; b) Transect F-F', located 9m downslope of Sp-3. The transition between sorted nets and non-sorted stripes are covered with *S. oppositifolia*. Note the bare soil instead of black crusts in the intertracks; c) Sp-1 site, near the edge of the lake. The contrast between the moss cover on the linear water tracks and black crust on the intertracks makes the features stand out. The bag on the picture is 30 cm wide; d) Location of Sp-4 and of transect G-G', where cyanobacterial mats covered a seepage (dry at the time of the photograph) streambed downslope of a water track, as opposed to the black crust on the edges and on the intertracks.

lake bed of the littoral zone, possibly reflecting periods of lower lake levels (Fig. 2.2a).

The mapping of a patterned ground network and the measurements of micro topographic transects showed the organization of the water tracks and their changes down the slope (Fig. 2.3). The network began at the upper part of the lower slope section, with sorted, elongated patterned ground. This section had irregular micro topography (transects D-D' and E-E'), where the depressions were occupied by clean gravel and cobbles, while the highest sections possessed a sandy and muddy matrix. Downhill from this area, the nets and polygons stretched and merged into stripes. The depressions in the patterned ground (transect F-F') were covered with *S. oppositifolia* and mosses, indicating near-surface water availability. As the stripes coalesced,

seepage occurred and the micro topography was progressively gentler (transects G-G' to I-I'), ending the striped pattern.

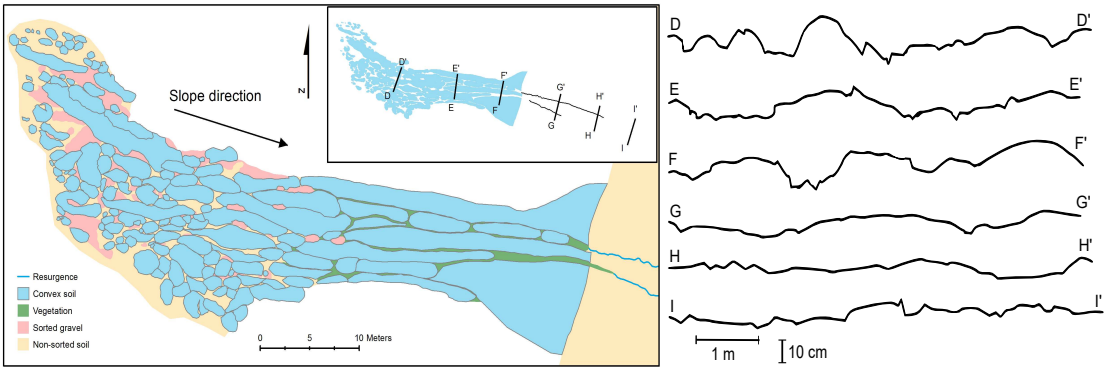

Figure 2.3. a) Map of sorted nets and stripes network with locations of soil pits and of micro-topographic profiles (insert). The extent of the mapped features corresponds to the "divide" of the network to the north and south and to a coarse backslope deposit to the west; b) Micro-topographic profiles with a 3.5:1 vertical exaggeration. The micro-topography gradually becomes less pronounced downslope, and no trace of a pattern is visible in H-H' and I-I'.

The physical characteristics of the moss-covered water tracks, 20 m from the edge of the lake, are summarized in Table 2. I. One conspicuous feature was a 10.2 ± 4.8 cm thick washed-out gravel layer of mean grain size 12.7 mm and with less than 5% sand content (mostly coarse) immediately beneath the wedge-shaped moss cover. Lifting up the moss cover revealed that this gravel layer, at the interface of the organic and mineral layer, contained free-flowing water. The intertracks were on average 4.5 cm (±3.1) (maximum = 10 cm) higher than the water tracks.

Table 2. I. Morphological characteristics of water tracks on Ward Hunt Island.

Characteristic	Width or depth (cm)			
	Mean ± SD	Min	Max	n
Width	29.7 ± 9.9	14.0	55	17
Organic matter thickness	6.2 ± 2.8	2.0	17	17
Gravel layer thickness	10.2 ± 4.8	0.0	>30	18
Active layer depth (2014)	48.9 ± 7.1	32.0	61.5	17

The soil properties across the water tracks and intertracks are given in Table 2. II. The most striking difference was in organic matter content, which was significantly higher in the first 5 cm

Table 2. II. Physical and chemical properties of water track and intertrack substrates at two

Properties	Water track		Intertrack		t-test	
	0-5 cm	5-10 cm	0-5 cm	5-10 cm	0-5 cm	5-10 cm
O.M. (% dry weight)	26.4 ± 3.2	8.3 ± 0.6	9.0 ± 1.2	4.4 ± 0.2	WT***	WT***
Carbonate (% dry weight)	3.9 ± 0.5	6.6 ± 0.6	7.9 ± 0.4	8.0 ± 0.4	IT***	IT*
SpC (µS cm^{-1})	611.5 ± 38.9	374.5 ± 29.0	487.2 ± 52.1	210.1 ± 11.7	WT	WT***
pH	7.42 ± 0.06	7.86 ± 0.05	7.76 ± 0.06	8.11 ± 0.03	IT***	IT***
G.W.C. (%)[1]	159.3 ± 30.8	33.8 ± 7.1	19.3 ± 1.5	17.8 ± 3.6	WT***	WT***
Mean particle size (mm)[1]	1.9 ± 0.5	4.0 ± 1.0	3.8 ± 0.4	1.7 ± 0.2	IT**	WT*

O.M.: organic matter; SpC: specific electrical conductivity; G.W.C.: Gravimetric water content; [1] Wilcoxon test for non-normal data; WT: Water track value is greater; IT: Intertrack value is greater; *significance of the p-value: * p <0.05, ** p <0.01, *** p <0.001. All ± values are standard errors.

of the water track soils than in the intertrack, reaching 26.4% ± 3.2% compared to 9.0% ± 1.2% (t = 5.4) ($p < 0.001$, n = 17). This difference was also observed at 5-10 cm depth, where the organic matter was twice as high in the water tracks compared to the intertracks. The water content was also much higher (factor of 8.3, W = 264, $p < 0.001$) in the water tracks than in the intertracks in the upper 5 cm of the profile, while the difference at 5-10 cm depth was less pronounced (1.9 times higher) but still highly significant (W = 255, $p < 0.001$). Grain-size analysis at these depths revealed a clear difference between the two locations. In the water tracks, the top 5 cm layer of the soil was almost equally composed of gravel and sand (43% and 47% of the sample weight, respectively) mixed with organic matter. It was underlain by the gravel layer noted above but also included some sand and organic matter in the 5-10 cm sample. In contrast, the intertracks were always dominated by gravel, and their surfaces contained the highest concentration of gravel: 67.8% versus 52.7% in the 5-10 cm range (W = 280, $p < 0.001$). There were also more fines in the 5-10 cm depth of the intertrack sections than in other locations or depths sampled (15.0% versus $\leq$ 10.0% elsewhere).

The active layer depths for water tracks and their intertracks in 2014, immediately prior to freeze-back, are shown in Fig. 2.4. The active layer was significantly deeper (W = 268.5, $p < 0.001$) in the intertracks, on average by 7.5 cm. This difference was consistent, except for a small number of measurements where local conditions, such as the presence of rocks, may have affected the measurements. The difference was smaller but still significant (t = 3.4, $p < 0.01$) after

correcting for micro topographic differences between the water track and intertrack in order to put all measurements on the same datum: this adjusted active layer depth beneath the water tracks was on average 2.5 cm (4.6%) shallower relative to adjacent soils.

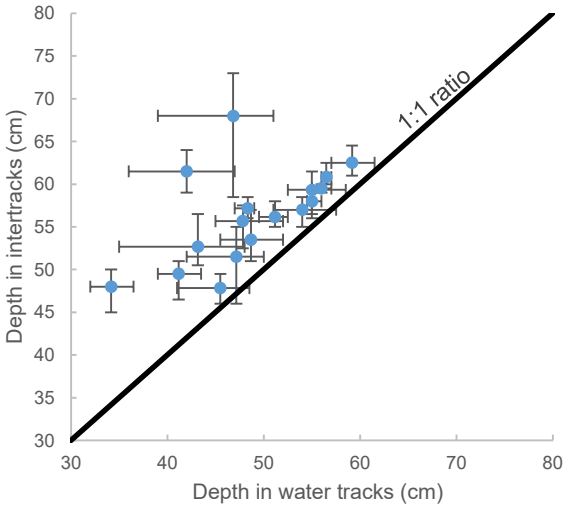

Figure 2.4. a) Active layer depth measurements in water tracks and their intertrack. Dots are the mean of triplicate measurements while bars represent minimum and maximum values.

2.3.3. Subsurface morphology

In soil pits Sp-1 to Sp-4 (locations in Figs 2.2 and 2.3), the intertracks had a coarse surface layer, along with varying proportions of biological soil crust and bare ground. The other intertrack profiles showed no obvious structure, with the soil always composed of a gravelly, angular diamict. In contrast, the water track sections of the soil all had distinct morphologies that differed from one soil pit to the next. In Sp-1, the vegetated water track contained a wedge of fibrous organic matter associated with the moss cover and mixing with the diamict to form a gravelly, organic-rich soil (Fig. 2.5). On each side of the wedge, a zone of washed-out gravel marked the transition between the organic cover and the rest of the soil, and their dimensions indicated the maximum area available for free water flow. The section shown in Fig. 2.5b was located just below the organic cover and had a rectangular shape 9.5 cm wide and 3.5 cm high, while that in Fig. 2.5c followed the right edge of the wedge of organic matter, measuring 13.5 and 4 cm in its long and short axis, respectively. Summer was almost at an end at the time of the excavation of the pit (8

August 2014), which was performed around 2200 when discharge was near its lowest daily rates. Even under those conditions, seepage was observed at the base of the gravel zone (Fig. 2.5c), with evidence of wetting throughout the rest of the soil profile downward.

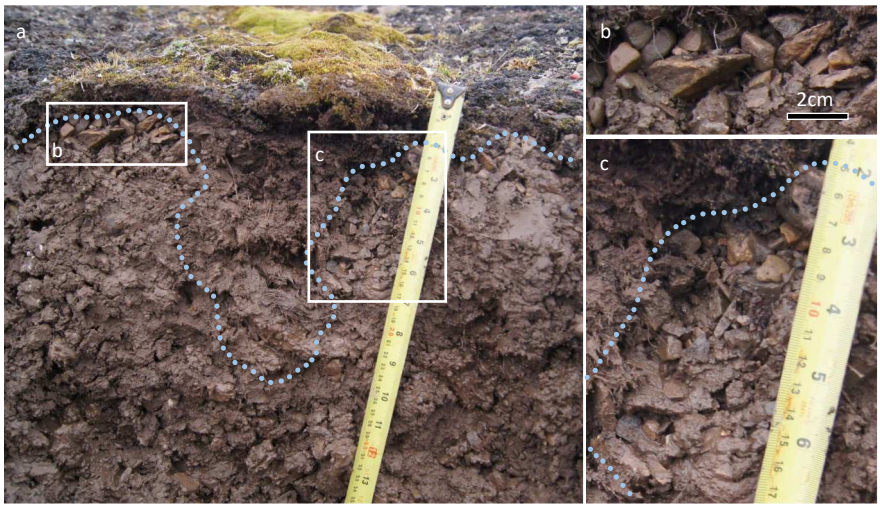

Figure 2.5. Soil structure at Sp-1. The blue dotted line marks the separation between the wedge of fibrous organic matter and the mineral soil. Rectangles are locations of clean, washed-out gravel concentration on each side of the wedge and are magnified in b and c.

The physical structure of Sp-2 and Sp-3 is given in Fig. 2.6. In Sp-2, the washed-out gravelly section was much greater than in other pits and had the form of an inverted wedge, with a width of 15 cm at the surface and 62 cm at the thaw front. The configuration of the active layer ranged from 30.5 cm at its minimum to 56 cm, as shown on the left side of Fig. 2.6. These properties might have been expected to favor water flow laterally from the gravel section toward the intertrack following the steepest micro topography. Instead, however, water was seen flowing at the bottom of the active layer in the coarse section only. Sp-3 covered two water tracks instead of one and showed two wedge-shaped gravel concentrations just beneath the vegetation wedges of the water tracks. Once again, the thaw front was shallower underneath the water tracks. Sp-4 and Backslope are not shown because their profiles were realtively uniform: Sp-4 showed a coarse diamict throughout the profile, while the first 25 cm of Backslope (the entire thawed region) was composed of washed-out gravel and stones.

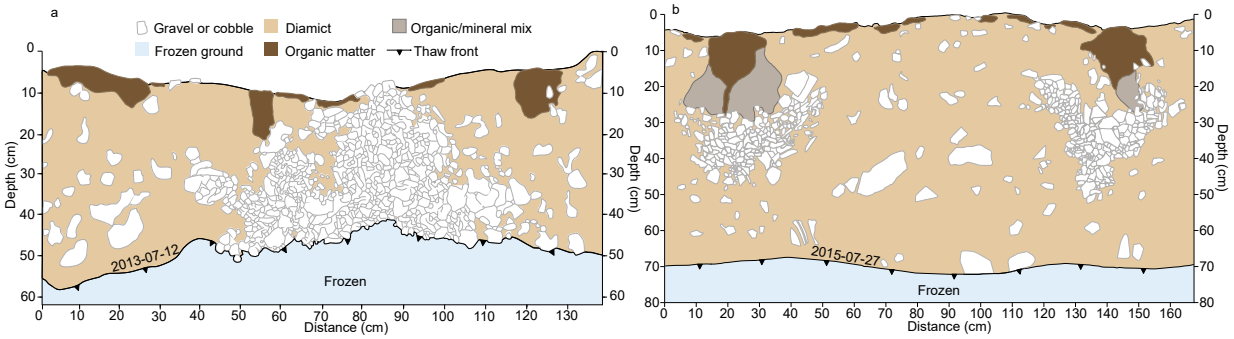

Figure 2.6. Soil structure at sites Sp-2 (a) and Sp-3 (b). Vertical axes begin at the highest point of the soil.

Soil properties of the sampling pits are given in Fig. 2.7. Compared to the adjacent intertrack, the water track of Sp-1 had higher organic matter and water content throughout its profile, along with higher mean particle size and specific conductance and lower bulk density and pH. However, there were large variations in these soil properties, particularly near the surface, and overall, there were no significant differences between the intertrack and water track locations. In Sp-3, the mean particle size showed a large increase between approximately 25 and 50 cm in the water track. The organic matter content was also larger at the top and at 15 cm depth in the water track than it was in the intertrack, and this in turn was reflected in the higher water content of the soil.

Backslope properties show the dominance of clean, washed-out gravel in the soil profile. The sample taken just below the thaw front of at the Backslope site showed higher fine sediment content, with little organic matter. This sample also had the highest carbonate content, likely caused by the absence of wash in the frozen ground. Sp-4 also showed distinct profile properties, with grain size increasing with depth, while water content and organic matter content diminished. The 45 cm depth marked a sharp change in all variables, with the percentage of organic, fine, and sandy material as well as the SpC all dropping, while pH, gravel content, and carbonate concentrations increased.

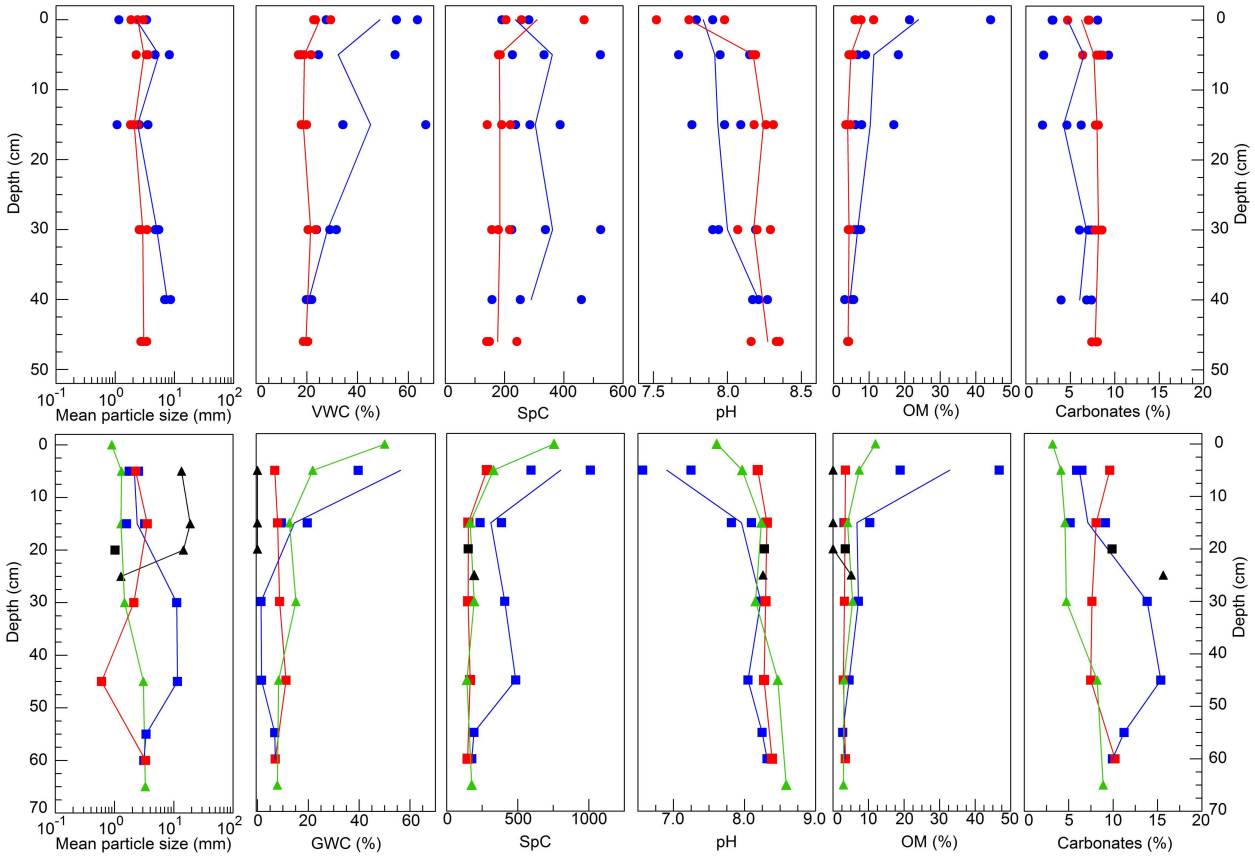

Figure 2.7. Soil properties of soil pits. Points are individual samples and lines connect the means at each depth. Blue circles: Sp-1 water track; red circles: Sp-1 intertrack; black square: Sp-2 intertrack; blue squares: Sp-3 water track; red square: Sp-3 intertrack; green triangles: Sp-4; black triangles: Backslope site; VWC: Volumetric water content; GWV: Gravimetric water content; SpC: Specific conductivity (µS cm^{-1}); OM: organic matter content (% of dry weight of sediments < 2 mm).

2.3.4. Hydrology

Water flowed below the surface in the water track sections of the slope, while at another sites on the slope, several hundred metres to the south, the water flowed at the surface in distinct rills that extended from a perennial snowdrift. Fig. 2.8 shows the discharge measurements in a water track and one of these rills in 2013, along with snowmelt and air temperature data from the weather station. The onset of snowmelt and flow was late during the 2013 summer, reflecting the cold air temperatures (Paquette et al., 2015). While the rill registered greater discharge than the water track, both exhibited a strong diurnal variation. Peak flows were attained around the same time in late afternoon in both sites, between 1500 and 1700, while low flows were usually between 0100 and 0700 in the rill and between 0300 and 0800 in the water track. Maximum discharges

were recorded in both flow paths on 17 July, at midnight in the rill and at 0100 in the water track, as part of a discharge event that had begun during the afternoon of 16 July. This event lasted longer in the rill than in the water track, and was followed by a return to flows similar to previous conditions after 19 July.

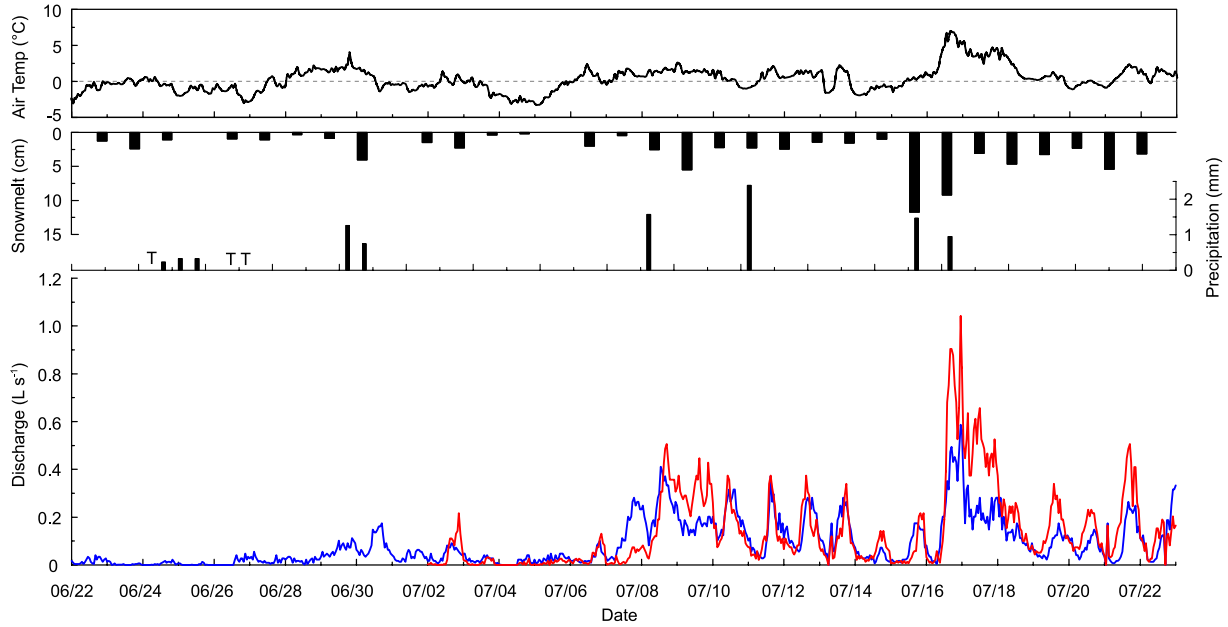

Figure 2.8. Air temperature, daily snowmelt (snow thickness), precipitation (T for trace) and discharge in a rill (red line) and in a seep fed by a water track (blue line) in 2013. Discharge rates responded rapidly to snowmelt, with almost no delay between the water track and the rill.

The samples taken at the junction of the gravel and organic layer in the water track had the highest hydraulic conductivity, with values that were an order of magnitude higher than in the organic material (Table 2. III). By comparison, the diamict had a low hydraulic conductivity, seven orders of magnitude less than in the subsurface flow path. This low value was mostly due to the low porosity typical of gravel-fine mixtures (Dunn and Mehuys, 1984). Our tracer velocity tests indicated a flow speed that was two times higher than that measured in the laboratory, with values that range within the theoretical conductivity of gravel-dominated layers (Fetter, 2001).

Table 2. III. Hydraulic properties of a water track and intertrack. ks is the saturated hydraulic conductivity, with standard deviation in brackets. The first two samples were measured with the ksat device, the third was measured with a permeameter, and the fourth was based on tracer tests. WT: water track; IT: intertrack.

Location, type	k_s		Bulk density	Porosity
	(m d^{-1})	(cm s^{-1})	(g cm^{-3})	(%)
WT, semi-organic	2.4 (0.62) x 10^2	2.7 (0.07) x 10^{-1}	1.29	37.9
WT, organic	4.0 (0.44) x 10^1	4.6 (0.5) x 10^{-2}	0.64	54.6
IT, diamict	2.4 (1.3) x 10^{-5}	2.7 (1.5) x 10^{-8}	1.95	25.4
WT, vegetated	5.3 (1.4) x 10^2	6.1 (1.6) x 10^{-1}	N/A	N/A

2.4. DISCUSSION

2.4.1. Formation of the water tracks and significance for slope hydrology

Linear water tracks are an important feature of the Ward Hunt Lake watershed. These landscape features correspond to the definition of non-sorted stripes (Washburn 1956), a patterned ground with regular spacing, downslope orientation, and a vegetation cover that contrasts with the relatively bare ground of the intertracks. The wedge shape of the vegetation, their width, and the concentration of stones at the surface of the soil were all consistent with this description. Upslope from these non-sorted stripes, however, the network of gravel and vegetation patches between elevated grounds was more of a hybrid between sorted (segregation of coarse and fine sediments) and non-sorted stripes.

In patterned ground, the shape of the pattern is generally affected by the slope gradient and the availability of fines (Washburn, 1979). The patterns at the upper end of the water track network corresponded to a series of debris islands followed by circles or polygons, nets, and finally stripes that form the logical succession of patterned ground along an increasing slope. In this case, however, the slope did not increase along the succession; instead, it decreased from values between 5° and 17° to more steady values between 3.6° and 9.3°. The reason why the patterned grounds were better developed and became elongated downslope is still uncertain, but our observations suggest two potential reasons: a downslope decrease in winnowing and the existence of a gradient

of sorting potential in the material.

The first reason, decreased winnowing, relates to soil morphology and to the organization of the hydrological network. As the inverse wedge shape of the gravel layer in Sp-2 and the complete absence of fine particles in the active layer at the Backslope site suggest, leaching of fine sediments likely accounted for most of the concentration of gravel, with this process enlarging the wedge as the thaw front progressed in spring. Sp-2 and Sp-3 exhibited a clear separation between the washed-out, coarse sections of the patterned ground and the finer grained areas in between. This distribution of sediments, with their contrasting hydraulic conductivity, indicated the preferential flow in the coarse section, as observed. The presence of a binding organic layer at Sp-3 and the slightly lower slope at Sp-1, decreasing velocities in this water track, could account for the differences between the structures of both water tracks. The network formed in the upslope part of the network as shown in Fig. 3 also likely played a role channeling water toward the vegetated water tracks. In a classic study of sorted stripes, Caine (1963) observed that most of the drainage along a network of patterned ground occurred in the coarse section of the stripes, eluviating fine material along the process. Horwath et al. (2008) also hypothesized that the coarse sandy and loamy gravel accumulation observed along vegetation and sand wedges at their site favored slope drainage but did not mention winnowing as part of the formation process. The erosion of soil particles is likely favored by decreased sediment cohesion following freeze-thaw (Dagesse, 2013) or by localized high velocities caused by factors such as a steeper local hydraulic head, turbulent flow through gravel layers, or interception of the thaw front with ice lenses (Dyke and Egginton, 1988). These particles may then be transported through the network until the emergence of the water track as overland flow. Leaching of fines from gravel-rich slopes is known to occur in polar deserts (Woo and Xia, 1995), and evidence from Antarctica suggests that water tracks can create favorable flow conditions when sufficient flow velocities are reached, through either large enough hydraulic gradients or high conductivities (Schmidt and Levy, 2017). At that point on the slope, the surface flow becomes a losing stream, dissipating water into the surrounding soils and depositing the suspended sediments along the slope. This deposition process could explain the

absence of sorting in Sp-4 as well as the increasing amounts of fines and the decreasing amount of carbonates towards the soil surface. Similar stratigraphic evidence was found where surface runoff and seepage occurs (Woo and Steer, 1986, Woo and Xia, 1995) and has also been reported at another site on Ward Hunt Island (Verpaelst et al., 2017).

The second reason explaining the shape of the pattern ground is the gradient of sorting potential in the slope caused by changes in soil material, where the coarser deposits in the upslope section would be less easily sorted than the finer material downslope. Continuous eluviation (removal of material by running water) of fines at the Backslope site along with irregular slope angles would have prevented the formation of continuous and regular elongated polygons and stripes by removing the frost-susceptible sediments. Kessler and Werner (2003) showed that availability of coarse material and the sorting capacity of the soil can affect sorting and result in the formation of nets or polygons. The Goldthwait (1976) chart classifies patterned ground transitions according to the relation between grain size fraction < 0.074 mm and slope gradient; according to this classification, the soils at Sp-2. Sp-3, and Sp-4 would possess the grain size and slope for the sorted stripes category, while Sp-1 soils would be at the transitional boundary between stripes and nets and the Backslope would fall into the non-sorted category. A sorting potential gradient could therefore partially explain the difference in patterned ground shape between these areas. While the accumulation of gravel or stones at the interface of peaty layers has been previously observed in the Low Arctic (Nicholson, 1976) and High Arctic (Horwath et al., 2008), the origin of this feature is not clear, and both studies attributed it to differential frost heave. At Ward Hunt Island, the stones showed no evidence of preferential vertical orientation, which would be expected in any periglacial concentration of rocks by mass movement and sorting (Watson and Watson, 1971, Washburn, 1979, Van Vliet-Lanoë, 1991). The higher organic matter content measured at all depths in Sp-1 and Sp-3 and the high gravel content present at the surface in all intertracks suggest, however, that some freeze-thaw sorting occurs. This process can be responsible for carrying organic matter to depths and burying it, and frost-pushing and pulling may create a gravelly soil surface (Horwath et al., 2008, Hallet and Prestrud, 1986, Bockheim,

2007, Bockheim and Tarnocai, 1998, Mackay, 1984). Whether the vegetated water tracks were initiated by eluviation or by sorting remains unresolved, but a case can be made for the latter as the starting point because of the general appearance of the network.

The genesis of water tracks on Ward Hunt Island contrasts with their formation process at Imnavait Creek, Alaska, where the water tracks are interpreted as rudimentary channels that never completely developed due to the restricting effect of permafrost on soil erosion (McNamara et al., 1999). For the Ward Hunt Island water tracks, a combination of periglacial and azonal processes caused the formation of a drainage network that was not linked to the formation of a classical drainage network. The formation process for these water tracks resembles that for soil pipes, except for their retention of a gravel lag because of the coarse nature of the parental material. Soil pipes are usually initiated by eluviation at the peat-soil interface, where the difference in conductivity between two materials favors the erosion of the finer, less porous material (Jones, 1971). On permafrost slopes, a shallow thaw front and the presence of thick organic mats create ideal conditions for high-velocity flow at and just below the interface of the organic and mineral layers (Carey and Woo, 2000). Our hydrographic comparison of a seeping water track with that of a rill shows that the behavior of both channels was similar, responding rapidly to snowmelt by exhibiting a strong diurnal cycle and receding quickly when temperatures or insolation dropped. Such dynamics are typical of surface flow on polar desert slopes during snowmelt periods (Woo and Steer, 1983). The registered flow velocities, the rapid response of the hydrograph to input of meltwater from the upslope snowdrifts, and the limited storage in the surrounding soils make the water tracks on Ward Hunt Island behave more like a rill than simply a zone of preferential soil water flow. This is also the behavior proposed by Woo (2012, p. 245) for sorted stripes, but it differs from the behavior of the water tracks in Imnavait (saturation excess flow up to 14 L s^{-1}, but usually less than 1 L s^{-1}; McNamara et al., 1998) and in the Antarctic Dry Valleys (groundwater flow averaging 5.4 x 10^{-3} L s^{-1}; Levy et al., 2011).

The maximum difference between the measured hydraulic conductivity of water tracks and intertracks at Ward Hunt Island was seven orders of magnitude; this shows that intertracks play a negligible role in groundwater flow within the studied slope section. Soil pipes regularly become the dominant flow pathway in non permafrost environments, greatly affecting the hydrographic characteristics of small catchments (Uchida et al., 1999), and can even account for 100% of total runoff down slopes during precipitation events (Uchida et al., 2005). Our observations show the strong, controlling relationship between patterned ground and slope hydrology, a link rarely highlighted in periglacial regions. This type of landscape feature is widely distributed throughout the vast landscapes of the High Arctic, and geomorphological processes involved in the formation of patterned ground are likely to play a central role in the establishment of drainage patterns. Although strict nomenclature is not always respected, similar links have been established in periglacial landscapes. Woo et al. (1994) witnessed rapid flow through blockstreams and stone stripes, where alpine conditions (coarse sediment, steep slopes) favored free subsurface flow. In a study of rill flow and erosion in polar desert conditions, Wilkinson and Bunting (1975) identified flow through stone stripes as an important provider of water to rillwork. Hodgson and Young (2001) measured a three order of magnitude increase of hydraulic conductivity between the top of frost mounds, composed mainly of fine-grained material, and the low-lying gravelly channels in between the frost mounds. Areal weighting of these features modified their modeled groundwater flow output by 28%-48% as opposed to a general calculation of groundwater flow. Quinton et al. (2000) also measured a similar scale variation of soil hydraulic properties between earth hummocks and inter-hummocks of the Arctic tundra, where the relative contribution of inter hummock flow reached upwards of more than 99 % of the total subsurface flow on the studied slope sections. In the case of Ward Hunt, surface conditions are closer to polar desert or alpine environments than Arctic tundra, and hydraulic properties do not depend on the presence of living peat but rather on sediment properties and organization. Nonetheless, at Ward Hunt Island, the ubiquity of water tracks on the slopes and the presence of multiple snowdrifts upslope imply that most of the meltwater reaching the lake from the snowdrifts of Walker Hill transits through

patterned ground as preferential subsurface flow.

2.4.2. Thermal role of running water

On Ward Hunt Island, the active layer depth of water tracks was consistently and significantly shallower than in intertracks, on average by 7.5 cm (13%). A similar behavior where shallower thaw occurred in preferential flow zones has been reported in cold-room simulations when air temperatures were higher than water temperatures (Veuille et al., 2015). The dominant paradigm in permafrost environment is that running water has a warming effect on the active layer because of convective heat transfer to the underlying ground. For instance, running water can initiate thermokarstic features such as thermo-erosion gullies (Fortier et al., 2007, Bowden et al., 2008), thermo-erosional niches (Kanevskiy et al., 2016), or retrogressive thaw slumps (Burn and Lewkowicz, 1990) and can damage buildings, roads and other infrastructure by increasing the active layer depth (de Grandpré et al., 2012, Zottola et al., 2012). In the polar desert water tracks of Taylor Valley, Antarctica, the active layer was more than twice as deep as in the rest of the slope (45 versus 19 cm; Levy et al., 2011), while in Alaska tundra, it was over 50% greater than in intertrack soils (Hastings et al., 1989). A combination of factors prevented running water from preferentially thawing the active layer in the water track on the slopes of Ward Hunt Island. Firstly, the cold air temperatures and the short residence time of water through the slope allowed little opportunity for the flowing water to warm up. This water came from snowdrifts, and it entered the hydrological network at or near 0 °C, reducing the amount of heat available for advection. Secondly, the structure of the water tracks kept water moving near the surface of the soil, preventing effective thermal exchange with the thaw front and acting as a buffer for conductive exchanges by cooling the soil near the surface. The structure of the water track thus created a two-layer system, with the near-surface layer dominated by convective heat transfer and setting the boundary conditions for the conductive heat transfer in the deeper soil column. Thirdly, the thermal conductivity (k) and the heat capacity (C_p) of the porous peat or gravelly layers created different conductive heat transfer conditions than in the regular soil. Calculation of these parameters was done using the following values: our data for porosity and density, parameters from Farouki (1981, pp. 12 and

42) for C_p in soils and peat as well as k for gravel, equation 2.5-12 and figure 2-28 in Andersland and Ladanyi (2004, pp. 46-51) for k values in the soil and peat respectively; and average values of Schön (2004, pp. 373) for C_p in limestone gravel. Assuming saturated conditions, the peat, gravel, and intertrack had C_p values of 2.84, 2.86, and 2.50 J g^{-1} K^{-1}, respectively, and k of 0.25-0.4, 1.79, and 3.24 W m^{-1} K^{-1}. Thermal conductivity is therefore much higher in the intertrack, while heat capacity is only slightly lower in the intertracks. These differences between water track and intertrack near-surface thermal properties were enough to prevent the heat conduction in the water tracks, at least early during the period when the thaw depth was still shallow. This thermal behavior is common in patterned ground, which often exhibit thicker thaw penetration under the finer or barren sections (Shilts, 1978; Mackay, 1980; Van Vliet-Lanoë, 1991).

2.4.3. Water tracks in the High Arctic

Water tracks have been described at only a few locations with most information from either the North Slope of Alaska or the McMurdo Dry Valleys, Antarctica. The observations from these two contrasting landscapes (Arctic tundra versus polar desert) illustrate how water tracks can vary in morphology and functioning (Table 2. IV), but all studies to date agree on the dominant role that water tracks can play in headwater basin hydrology (Levy et al., 2011; Kane et al., 1991; McNamara et al., 1997). The water tracks of Ward Hunt Island also played such a role. They did not carry water across the entirety of the slope but were important for rerouting that water and concentrating it in highly conductive soils. They began near the front of every snowdrift where patterned ground and washed-out deposits were observed. Figures 2.9a and 2.9b show the front of a nivation hollow similar to the 'wetlands' described in Woo and Young (2003) and a patterned ground network on Ward Hunt Island, with their vegetated water tracks. The water tracks in figure 2.9a further fed into a block stream, but in other cases, where the slope angle permitted, led to solifluction lobes. In all cases, water was channeled underground and the groundwater flow velocities were controlled by these features.

Table 2. IV. Morphology of water tracks at three sites in the polar regions. nd: no data provided.

Site	Width (m)	Length (m)	Spacing (m)	References
Imnavait Creek (Alaska)	5-20	250	10-20	Chapin et al. (1988), Stieglitz et al. (2003)
Taylor Valley (Antarctica)	1-3	200-1900	nd	Levy et al. (2011)
Ward Hunt Island (High Arctic Canada)	0.2-3	< 100	1-2	This study

In addition to the reported occurrences mentioned above (Wilkinson and Bunting, 1975; Woo et al., 1994), similar features have been observed in other areas of the Canadian Arctic, for example, on southern Melville Island (Cape Bounty, 74.94°N, 109.61°W) and near Resolute Bay on Cornwallis Island 74.73°N, 94.96°W) (Figs 2.9c and 2.9d), near a site where polar desert hillslope hydrology was extensively studied in the early 1980s (Woo et al., 1981; Woo and Steer, 1982; 1983; 1986). In both of those locations, water flow is likely to occur preferentially through the coarse section of patterned ground and to exit the soil at the break of slope. There was also a small alluvial fan showing evidence of recent sedimentation in a small resurgence downslope of the site in Fig. 2.9c, demonstrating the potential of the underground network for soil erosion. These small-scale features strongly influence hillslope hydrology and water quality by rerouting flow and by supplying fine sediments to downslope soils, streams, lakes, and wetlands. The presence and properties of patterned ground on sloping terrain, whether it is sorted or non-sorted in appearance, are likely to have a controlling effect on the hydrologic properties of unincised hillslopes in permafrost landscapes.

2.5. CONCLUSIONS

Water tracks are a common feature of high-latitude environments, but their characteristics differ greatly among regions. Our study at Ward Hunt Island in a High Arctic polar desert catchment describes a new geographic setting for such features. The water tracks in this catchment were initiated by the combination of sorting processes linked to patterned ground formation and of fine material eluviation. They were part of a regularly spaced network of patterned ground acting as small-scale watersheds, channelling snowmelt water down the slope in highly conductive gravel layers. In addition to increasing the velocity of groundwater transfer from snowbanks to

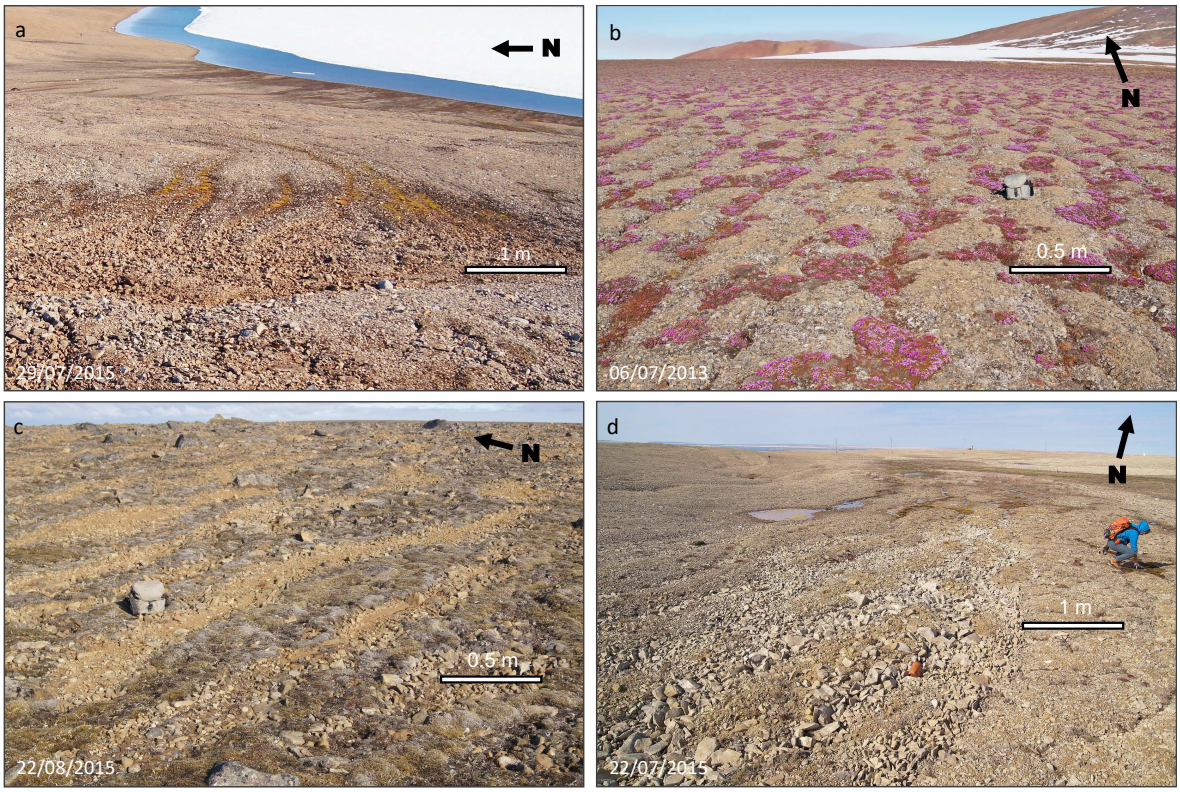

Figure 2.9. a) Patterned ground and water tracks at the front of a nivation hollow on Ward Hunt Island, feeding into a block stream (not pictured); b) Water tracks on gently sloping terrain. The high gravel and organic matter content allowed water to drain efficiently in the coarse section of the patterned ground; c) Patterned ground on sloping terrain on Melville Island, where the very coarse, stony sections were devoid of fines and were covered by vegetation (moss), giving an unsorted appearance. A small fan of recently deposited sandy sediments was observed downslope, indicating both a channelled flow and fine sediment removal; d) Sorted patterned ground on Cornwallis Island followed the typical elongation sequence along an increasing slope angle. Water can be seen seeping further downslope, at the junction of multiple stripes.

the lake, they were also a mechanism of underground erosion and sediment transport. They were widespread along low-angle slopes and collected meltwater from snowdrifts and were therefore the dominant flow paths for the water traveling downslope to the lowlands. The water tracks were characterized by soil conditions of increased water and organic matter content, lower pH, and higher dissolved solid concentrations. These hydrological features also had a thermal effect by cooling the near surface with fast-flowing snowmelt water, thereby restricting the extent of active layer deepening.

Some uncertainties exist on the definition and role of water tracks in the periglacial landscape. As shown here, water tracks can possess different characteristics and thermal behaviors according to their morphology and location. Their formation can be the result of multiple processes, and the origin of water tracks may vary according to local conditions. Our results show that patterned ground can play a controlling role in slope hydrology by forming water tracks that greatly modify soil properties, ground thermal regime, and drainage pathways.

2.6. ACKNOWLEDGEMENTS

This research was conducted with the financial support of the Natural Sciences and Engineering Research Council of Canada (NSERC), including the Discovery Frontiers project Arctic Development and Adaptation to Permafrost in Transition (ADAPT), the Networks of Centres of Excellence program ArcticNet, the Canada Research Chair program, the Northern Scientific Training Program, the Canadian Foundation for Innovation: Canadian Northern Studies Trust, Centre d'études nordiques (CEN), and Fond de Recherche du Québec-Nature et Technologie (FRQNT). Logistical support was provided by the Polar Continental Shelf Program (PCSP), and Parks Canada graciously granted us the use of their facility. The authors would like to thank I. de Grandpré, M. Verpaelst, P. Bégin, and D. Sarrazin for field assistance and three reviewers for their insightful comments and advice.

Chapitre 3

HILLSLOPE WATER TRACKS IN THE HIGH ARCTIC : SEASONAL FLOW DYNAMICS WITH CHANGING WATER SOURCES IN PREFERENTIAL FLOW PATHS

Abstract

Preferential subsurface flow paths known as water tracks are often the principal hydrological pathways of headwater catchments in permafrost areas, exerting an influence on slope physical and biogeochemical processes. In polar deserts, where water resources depend on snow redistribution, water tracks are mostly found in hydrologically active areas downslope from snowdrifts. Here we measured the flow through seeping water track networks and at the front of a perennial snowdrift, at Ward Hunt Island in the Canadian High Arctic. We also used stable isotope analysis to determine the origin of this water, which ultimately discharges into Ward Hunt Lake. These measurements of water track hydrology indicated a glacio-nival runoff regime, with flow production mechanisms that included saturation overland flow (return flow) in a low sloping area, throughflow or pipe-like flow in most seepage locations, and infiltration excess overland flow at the front of the snowdrift. Each mechanism delivered varying proportions of snowmelt and ground water, and isotopic compositions evolved during the melting season. Unaltered snowmelt water contributed to $> 90\%$ of total flow from water track networks early in the season, and these

Paquette, M., Fortier, D. et Vincent, W. F. (2018). Hillslope water tracks in the High Arctic: Seasonal flow dynamics with changing water sources in preferential flow paths. *Hydrological Processes, 32*(8), 1077-1089. doi: 10.1002/hyp.11483

values fell to $< 5\%$ towards the end of the melting season. In contrast, infiltration excess overland flow from snowdrift consisted of a steady percentage of snowmelt water in July (mean of 69%) and August (71%). The water seeping at locations where no snow was left in August 2015 was isotopically enriched, indicating a contribution of the upper, ice-rich layer of permafrost to late summer discharge during warmer years. Air temperature was the main driver of snowmelt, but the effect of slope aspect on solar radiation best explained the diurnal discharge variation at all sites. The water tracks in this polar desert are part of a patterned ground network, which increases connectivity between the principal water sources (snowdrifts) and the bottom of the slope. This would reduce soil-water interactions and solute release, thereby favoring the low nutrient status of the lake.

3.1. INTRODUCTION

Hillslopes are a basic unit of natural hydrological systems, and runoff-generating interactions between precipitation and geomorphological features is a fundamental process that determines hillslope flow paths. In periglacial areas, the active layer thermal regime restricts water infiltration and circulation to shallow depths, and the heterogeneous distribution of snow creates spatial and temporal variations in water supply (Woo et al., 1981; Woo, 1983; McNamara et al., 1998; Woo and Young, 2003). In addition, hydrological phenomena affecting shallow groundwater operate at a faster rate in sloping terrain, mainly because of higher hydraulic gradients and flow velocities, and these rates can be exacerbated by either local or widespread high hydraulic conductivity materials (Woo et al., 1994; Quinton and Marsh, 1999). This combination of variable water inputs, shallow flow paths, topography and material properties can create preferential flow paths such as water tracks, which often dominate hillslope hydrology in periglacial regions.

Water tracks are subsurface flow pathways of diverse morphology, usually in permafrost areas, whose principal hydrological role is to carry snowmelt water and sometimes rainfall downslope as subsurface flow (Kane et al., 1991; McNamara et al., 1998; Gooseff et al., 2013; Rushlow and

Godsey, 2017). Water tracks have been the object of study mostly in Alaska and Antarctica, yet they have been reported in other parts of the periglacial domain, albeit sometimes under other terminologies (Nicholson, 1978; Woo and Xia, 1995; Curasi et al., 2016). Their importance in the periglacial landscape extend beyond that of a simple hydrological pathway, as they play specific roles in heat transfer and active layer development (Hastings et al., 1989; Gooseff et al., 2013; Paquette et al., 2015; Levy and Schmidt, 2016; Paquette et al., 2017), solute transport (Levy et al., 2011) and nutrient and carbon cycling (Oberbauer et al., 1991; Cheng et al., 1998; McNamara et al., 2008; Ball and Levy, 2015). They also play a role in the development of the landscape, acting as an immature drainage network (McNamara et al., 1999), as moisture provider for slow mass wasting processes (Verpaelst et al., 2017) or as indications of denudation by leaching of fine material (Paquette et al., 2017).

Water tracks in polar desert landscapes are known to be preferential pathways for the water flowing from snowdrifts toward the bottom of the slopes (Paquette et al., 2017). These pathways mainly take the shape of gravel lag conduits and patterned ground, playing a hydrological role similar to soil pipes by locally increasing underground hydraulic conductivity. Specifically at Ward Hunt Island, a high latitude location at the northern tip of Canada, water track networks have been identified as principal flow paths linking hillside snowdrifts to the ultra-oligotrophic (Villeneuve et al., 2001) waters of Ward Hunt Lake. Geomorphologically dependant flow paths and flow regimes greatly influence water quality and characteristics, exerting a fundamental control on limnological conditions (Quesada et al., 2006), and although the water track morphology has been described in detail, their hydrological regime remains to be investigated. Specifically, little is known about the degree of interaction between water track flow and soil water. The objectives of the present study were to determine the discharge regimes, including delivery time and flow generation mechanisms, and the origins of the water coming from water tracks and seeping at the bottom of a polar desert slope. Our overall aim was to define hydrological functioning of water tracks on hillslopes, and their role as the primary link between precipitation and downstream systems in the High Arctic

polar desert environment.

3.2. STUDY SITE

Northern Ellesmere Island is a partly glaciated, alpine landscape at the northern edge of the Canadian High Arctic. Aridity limited ice advance during the Wisconsinian, a portion of the landscape therefore pre-dates the last glacial maximum and could have escaped glaciations for as much as $>$ 400 000 years (Lemmen and England, 1992). Among these areas, Ward Hunt Island is located 6 km off the northern coast of Ellesmere Island (Figure 3.1). It features hills with rounded summits, and their slopes are mantled by patchy glacial drifts veneer and frost-shattered, colluvial debris. The studied hillslope is located at the foot of such a hill (Walker Hill, elevation: 436 m above sea level (a.s.l)), whose eastern slope follows a concave-up profile with slope angle values ranging from 29.5° in the upper middle slope to 3.5° at the toe. The middle section of the slope, just above the maximum change of slope and Holocene sea levels of $\geq$ 62 m a.s.l. (Lemmen, 1988), harbours two rows of annual snowdrifts which quickly become the only remaining snowmelt sources after a few days of thawing. The geology of Walker Hill is primarily carbonates (Trettin, 1991), and bedrock exposures are rare on the studied sections. Surface material is a patchwork of glacial drift and gelifracted bedrock. The mean annual air temperature is -17.8 °C (1995-2016), with only July having a positive mean, of 1.5 °C (CEN, 2016). Further descriptions of the physiography, geomorphology and ecology of Ward Hunt Island and of the hillslope in the present study are given in Vincent et al. (2011) and Paquette et al. (2017).

3.3. METHODS

The lower slope of Walker Hill exhibits surface runoff and alluvial reworking of sediments at discrete locations, mostly at the front of snowdrifts as well as at the bottom of the slope, where water tracks merge and seepage occurs (Paquette et al., 2017). These locations were chosen to investigate hydrological regimes of water tracks, as the seepage allows direct water sampling and measurement of discharge. Measurements were performed for the greater part of the snowmelt

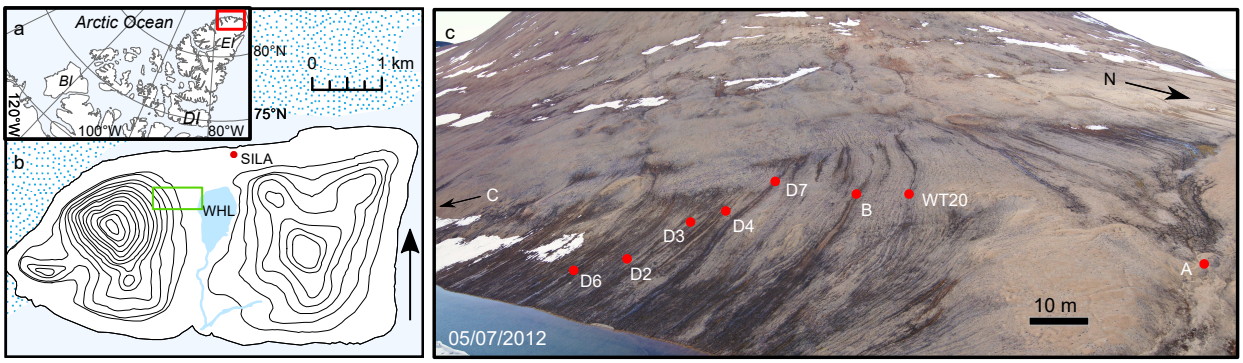

Figure 3.1. (a) Location of Ward Hunt Island in the Arctic Archipelago. EI: Ellesmere Island; BI: Banks Island, DI: Devon Island. (b) Topography of Ward Hunt Island (30 m isolines), with location of the studied slope section. SILA: weather station; WHL: Ward Hunt Lake. (c) The lower slope of Walker Hill, showing the measurement sites. The picture was taken after an unusually warm early summer, and snowmelt was already well advanced.

season in 2013 and 2016, and some discrete measurement were also made in 2014 and 2015. A total of three cutthroat flumes were installed (A, B and C, Figure 1); Seep A was positioned at the downslope end of a relatively flat wetland, where sorted polygons were the main surface landforms. Seep B was located where a network of water tracks merged and seeped, and seep C was located at the front of a perennial snowdrift. The flumes placed at those three locations were snuggly fitted into the ground and equipped with a Hobo U20 water pressor sensor (accuracy of ± 0.14 cm; Onset, Bourne, USA). Water levels (h_u, cm) were obtained from absolute pressures through barometric compensation and were then used to calculate free flow discharge (Q_f, cm^3 s^{-1}) using the equation

$$Q_f = K_f \cdot C_f \cdot h_u^{n_f} \tag{3.1}$$

where K_f is a free flow correction factor calculated from the specific dimensions of the flume, C_f is the free flow coefficient and n_f is the free flow exponent, both of which can be extracted from tables depending on the flume standard dimensions (Siddiqui et al., 1996). Although care was taken that no water flowed underneath the flumes, which was successful at seeps B and C, the coarse nature of the sediments at seep A still allowed some subsurface flow. In 2016, another U20 was placed in a stilling well in the middle of a water track seepage (D6). Discharge values for

this location were calculated using a rating curve obtained by the discrete measurements method detailed below (n = 16, R^2 = 0.87).

Discrete discharge measurements were used to monitor flow in other seeps of similar morphology to B (D2, D3, D4 and, D7) and in a vegetation-covered water track (WT20). They consisted of dilution and tracer gaging tests using a NaCl mixture and an electrical conductivity probe. Discharge (Q) was then calculated as

$$Q = \frac{V}{t} \cdot \frac{C_i}{C_m} \tag{3.2}$$

where V is the volume of the injected solution, t is the amount of time taken for the passage of the tracer slug, C_i is the concentration of the injected solution and C_m is the mean concentration of the slug (Whiting, 2005). These measurements were performed daily when possible (usually in the afternoon), and sometimes twice a day in the morning and in the afternoon.

Two pairs of stilling wells were installed, upslope from seeps A and B, and equipped with a U20 water level logger. Each pair occupied a different position, either the "coarse" or "fine" grain-size sections of patterned grounds networks, where water flowed as determined in Paquette et al. (2017). As water is expected to travel preferentially through the coarse sections, the paired sensors provided flow direction, either towards the coarse or the fine sections. Thaw depth was measured 4 times at each well during the monitoring period, and wells were repositioned deeper when thaw depth increased. In the case of seep B, wells were not placed directly upslope from the flume, as disturbances would have affected other experiments, but rather in the adjacent patterned ground sub-watershed where soil pits were made previously (Paquette et al., 2017). The wells at seep B could not therefore be used to monitor any water pulse through the system, as the specific source and the pathways would have differed at this site.

Meteorological variables were measured at the SILA weather station located on the north shore of the island (outside of the watershed) and recorded on a CR10X data logger (Campbell Scientific,

Edmonton, Canada). Air temperature was measured with a thermistor in a solar radiation shield, snowmelt was measured as snow height change using a Sonic SR50 sensor (Campbell Scientific, Edmonton, Canada) positioned over a snowdrift and incoming solar radiation was collected using a LI-200 (Li-Cor Biosciences, Lincoln, USA). Hourly solar radiation was corrected to account for the slope angle (mean = 18.5°) and aspect (mean = 75.1°), both determined from the random sampling (5% of data points) of a digital elevation model of Walker Hill. Water sampling for deuterium and ^{18}O concentrations was performed discretely every few days in 2013, and for a few days in 2014 and 2015. In 2016, samples were taken at least twice a day, in the morning and in the evening (estimated time of high and low flow conditions) at seep A, and often a third time at mid-day at seep B. In order to measure the daily variation in water sources at seep B, isotopes were sampled every hour for 24-hour in 2016. Precipitation was sampled by digging snow pits and collecting snow at 10 cm depth intervals.

Isotopic signatures of soil water were determined by melting ice in cores of the frozen active layer collected during mechanical coring operations, using a portable earth-coring system. Permafrost samples were collected the same way, by drilling to a maximum of 3 m depth in the ground. Cores were thawed in sealed and vacuumed plastic bags, from which water was then drained. Snowpack composition was sampled by digging snow pits in snowdrifts and by sampling every 10 to 20 cm. Fresh snow and rainfall samples were also collected during precipitation events and the fallen amounts were measured using a metric rain gauge, read twice a day at 700 h and 1900 h. All isotopic measurements were made with an LGR isotope analyser at the Facility for Biogeochemical Research on Environmental Change and the Cryosphere (FaBRECC) of Queen's University. Accuracy of the measurement was better than 0.25 ‰ for ^{18}O and 1.5 ‰ for deuterium.

The relative contributions from snowmelt and soil water (active layer ice) to discharge were estimated using a two-component separation technique (Sklash and Farvolden, 1979; Carey and Quinton, 2005) using ^{18}O as a tracer. The fractional contribution from each source was calculated as

$$Q_1/Q_T = \frac{(c_T^{t_1} - c_2^{t_1})}{(c_1^{t_1} - c_2^{t_1})} \tag{3.3}$$

where Q_1 is the contribution from snowmelt, Q_T is the total runoff, c_T is the concentration of the observed tracer in the runoff and c_1 and c_2 are the concentrations of the tracer in snowmelt and in active layer ice respectively. Uncertainty resulting from equation 3.3 (W_{f_1}) can be attributed to analytical error in the measurement of c_T and to the standard error of the mean calculated for each end member, and was calculated by applying the method described by Genereux (1998)

$$W_{f_1} = \sqrt{\left[\frac{c_T - c_1}{(c_1 - c_2)^2} W_{c_2}\right]^2 + \left[\frac{c_2 - c_T}{(c_T - c_2)^2} W_{c_1}\right]^2 + \left[\frac{1}{c_1 - c_2} W_{c_T}\right]^2} \tag{3.4}$$

where W represents the uncertainty for the variables specified by the subscripts. Part of the snowmelt water refreezes during the snowmelt process and isotopic fractionation will therefore occur, modifying the values of the modeled contribution. The relationship between initial water δ^{18}O isotopic composition (δ_o), the composition of the ice (δ_i) and of the residual water (δ_w) freezing in an open system was calculated as in Lacelle (2011)

$$\delta_i = \delta_o + \ln(\alpha_{i-w}) \cdot 1000 \cdot \ln f + \ln(\alpha_{i-w}) \cdot 1000 \tag{3.5}$$

$$\delta_w = \delta_o + \epsilon_{i-w} \ln f \tag{3.6}$$

where $\ln(\alpha_{i-w}) \cdot 1000$ equals 3.018 for δ^{18}O and 15.228 for δ^2H, while ϵ_{i-w} equals 3.022 and 15.345, and f is the residual fraction of water (O'Neil, 1968; Lacelle, 2011). Statistical analysis was performed using R 3.1.1 (R Core Team 2014), and wavelet analysis of the bivariate time series was accomplished using the WaveletComp package (Roesch and Schmidbauer, 2014).

3.4. RESULTS

3.4.1. Discharge regimes

The discharge regimes of all monitored sites showed a diurnal cycle that began a few days after the onset of snowmelt (Figures 3.2 and 3.3). Positive air temperatures led to rapid rises in discharge in all seeps, while the returns to freezing temperatures were associated with extended recessions. 2013 was a relatively cold year when comparing with Ward Hunt climatic conditions (Paquette et al., 2015, Figure 3.2a). The melting season began in late June, but steady $> 0°C$ temperatures only occurred starting in mid-July. In contrast, summer 2016 began quite early and remained steadily warmer, except mainly for a blizzard that occurred from June 23 to 25, which filled up all the flumes and the seeps with snow and interrupted water flow (Figures 3.3a, 3.3d and 3.3h). Because of warmer climatic conditions, accumulated snowmelt had already reached more than 100 cm on July 1, compared to 15 cm on the same date in 2013 (Figures 3.2b and 3.3b).

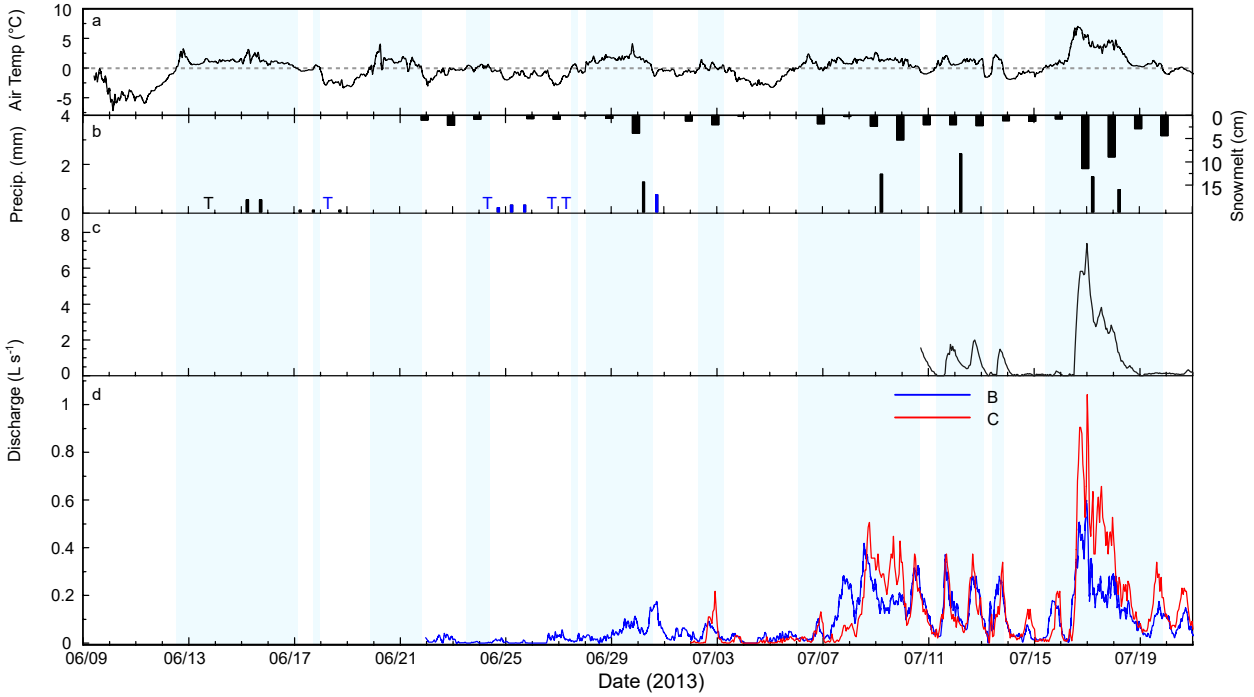

Figure 3.2. Meteorological and hydrological data from 2013. Blue areas have positive air temperatures while white areas are below freezing.: (a) air temperature; (b) rainfall (black), snowfall (blue), and daily snowmelt, T = trace; (c) discharge in seep A; (d) discharge in seeps B and C.

The timing and magnitude of flow conditions differed between the two years. In 2013, steady discharge only began on July 6 and peak discharges at all sites were registered during the night of July 16 to July 17. Prior to this period, the melting season was steadily interrupted by cold spells where snowmelt was minimal (3.2c and 3.2d). In contrast, 2016 had steady discharge very early on, starting on June 10 at seep A (Figure 3.3i) and on June 9 at seep B (Figure 3.3h), and both reached their peak discharge a few days later, on June 13. The flume at seep C remained covered by snow until later in June, but also began registering high discharge values early in the season as compared to 2013 (Figures 3.2d vs 3.3h). Its highest discharge, however, was recorded much later than in the other seeps, on July 3rd, and was coincident with a peak of air temperatures above 10°C for several hours.

Greater overall daily discharge was recorded in 2016, with daily peak discharge regularly exceeding those occurring in 2013 (Table 3. I). Maximum discharge was reached in 2013 at seep A, which had by far the largest discharge measurements of all seeps, ranging about an order of magnitude above the others. Seep B saw the opposite of seep A, as the largest discharge registered in 2013 was exceeded on 7 occasions during 2016, while seep C recorded similar maxima in both years. The 2016 monitoring period was long enough and had the appropriate timing to record flow recession to base levels or to the end of flow in seeps A, B and D6 (Figures 3.3h and 3.3i).

Discretely measured discharge of active seeps located around B and D6 provided an account of the spatial variation (Figure 3.3j). Seeps typically possessed discharge values smaller than those of seep B, which was also the first to become active in the season. D4 showed the greatest

---

Figure 3.3 ***(facing page).*** Meteorological and hydrological data from 2016. Blue areas have positive air temperatures while white areas are below freezing. (a) air temperature; (b) rainfall (black), snowfall (blue), and daily snowmelt, T = trace; (c) active layer thawing front depth; (d) water level (blue line), thaw front depth (dotted line and dots) and depth to the bottom (broken line) of a well upslope from seep A, in the fine section of patterned ground; (e) same as (d), but in the coarse section of patterned ground; (f) water level (blue line), thaw front depth (dotted line and dots) and depth to the bottom (broken line) of a well, in a water track upslope from seep B; (g) same as (f), but in the intertrack section; (h) discharge in seeps B and C and at site D6; (i) discharge in seep A; (j) discharge in other seepage sites, the rectangle is enlarged in the insert on the right.

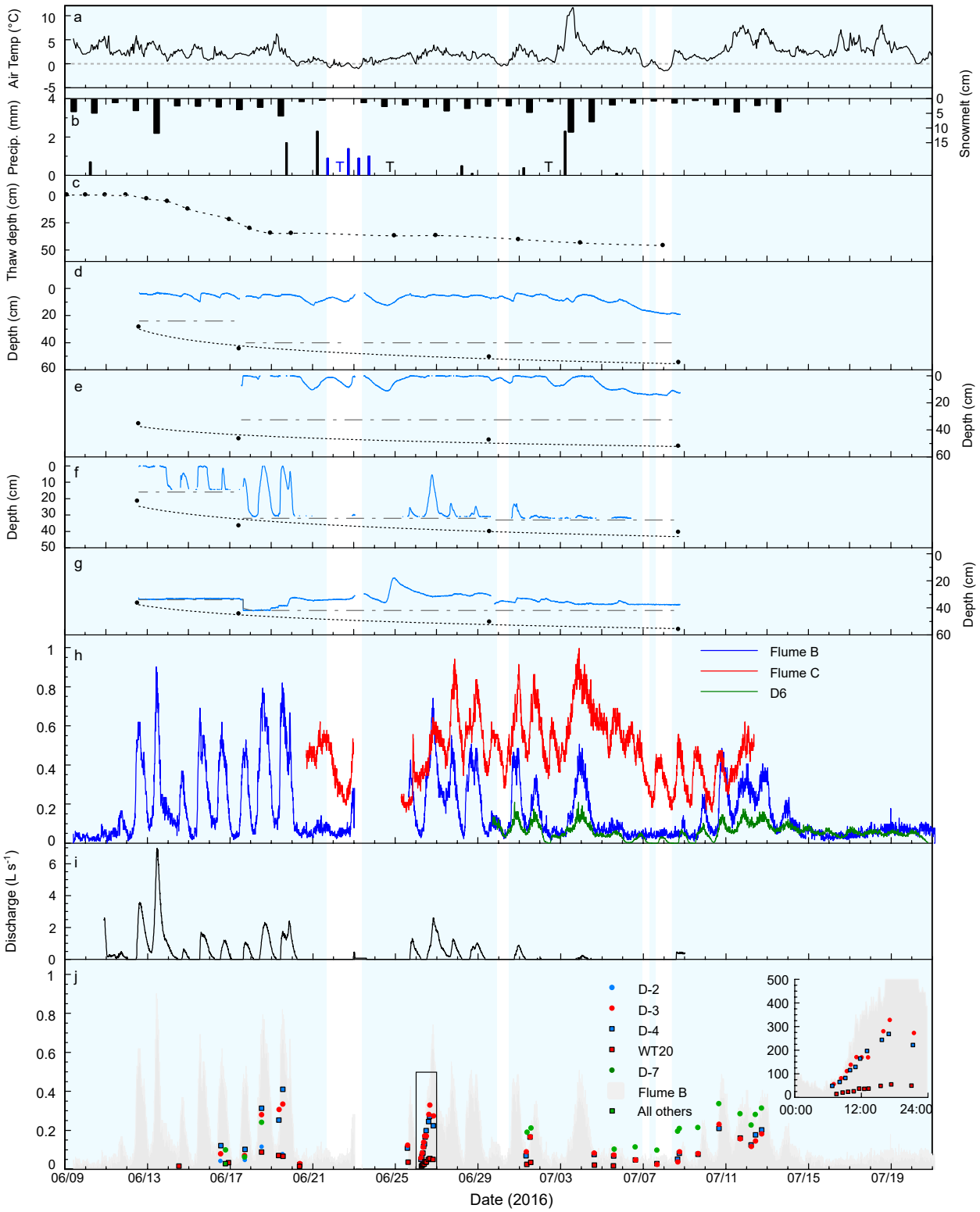
a
Air Temp (°C)
10
5
0
-5
b
Precip. (mm)
4
2
0
T
T
T
Snowmelt (cm)
0
5
10
15
c
Thaw depth (cm)
0
25
50
d
Depth (cm)
0
20
40
60
e
Depth (cm)
0
20
40
60
f
Depth (cm)
0
10
20
30
40
50
g
Depth (cm)
0
20
40
60
h
1
0.8
0.6
0.4
0.2
0
Flume B
Flume C
D6
i
Discharge (L s-1)
6
4
2
0
j
1
0.8
0.6
0.4
0.2
0
D-2
D-3
D-4
WT20
D-7
Flume B
All others
500
400
300
200
100
0
00:00
12:00
24:00
06/09
06/13
06/17
06/21
06/25
06/29
07/03
07/07
07/11
07/15
07/19
Date (2016)

Table 3. I. Discharge values (L s^{-1}) at seepage sites in 2013 and 2016.

Site	Mean		Maximum	
	2013	2016	2013	2016
A	0.93	0.89	7.39	6.97
B	0.06	0.16	0.47	0.90
C	0.13	0.48	0.94	1.00
D6	-	0.06	-	0.21

relative value early in the season of 0.40 L s^{-1}, followed closely by D3 and D7. Seep D2 registered some discharge early in the season, but quickly dried up before the June 23 snowfall. WT20, short for water track 20, did not seep but rather flowed through a gravel conduit underneath a cover of mosses (see Paquette et al. 2017 for details on water track morphology). It maintained low discharges (mean of 0.03 ± 0.016 L s^{-1}) even during warm events, but reached its maximum capacity (0.06 L s^{-1}), and water was at times seen flowing on top of the vegetation. Flow in D7 increased later in the season and its highest levels (0.33 L s^{-1}) were recorded during the second week of July. The recorded values even surpassed the discharge from seep B during this period, when it became the most active of all seeps in the area. The monitoring of D3, D4 and WT20 performed over 15 h on June 26 showed a rise of the hydrograph simultaneous with seep B, followed by recession.

The timing of daily maximum and minimum discharges vary only slightly between sites, unlike the discharge amplitude which can vary by more than an order of magnitude. All locations typically experienced low flow conditions in the early morning and peaking flow levels late in the afternoon or during the evening. Iterative, multiple regressions were performed on 2016 discharge measurements, using air temperatures and slope-corrected solar radiation as explanatory variables (Table 3. II). The iteration consisted of using discharge values with a delay of between 0 and 23 hours, to correct for a potential time delay between environmental variables and discharge. All data showed a relatively small standard variation in the Pearson correlation coefficient (r) for air temperature compared to radiation. A and B showed a discharge with a stronger correlation to radiation, while C and D6 variations were more correlated to air temperatures. Overall, discharge

is always positively related to air temperatures, while the diurnal radiation regime on the slope created a time-sensitive correlation with discharge. Wavelet analysis of the time series measured the strength of the diurnal signals of the variables. Air temperatures did not vary according to a 24h period (average p-value of 0.358), but radiation showed a strong diurnal variation (average p-value < 0.05), caused mainly by the effect of slope angle and aspect. Cross-wavelet analysis of radiation and discharge showed a strong coherence over daily periods, most of all when temperatures were above 0°C (Figure 3.4). The cross analysis also provided a measure of time delay when both time series cycles best overlapped. Time delays were over 6 h in every case and increased during the season in all locations except C. The delays reached more than 16 h in A, 14 h in B and more than 18 h in the case of D6. At seep C, time delays went from 12 h to approximately 8 h at the end of the monitoring period.

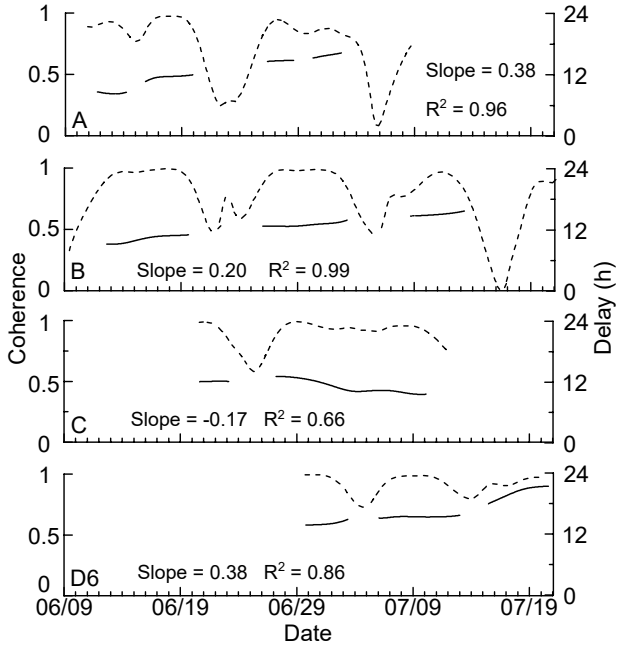

Figure 3.4. Coherence (dotted line) between solar radiation and discharge variation in seeps A, B, C and D6, and delays (full line) between their respective cycles, as determined from wavelet analysis. Also shown are the slope and coefficient of determination (R^2) applied to the delay.

Wells installed upslope from site B showed contrasting water level behavior between the coarse and the fine section of the patterned grounds (Figures 3.3f and 3.3g). The coarse section (water track section, Figure 3.3f) exhibited water levels that behaved almost identically to the

hydrograph of seep B. They peaked and collapsed rapidly during diurnal episodes, with the highs occurring at a mean of 104 minutes after B peaked (σ = 59, n=18). This delay could be an artefact caused by placing the well upstream another sub-watershed next to B, to avoid disturbing sediments concentrations which were monitored in another study. Water levels often rose to the surface or near surface early in the season, but peaks became rarer and weaker as the season went on. In the fine section (intertrack section, Figure 3.3g), levels were much steadier, rarely rising closer than 0.3 m from the surface. Small amplitude peaks sometimes followed the main peaks in the coarse well, but the biggest peak occurred just after the onset of snowmelt following the June 23-25th snowfall.

Table 3. II. Partial correlations (r values) between discharge at each seepage site and meteorological variables. Delays of 0 to 23 hours were applied to discharge measurements.

Meteorological variable		Pearson r			
		A	B	C	D6
Air Temp.	Min	0.09	0.03	0.31	0.23
	Max	0.29	0.25	0.54	0.53
	Mean	0.19	0.13	0.47	0.43
	SD	0.07	0.09	0.07	0.09
	Delay*	7	6.5	6	10
Radiation	Min	-0.14	-0.28	-0.4	-0.24
	Max	0.43	0.48	0.24	0.42
	Mean	0.17	0.13	-0.05	0.1
	SD	0.20	0.27	0.21	0.24
	Delay*	11	12	12	15.5

*delay in hours at maximum correlation

The wells upslope from seep A had a more correlated response between them (Figures 3.3d and 3.3e). The coarse sediment well (Figure 3.3e) had the most variable behavior, with amplitudes exceeding those in the finer sediment well (Figure 3.3d). Its level often rose to the surface during high discharge periods, and the rise occurred slightly earlier than in the finer well. Both wells maintained a high water table throughout the monitored period, which had begun to drop by the end of the monitoring record.

3.4.2. Water isotopes

Our isotopic measurements of snowpack and collected precipitation are the only recent values that can be used to establish a local meteoritic water line for Ward Hunt Island and vicinity. The Global Network for Isotopes in Precipitation (GNIP) database includes $\delta^{18}O$ and δD values for monthly means at Alert, Nunavut., spanning five years from 1989 to the end of 1993 (IAEA/WMO, 2017), providing a local meteoritic water line (LMWL) of $\delta D = 7.68 \pm 0.12 * \delta^{18}O + 3.37 \pm 3.82$ ($n = 58$, $R^2 = 0.99$). Rainfall may be more frequent at Alert than at our site, as total June-July precipitation averaged 42 mm at Alert but only 9 mm and 9.6 mm in 2013 and 2016 on Ward Hunt Island. The reduced major axis regression calculated for the Ward Hunt LMWL was $\delta D = 7.83 \pm 0.23 * \delta^{18}O + 1.15 \pm 6.24$ ($n = 55$, $R^2 = 0.95$). The slope of the ordinary least squared regression was not significantly different from the Global Meteoritic Water Line (GMWL, Craig, 1961, F-value = 1.81 p = 0.182) or from the LMWL of Alert (F-value < 0.01, p = 0.952, Figure 3.5).

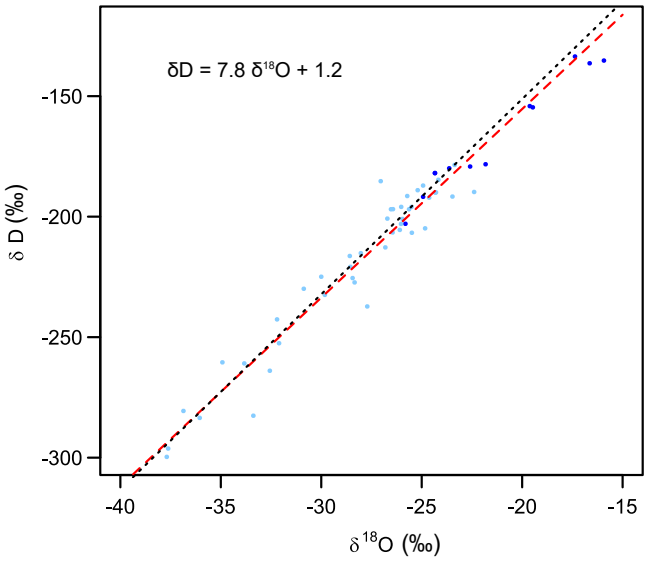

Figure 3.5. Isotopic composition of precipitation on Ward Hunt Island displaying snowfall (light blue), rainfall (dark blue), the global meteoritic water line (black dotted line) and the local meteoritic water line (red broken line).

Water stable isotope values for of $\delta^{18}O$, δD and d-excess of precipitation and ground ice are presented in Table 3. III. Permafrost ice had the heaviest ratios, close to sea water in some cases, followed by rainfall, active layer ice, and snow. Snow and active layer ice isotopic compositions

Table 3. III. Measured isotopic composition of water sources at Ward Hunt Island.

		δ^{18}O				δD				*d*-excess			
Source	n	Mean	SD	Min	Max	Mean	SD	Min	Max	Mean	SD	Min	Max
Precipitation													
Rain	12	-21.4	3.5	-25.8	-15.9	-167.5	23.7	-203.0	-133.5	3.5	6.5	-7.8	12.8
Snow	43	-28.3	4.1	-37.7	-22.4	-219.7	33.5	-299.7	-178.5	6.5	8.9	-15.6	31.0
Soil water													
Active layer ice	15	-22.6	1.3	-24.6	-19.1	-176.4	9.0	-195.3	-156.7	4.5	4.5	-4.2	10.8
Permafrost ice	83	-16.2	7.1	-27.1	-1.2	-124.9	55.1	-203.7	-30.9	4.4	8.6	-30.7	27.1

were used for end-member values in the mixing model, as rainfall amounts were small and permafrost ice, by definition, could not be a contributor of runoff before the active layer has thawed completely. They were applied to isotopic compositions, as shown in in Figure 3.6, which combines all samples of surface runoff taken between 2013 and 2016. Standard error of the mean for snow (0.63) and active layer ice (0.35), along with the average analytical error of the samples (0.15) amounted to uncertainty values averaging (± standard deviation) 8.0% (± 2.2%). A seasonal trend is visible in all locations, as June values plot much closer to the snow mean end-member, while July and August values plot progressively closer to the active layer ice average ratio, even surpassing it during low flow conditions in August 2014, a few days prior to freeze back. Samples plot mostly along or slightly to the left of the LMWL, except for seep A samples which plot on the evaporative side of the line. Two-component mixing results for seep B are presented in Figure 3.7 as fractions of snowmelt contribution to discharge. High values with large variation are found early in the season, as snow is still present in the vicinity. A significant (F-value = 285.6, $p < 0.001$) decreasing trend in direct snowmelt contribution appears as the thawing season progressed and as snowdrifts became the only contributors of snowmelt, and late data suggests an increasing contribution from soil water or active layer ice (Figure 3.7a). Details of a 60 h period including the hourly sampling period did not show any clear trend that can be associated with either the rise or fall of discharge (Figure 3.7b). The mixing model results for all analysed seeps, combining samples taken from 2013 to 2016, are presented in Table 3. III. All seeps showed a drop of snow contribution during the year, except for seep C which still possessed relatively large Q_1/Q_T values even in early August.

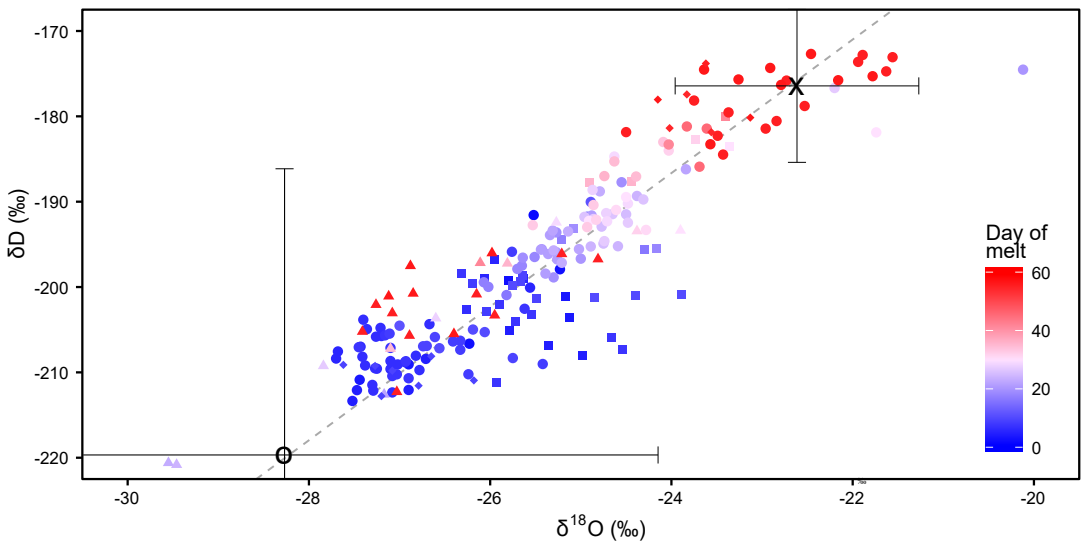

Figure 3.6. Isotopic composition of surface runoff between 2013 and 2016. Colors depend on sampling day, starting from June 10 (the earliest runoff recorded). Sites are represented by marker shape. Seep A: square; seep B: filled circle; seep C: triangle; others: diamond. The O and X are snow and active layer ice with standard deviations, the end-members for the mixing model.

3.5. Discussion

3.5.1. Hydrological regime of water tracks

The water track seeps on Ward Hunt Island exhibited large diurnal variations in discharge, but, except for seep A, did not show any pronounced seasonal peak. Snowmelt water delivery in the seeps was dependant on air temperature, but the diurnal variation in discharge appeared to be controlled by the hourly variations in incident solar radiation, indicating the importance of slope aspect on snowmelt at high latitudes when summer temperatures hover just above 0°C. In addition to strong diurnal cycles, the seeps did not return to baseflow conditions; instead, the recessions were interrupted by a new discharge event when incident radiation rose again. The influence of slope characteristics on energy input has long been identified as important for snowmelt production (Dunne and Black, 1971), however Hardy (1996) noted a less prominent role of radiation compared to air temperature for discharge in nearby Taconite Inlet (inflow to Lake C2). Our findings indicate that a combination of steep topography and slope aspect can play a similar role to sunset in the energy balance at polar latitudes. The importance of solar radiation for snowmelt production had been similarly shown by measurements and models for other high

Table 3. IV. Monthly proportion of snowmelt water (Q_1/Q_T) in runoff for each seep. Values include all years.

	June				July				August			
	Mean	SD	Min	Max	Mean	SD	Min	Max	Mean	SD	Min	Max
Seep A	0.49	0.12	0.23	0.66	0.24	0.12	0.13	0.4	-	-	-	-
Seep B	0.66	0.2	0.34	0.9	0.33	0.12	< 0	0.52	0.04	0.14	< 0	0.33
Seep C	-	-	-	-	0.71	0.33	0.22	> 1	0.69	0.06	0.39	0.85
All Seeps (11)	0.77	0.27	0.51	0.89	-	-	-	-	0.20	0.09	0.08	0.30

latitude locations (Young and Lewkowicz, 1990; Young et al., 1997; Woo et al., 1999, Hoffman et al., 2014), as well as in alpine conditions in the subarctic (Quinton et al., 2004). It has also been demonstrated in boreal forest and tundra environments (Dunne et al., 1976; Hamlin et al., 1998), with a day-night regime. Based on the classification of northern hydrological regimes by Church (1974), water tracks showed a proglacial regime, but within a nival catchment. Seep A was more similar to a nival regime, as it peaked intensely during both season. The reaction of individual seeps to the production of snowmelt varies, with three distinct mechanisms for runoff generation: saturation overland flow (return flow), throughflow (or pipe flow) and infiltration excess overland flow (Hortonian overland flow).

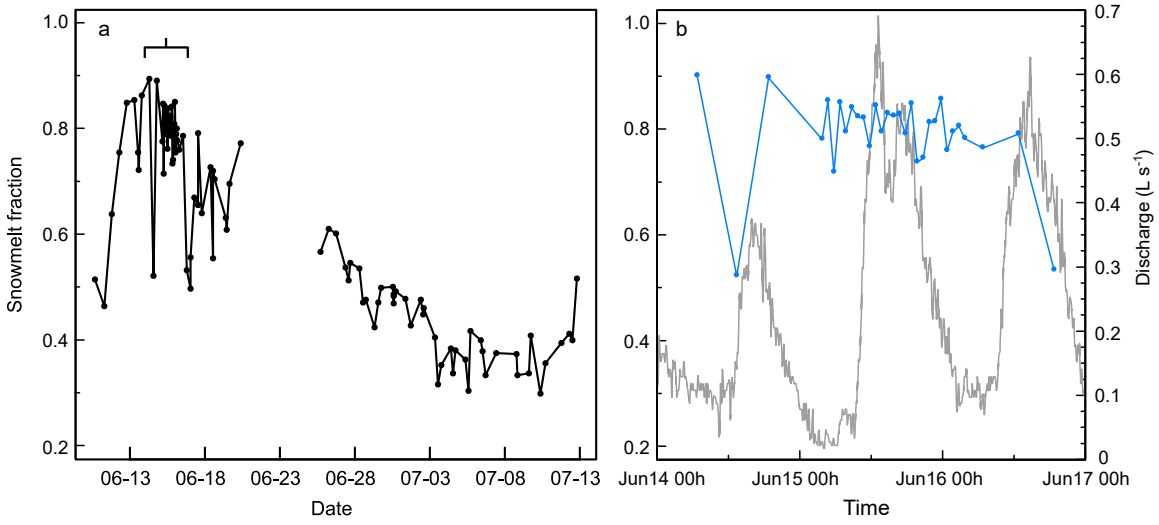

Figure 3.7. Mixing model results in seep B, showing the relative contribution of snowmelt to total discharge. a: seasonal pattern with timing of the hourly sampling period; b: evolution of the contribution (blue) and of discharge (grey) during a 60-hour period, including a 24-hour period of hourly sampling.

3.5.2. Flow regime in sloping sections: Throughflow

In seep B, pulses of water transited through the coarse sections of patterned ground with only minimal interaction with surrounding soils, where fluctuations in water table were muted. This preferential flow path was also suggested by the absence of a pattern in the isotopic composition of runoff as the hydrograph rose and fell during a 24-hour period. In addition, the mixing model results showed a strong event water component, especially early in the season. This type of flow is similar to throughflow and pipe flow, and these were likely the dominant mechanisms of flow generation in the water track networks leading to seep B. Since D6 and other seeps (D3, D4, D7 and WT20) behaved similarly, it may be that all the lower slopes seeps and their water track networks behaved in the same way. However, as was shown by the delay between water pulses in seep B and its wells, the exact timing and intensity could vary depending on the water track network configuration and location. When water flowed preferentially in coarse material of a hydraulic conductivity up to 7 orders of magnitude greater than the surrounding soils, it could flow through the slope with little dependence on antecedent moisture conditions in these surrounding soils. The downstream movement of water in the fine-grained portion is limited, however, because of the extremely low hydraulic conductivity of the soil (10^{-5} m d^{-1}). The moisture in this portion of the ground cannot contribute to the downstream system, except if it was to return to the coarse-grained section when snowmelt inputs (and hydraulic head) diminishes in the coarse section. This did not seem to occur in the wells at seep B. These water tracks might therefore be considered as losing streams even before they emerge, as they contribute to local groundwater recharge instead of depending on groundwater levels to be able to flow.

Similar underground stream-like flow is known in alpine and periglacial landscapes. On steep and bare alpine slopes underlain by permafrost, the presence of gelifracts and coarse slope deposits can favor infiltration and rapid subsurface flow (Woo et al., 1994). Large spatial variations in hydraulic properties of soils have also been documented in periglacial areas in the past, notably by Hodgson and Young (2001), and by Quinton et al. (2000) and Quinton and Marsh (1998) who found a three- to six-fold increase in k_s values in inter-hummock areas. Similar to the data from

the coarse sediment well at seep B, these areas were also highly responsive to daily variations in snowmelt and were by far the greatest contributors of snowmelt water at the plot scale. However, the runoff generation process was different in seep B than in these locations, where a water table rise was necessary in order to activate these preferential flow paths of highly conductive peat.

3.5.3. Flow regime in flat areas: Saturation overland flow

Seep A rarely exhibited continuous flow; its discharge regime rather indicated a fill and spill behavior, or a return flow produced by saturation overland flow, much like in southern low-lying wetlands. This explains the relatively low direct contribution of snowmelt to discharge, which showed a good amount of mixing with pre-event water even early in the season. The relatively flat, sorted polygon network upstream from the seep location experienced elevated water table prior to discharge events. The polygonal network experiencing water tables fluctuations acted as a variable source area as defined by Dunne et al. (1975). The shallow gravel pathways of the coarse-grained portions of the patterned ground network formed the preferential drainage network, which was mainly underground as is usually the case for water tracks. In 2013, the extended low temperatures caused a lack of sufficient water input from the upslope snowdrifts, preventing flow conditions from filling the network and producing runoff. Flow ceased completely during the season, as the thawing of the active layer increased the amount of water necessary to saturate the area. The different flow dynamics between these water tracks and those upslope from seep B and other seeps could be explained by the low slope of the area ($< 3°$) compared to the other networks ($< 9.7°$), which prevented the formation of a large hydraulic gradient.

The conceptual framework for runoff generation for Arctic tundra landscapes described by Quinton and Marsh (1999), Carey and Woo (1999, 2001) and Carey (2003) could extend to this area. In our case, however, the inter-hummock peat network of their framework are replaced by the gravel networks of the polar desert polygonal terrain. This polyvalence of their framework underscores the hydrological importance of microtopography and soil surface properties, even in

very different periglacial landscapes.

3.5.4. Flow regime in front of snowdrifts: Infiltration excess overland flow

Seep C, located at the front of a large perennial snowdrift, had a unique behavior amongst the monitored seeps. It showed the greatest annual variation in mean discharge, but maximum discharge remained similar in 2013 and 2016. In addition, it showed a relatively high correlation between discharge and air temperature, while also maintaining a high amount of event water contribution during late summer and a diminishing delay between maximum radiation and maximum discharge. This hydrological signature indicates that the direct link with the event water source (the snowdrift) increased as the season progressed, indicative of infiltration excess overland flow. A negative slope relationship for the delay against melt season progression was also measured by Dunne et al. (1976), Lewkowicz and French (1982) and Lewkowicz and Young (1990a) who observed that thinner snow covers had the fastest response time to daily maximum energy input, as meltwater waves take less time to cross thinner snow covers and can create more efficient flow pathways during the season. Seep C showed a contrasting pattern, with the negative slope of its delay between maximum energy input and maximum discharge being opposite to that measured in the other seeps, where delays increased as the season progressed. The steady high proportion of event water in seep C throughout the season also differed from the other seeps, which registered a diminishing contribution of event water over the course of the season. The increased lag in other seeps could be explained by the increased thickness of the active layer, which obstructs event water flow and force it to travel through less conductive, sandier sediments at depth. It could also result from the increased distance to snowdrifts, as snowdrifts on the lower slopes of Walker Hill melted before snowdrifts at higher altitudes, further delaying the arrival of the meltwater wave.

3.5.5. Ground ice contribution to runoff

Water in each of the seeps (except in seep C) had an isotopic signature close to that of active layer ice late in the season, and some seeps began discharging again in August 2015, when

snowdrifts had already disappeared for a few days. These waters probably came from the thawing of the ice-enriched transient layer, as defined in Shur et al. (2005). Summers were colder in 2013 and 2014 (respectively 55.2 and 55.3 melting degree days; CEN, 2016), and no seepage was detected during fieldwork in August 2014. These summers would have increased transient layer ice-content, due to a thinner active layer, as is usually the case during colder years (Shur, 1988). In contrast, 2015 had nearly twice as many melting degree days (105.1), which should have caused the melting of some of the ice in the transient layer.

Ground ice is usually not identified as an important contributor to streamflow in polar desert (Woo and Steer, 1983). However, late-season ionic enrichment of streamflow has been measured and attributed to ground ice melt in at least one other High Arctic locations (Lamhonwah et al., 2017). In addition, similar late-season seeps in the McMurdo Dry Valleys, Antarctica, had also been attributed to the melt of ground ice, which was initially formed during snowmelt periods in colder years (Harris et al., 2007). Overall, even without the late summer contributions of ground ice, seeps and water tracks that were not in the downslope vicinity of a snowdrift experienced a modification in their contributing source during the season. This indicates that ground ice was present in the active layer on the coarse, steep slopes of this polar desert. An extended warm season would therefore increase water availability, reducing water stress for plants and increasing inputs into the lake.

3.5.6. Mixing model uncertainties

Isotopes are one method of performing hydrograph separation to measure event water contribution, but are subject to known shortcomings. In regular hydrograph separation, “new” water will usually come from a time-specific rainfall event, and will mix with the “old” water present in the soil just prior to the beginning of the event. In our case, the definition of event or “new” water and pre-event or “old” water is not straightforward, since every day produces an event, yet 24-hour old water does not fall clearly in the “old” water category. It is possible that a fraction of snowmelt water remains in the soil and is only mobilized after a day or two, or during low flow period, yet

because of the low potential for evapotranspiration caused by thin or absent vegetation cover and by low energy inputs (temperatures and radiation) between events, this water would possess an isotopic composition close to snowmelt water and might not be detected as pre-event water. This rationale justifies the construing of pre-event water as water present in the soil during freeze-back i.e. active layer ice.

The only indication of a potential evaporative effect was from the data at site A, which plotted either close to or clearly to the right of the LMWL. These individual points taken through multiple events cannot be used to create an evaporation line, as they are not sampled in a standing water body and are separated by various inputs of event water, which might not possess the same original isotopic composition. This interpretation however is consistent with the fill and spill behavior indicated by the hydrograph shape and by the wells data, and suggests an extended transit time for meltwater compared to other seeps measured in this study. In the case of seep A, identification of any event water is less clear, as the δ^{18}O values of snowmelt were likely modified during its transport as groundwater.

Another difficulty in interpretation is that snowmelt signature is not equal to the signature of the snowpack or to fresh snow. The δD to δ^{18}O relationship of the snowmelt will typically show a lower slope than the snowpack, which also possess a lower slope than fresh snow (Zhou et al., 2008; Lee et al., 2009). This could explain why June values in seeps B and C and in other seeps plot to the left of the LMWL early in the season (late in the season as well for C) as the slope of the seeps ratios (7.4) is significantly lower than the LMWL (F-value 13.8, $p < 0.001$). This process is caused by fractionation during refreezing in the snowpack (or in the soil), as part of the water is turned back to ice. The residual water (δ_w) will therefore always plot to the left of the MWL. In our case, the difference between runoff and the LMWL is typically $<$ 1 ‰. Using equation 3.5 and 3.6 and the average snow signature of -28 ‰ and -220 ‰, this difference would be compensated with a re-freezing of $\leq$ 30% of the snowmelt water as it travels through the snowpack and the cold soil. Taking into account the average δ^{18}O residuals of the

reduced major axis regression used for the LMWL (0.8 ‰), only a small fraction (7 %) of the snowmelt needs to be refrozen either in the snowpack or in the soil in order to obtain values that are outside the residual range of the LMWL. High Arctic snowpack can develop substantial ice layer at their base or within the snow layers (Woo and Heron, 1981; Lewkowicz and Young, 1990b) and Marsh and Woo (1984) have demonstrated that between 28-46% of the surface melt can re-freeze in the snowpack prior to the onset of snowmelt runoff. The required range of 7-30 % of refreezing is therefore reasonable, particularly for thick snowdrifts as encountered on the slopes of Walker Hill, or for the predominantly subsurface flows that refreeze in the active layer.

The signature of freeze-out fractionation and evaporative fractionation are sometimes undistinguishable in cold environments (Throckmorton et al., 2016), which brings into question the interpretation of evaporative enrichment based on the isotopic signatures at seep A. Using equation 3.5 with the mean snow signature, the enriched samples from seep A (the cluster to the right of the LMWL) also plotted close to the first ice that woud have formed after a 10% re-freezing of this snow (δ_i = -25.3‰, -206.4‰). However, these samples were from the early melting season, and without a process by which the re-frozen ice would reach the seep before the residual water, they must be interpreted as evaporative enrichment.

The re-freezing of snowmelt within the pack causes snowmelt isotopic compositions to show a depleted (more negative) signature early in the season, which leads to the overestimation of snowmelt contributions. This is followed by an enrichment in ^{18}O and the overestimation of groundwater mixing as the season progresses (Obradovic and Sklash, 1986; Cooper et al., 1993; Taylor et al., 2002). Taylor et al. (2002) used literature values to identify an average increase of the isotopic ratio by 3-5‰ during the snowmelt season. In our study, the difference between the end member δ^{18}O ratios is only 5.7‰ and would be reduced to 3.2‰ by the end of the season in the case of a 5‰ seasonal increase. Applying such a 3 to 5‰ linear correction to the snowmelt average value to the data presented in Figure 3.7 gives Q_1/Q_T ratios (standard deviation) of 0.58 (0.09) to 0.55 (0.08) for June and 0.46 (0.07) to 0.54 (0.11) for July, compared to original values

of 0.64 (0.14) in June and 0.39 (0.05) in July. These corrected values diminish the seasonal variability in snowmelt contribution and the role of groundwater mixing later on.

The percentage of event water yielded by the water track seeps (weighted for discharge) over the entire season was 48 % at seep A and 60 % at seep B. These values are among the highest recorded values for northern catchments according to a compilation by Taylor et al. (2002), where values exceed 50% steadily in only 6 out of 20 studies. They are also higher than values reported for a subarctic watershed, where event water contribution averaged between 10 and 32 %, and never reached higher than 55 % for a single event (Boucher and Carey, 2010). In Svalbard, only glacier-fed rivers had meltwater steadily dominating the discharge (Blaen et al., 2014), with the rest of the inputs dominated by groundwater. In this polar desert landscape, a combination of nivation processes and soil sorting has allowed the establishment of a drainage pattern dependant on the characteristics and processes of this cold environment, consistent with the cryo-conditioning of cold region landscapes (Berthling and Etzelmüller (2011). Local accumulations of thick snowdrifts dominate snowmelt hydrology, while micromorphology of the slopes and soil organisation dictate flow paths and meltwater delivery, together enhancing the structural connectivity of the landscape (Bracken and Croke, 2007; Turnbull et al., 2008; Bracken et al., 2013). Feedbacks and the effects of flow paths on water quality and on slope evolution remain to be evaluated, but water tracks can act as the dominant carriers of snowmelt water through polar desert slopes. In this particular case, the efficient transfer of water to Ward Hunt Lake is a result of enhanced connectivity between the snowdrifts and the water body. These findings imply that water is rapidly conducted through the slopes with little opportunity for soil-water biogeochemical interactions, which would help explain the low nutrient status of the lake.

3.6. CONCLUSIONS

Polar desert water tracks in the High Arctic can be efficient downslope carriers of snowmelt. Their runoff generation mechanisms depend on slope profile and on soil organisation, and are different from the front of a snowdrift, showing some interaction, albeit limited, with the surrounding soils. Early season runoff in the seeping water track networks of Ward Hunt Island were dominated by residual snowmelt water from re-freezing snowpack, while late season water had the isotopic signature of residual snow, ice and soil water. The water tracks differ from snowdrift seeps, which are dominated by snowmelt water throughout the season. While seeps dry up once snowdrifts have melted, some seeps were re-activated at the end of a warm summer. These had an isotopic signature that was heavier than active layer ice, towards that of permafrost ice, indicating a possible contribution from the thawing of the ice-rich transient layer. Together, the cold region processes of snowdrift and patterned ground formation have shaped the hydrology of this polar desert slope to enhance downslope connectivity, creating efficient pathways for evacuating water while minimizing interactions with the soil. Defining the hydrological regime of the water tracks draining the western slope of Ward Hunt Lake watershed provides a key step towards linking the limnological conditions of the lake to the characteristics of its watershed.

3.7. ACKNOWLEDGEMENTS

This research was conducted with the financial support of the Natural Sciences and Engineering Research Council of Canada (NSERC), including the Discovery Frontiers project Arctic Development and Adaptation to Permafrost in Transition (ADAPT); the Networks of Centres of Excellence program ArcticNet; the Canada Research Chair program; the Northern Scientific Training Program; the Canadian Foundation for Innovation: Canadian Northern Studies Trust; Centre d'études nordiques (CEN); and Fond de Recherche du Québec-Nature et Technologie (FRQNT). Logistical support was provided by the Polar Continental Shelf Program (PCSP) and Parks Canada graciously granted us the use of their facility. The authors would like to thank M. Lafrenière and S. Lamoureux

for the use of their facilities, and I. de Grandpré, M. Verpaelst, P. Bégin, G. Davesne and D. Sarrazin for their field assistance. We are also grateful to editor Jim McNamara, to Joseph Levy and to an anonymous reviewer for their comments on the manuscript.

Chapitre 4

PERIGLACIAL SLOPEWASH DOMINATED BY SOLUTE TRANSFERS AND SUBSURFACE EROSION ON A HIGH ARCTIC SLOPE

Abstract

Limnological conditions are vastly dependant on watershed characteristics, including sediment transport capacities. In the Arctic, water transport from the slopes to the water bodies of headwater catchments often occur through preferential subsurface flow paths known as water tracks. These flow paths are therefore the main conduits promoting matter transfer and slope modification. Because water tracks occur below the surface, they are expected to convey only dissolved solids, but recent studies have shown evidences of fine sediment leaching occuring below the surface. We investigated the transport of dissolved and suspended sediments in water tracks on a polar desert slope, the outlet of which is Canada's most northern lake, and linked this transport to slope and flow paths geomorphology. Solute transfers were dominated by carbonates, but other ions concentration increased when particularly warm summers promoted active layer thaw. Suspended sediment transport occurred in some of the water tracks, but was 5 to 10 times less important than solute transfers. They were supply-limited, as determined by the morphology and sediment availability in the flow paths, altogether indicating a good capacity for subsurface mechanical erosion. The amounts of suspended sediments varied greatly between sites. In this dry landscape dominated by snowmelt, the occurrence of surface seepage indicated sediment deposition sites, while subsurface flow promoted fine sediment leaching. These informations were used to complete

existing models of nivation slopes in polar deserts. It is uncertain how such a drainage network would adapt to important rainfall events, as it is well adapted to a strict nival regime implying large but very localized water inputs. The adaptation of the drainage system to new precipitation distribution and to increased permafrost thaw, as predicted by climate change models, should develop new sediment pathways and increased solute concentrations, with the potential to modify physico-chemical conditions in downstream water bodies.

4.1. INTRODUCTION

Catchment morphology exerts a fundamental control on limnological conditions in lakes of High latitudes (Quesada et al., 2006), and multiple studies have linked catchment processes to lake conditions in the Arctic (Hardy, 1996, Braun et al., 2000, Lewis et al., 2012, Stewart and Lamoureux, 2011, Tomkins et al., 2010). Among those processes, sediment and solute transport and deposition is often put forward. This transport depends on connectivity, described by Fryirs (2013) as the water mediated transfer of sediment between two different compartments of the catchment sediment cascade. In periglacial landscapes, connectivity is usually relatively low, as frozen ground can prevent the formation of first order drainage channels (McNamara et al., 1999) and because periglacial processes are mostly considered only effective in creating series of disconnected landforms, inefficient at transporting sediment from the slopes to the streams (Slaymaker, 2009). This can be obvious in polar desert landscapes, where low precipitation reduces the occurrence of surface flow and slopewash to pro-nival sites and to wetlands located at the break of slopes (Woo and Young, 2003, Woo and Xia, 1995).

The occurrence of highly spatially concentrated water inputs can create preferential subsurface flow paths, which designate the flow of water and solutes “along certain pathways, while bypassing other volume fractions of the porous soil matrix” (Gerke, 2006). In periglacial areas, these are often refered to as water tracks. Water tracks are subsurface flow pathways of diverse morphology, mostly studied in permafrost areas, whose fundamental hydrological role is to carry snowmelt

water and sometimes rainfall downslope as subsurface flow (Kane et al., 1991, McNamara et al., 1998, Gooseff et al., 2013). Studies of landforms and hydrology in High Arctic polar deserts have shown the dominant hydrological role of water tracks as networks of enhanced flow velocity and connectivity (Paquette et al., 2018). This occurs as water follows the path of least resistance through coarse areas of slopes and patterned ground, travelling in similar fashion to funnel flow as described in Kung (1990). It has been suggested therefore that those patterned ground were created by a mix of periglacial sorting processes and fine sediment leaching (Verpaelst et al., 2017, Paquette et al., 2017), indicating a capacity to increase the hydraulic conductivity of their substrate (Schmidt and Levy, 2017). Underground erosion in patterned ground has already been reported in the literature, as a process enhancing the surface expression of sorted stripes on frost affected slopes (Caine, 1963). This supposes they enhance sediment connectivity and are contributors to subsurface wash and to slopewash.

In general, relatively little is known on the role of subsurface wash in contemporary periglacial landscapes (French, 2007), but studies addressing it did prove its significance for chemical denudation (Lewkowicz, 1981, Pecher, 1994, Rapp, 1960, Williams et al., 2006). The subsurface wash of fines has been suggested in the past as a potential agent of periglacial slope modification, but only where coarse enough sediments allowed water infiltration (Tricart, 1967). However, there are to our knowledge no studies presenting values for subsurface mechanical slopewash in permafrost areas, possibly because they are expected of being low as compared to periglacial processes and surface wash. As such, it is not even mentioned in a recent sediment budget manual for cold environments (Beylich and Warburton, 2007). On temperate slopes, subsurface mechanical wash processes can be dominant pathways for sediment and solute transport through channels such as soil pipes (Jones, 1987, Verachtert et al., 2011), which have also been observed in periglacial area (Carey and Woo, 2000, Carey and Woo, 2002). The morphology of water tracks in the High Arctic and their hydrological behavior suggest they could act as subsurface denudation conduits through steep enough slopes. This behavior and function could be strongly affected by the projected modification of precipitation regimes toward a more landscape-distributed

rainfall regime, in contrast to the highly concentrated snow deposits observed here (Bintanja and Andry, 2017). Would that be the case, the water tracks could have wide implications for the impacts of climate change on sediment transport and biogeochemical processes in polar deserts.

The central goal of this paper is to test the hypothesis that significant subsurface wash of suspended sediments and dissolved solids occur in water tracks on a High Arctic polar desert slope. It combines discharge and load measurements in multiple water track seepage sites during the snowmelt period. These measurements convey the mode of transport and the amount of matter transiting toward the bottom of the slopes. Since water track flow is the most common flow pathway from the annual and semi-permanent snowdrifts (Paquette et al., 2017; 2018), the capacity of this feature to effectively carry material is fundamental for sediment delivery and slope evolution. Using topographic and geomorphologic transects, this paper looks to present a conceptual model of slope morphology and flow pathways, establishing the link between basin morphology and matter delivery affecting the downslope headwater catchment lake. This will provide a perspective on the stage of post-glacial evolution of this area.

4.1.1. Study site

The slope under study is located on Ward Hunt Island (WHI), at the northern fringe of the canadian High Arctic, 6 km off the northern coast of Ellesmere (83.08°N, 74.14°W). Ice surrounds the island, with the Ward Hunt Ice Rise to the north and west, and the Ward Hunt Ice Shelf to the southwest and formely to the south and east, an area now occupied by pack ice. At the center of Ward Hunt, at 26 m above sea level (a.s.l.) lays Ward Hunt Lake (WHL), an ultra oligotrophic, 0.35 km^2 headwater lake. The area experiences a polar desert type of climate with mean annual air temperature of -17.9 °C (1995-2015), and July is the only month averaging positive temperatures at 1.5 °C (CEN, 2016). It registers less rainfall than nearby Alert, NU (170 km to the southeast), where precipitation average 158 mm $year^{-1}$ (Environment Canada 2016). The region is in rapid transition, as perennial snow and ice volumes are steadily diminishing (Paquette et al., 2015, Mueller et al., 2017, Braun et al., 2004), largely altering ecosystems and

freshwater systems (Mueller et al., 2003, Veillette et al., 2008, Mueller et al., 2009). On Ward Hunt Island, glaciation levels reach < 200 m a.s.l., and the absence of glaciers is owed to aridity (Miller et al., 1975). The non-glaciated areas consist of landscapes where annual and perennial snowdrifts play a fundamental role, as the only providers of water for slopewash processes. The slope section studied in this paper links the western shore of Ward Hunt Lake to the foot of Walker Hill, a steep (22.5° to 29.5° graded slope on the eastern flank) carbonate hill rising to 436 m a.s.l where multiple perennial, semi-permanent and annual snowdrifts act as the main freshwater contributor to the lake (Figure 4.1). These snowdrifts are mainly organized in two irregular nivation benches transverse to the slope, the size of each snowdrift roughly depending on the size of its hollow. They are located just above the estimated Holocene marine transgression limit of 62 m a.s.l. (Lemmen, 1989). While seepage occurs for a short distance (< 20 m) at the front of snowdrifts, water mainly flows toward the lake by way of subsurface flow, often through coarse gelifracts or through patterned ground formed in colluvium mixed with glacial diamicton veneer, creating the preferential flow pathways called water tracks. As slope diminishes near the lake (3.5 to 9.7°), some water tracks seep to the surface prior to entering the lake. Further details on slope geomorphology and descriptions of physiography and ecology of the area are given in Vincent et al. (2011) and Paquette et al. (2017).

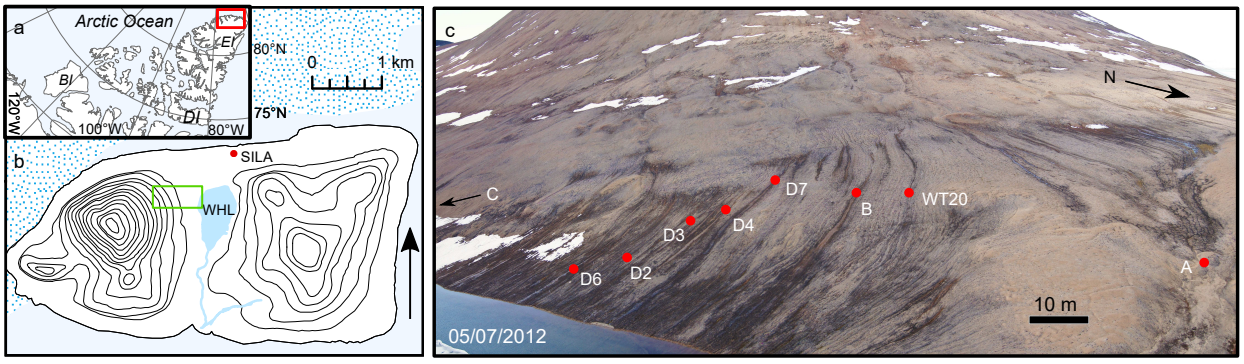

Figure 4.1. (a) Location of Ward Hunt Island in the Canadian Arctic Archipelago. EI: Ellesmere Island; BI: Banks Island, DI: Devon Island. (b) Topography of Ward Hunt Island (30 m isolines), with location of the studied slope section. SILA: weather station; WHL: Ward Hunt Lake. (c) The lower slope of Walker Hill, showing the measurement sites. The picture was taken after an unusually warm early summer, and snowmelt was already well advanced.

4.2. METHODS

4.2.1. Water tracks hydrology

The hydrology of water tracks was monitored for parts of the snowmelt season in 2016. Three methods were used depending on the type of flow monitored. Cutthroat flumes were installed where water track networks seep from the ground at sites A and B. The flumes were snuggly fitted into the ground so that no water flowed underneath them, and were equipped with a Hobo U20 water pressor sensor (Onset, Bourne, USA, accuracy ± 0.3 cm) corrected for barometric pressure variations using a second U20 positioned in the air. Water levels (h_u, cm) were then converted to free flow discharge (Q_f, $cm^3\ s^{-1}$) using a free flow correction factor calculated from the flume geometry according to

$$Q_f = K_f \cdot C_f \cdot h_u^{n_f} \tag{4.1}$$

where C_f is the free flow coefficient and n_f is the free flow exponent, both of which depend on the flume dimensions (Siddiqui et al., 1996). Discrete measurements of velocity were performed in other water tracks seepage locations using slug tests. Velocity was measured by dilution and tracer gaging tests with a sodium chloride mixture and an electrical conductivity probe. Discharge (Q, $cm^3\ s^{-1}$) was then calculated using

$$Q = \frac{V}{t} \cdot \frac{C_i}{C_m} \tag{4.2}$$

Where V is the volume of the injected solution (ml), t is the amount of time for the passage of the tracer slug, C_i is the concentration of the injected solution and C_m is the mean concentration of the slug (Whiting, 2005). At seep D6, stage was recorded by fitting a U20 sensor in a water level observation well inserted into the bed of the seeping stream. A rating curve was created using discrete velocity measurement to predict discharge according to stage (R^2 = 0.879, n = 16), a relation providing normally distributed residuals (Shapiro-Wilk test, p = 0.2018).

4.2.2. Subsurface wash

Measurements of subsurface wash included both suspended and dissolved solid measurement. Suspended sediments were measured twice daily during low and high flow (7:00 and 19:00) at the three monitored seeps, as well as every time discharge was punctually measured in other locations (D3, D4 and D7). Additional sampling was performed when high sediment concentrations were measured, in order to confine these events to their actual timeframe. Turbidity values in nephelometric turbidity units (NTU) were obtained by analysing 10 ml of water using a Lamotte 2020we turbidity meter (Lamotte, Chestertown, USA). For calibration, 0.3 to 0.5 L of water was sampled repeatedly and filtered through pre-weighted 0.7 µm glass fiber filters, which were dried at 105°C and weighted to obtain suspended sediments concentrations (SSC, mg L^{-1}, n = 136). SSC were linearly correlated to NTU (R^2 = 0.913, $p < 0.001$), residuals of the correlation were normally distributed (Shapiro-Wilk test, p = 0.387), and values below 4.3 NTU were considered negligible.

Geochemical sampling was performed in conjunction with measurement of suspended sediments. Seeping water was sampled from the field using tripled rinsed 500 ml Nalgene bottles. Permafrost cores (8.3-10.8 cm) were collected using a portable core drilling system and thawed in the laboratory in order to drain their water content. All samples were filtered for ion analysis using 0.22 µm PVDF membrane filters and stored in acid washed, triple-rinsed HDPE bottles kept at 4 °C until analysis. Major ions from 2013 to 2015 were analysed at the Quebec City Institut National de la Recherche Scientifique Research Centre on Water, Earth, and the Environment (INRS-ETE). Cations were determined using inductively coupled plasma atomic emission spectroscopy (ICP-AES) using a Varian Vista AX spectrometer (Agilent Technologies Inc, Palo Alto, California). Anions concentrations were measured using a Dionex ion chromatographer ICS-2000 (Thermo Fisher Scientific Inc, Waltham, Massachussets). For 2016 samples, both cations and anions were measured at the Facility for Biogeochemical Research on Environmental Change and the Cryosphere (FaBRECC) of Queen's University on a Thermo Scientific Dionex 5000 liquid ion chromatograph. Since pH measurements were mainly in the range 8.1-8.6, bicarbonate were

assumed to be the dominant species of carbonate. Bicarbonate concentration (mg L^{-1}) was then estimated from the charge balance of the samples using the sum of molar masses

$$HCO_3^- = \left[\sum cations - \sum anions\right] \cdot 61.0168\ g\ mol^{-1} \tag{4.3}$$

where 61.0168 is the molar mass of HCO_3^-.

Specific electrical conductivity (SpC) was monitored using a decagon ES-2 sensor connected to an EM50 data logger (Decagon Devices, Pullman, WA) in Seep A, B and for the end of the season at seep D6. In other seeps and water tracks, SpC was measured during discrete discharge measurement using a portable PCS Testr 35 (Oakton, Vernon Hill, Il). An ordinary least square (OLS) regression coerced to an intercept value of zero was applied to the relationship between the sum of major ions measured in water samples and SpC (Figure 4.2). The coefficient (0.65) was then used to convert SpC to dissolved solid concentrations (DSC, mg L^{-1}). The OLS coefficient was preferred to a reduced major axis (RMA) regression because of the relatively small error in the measurement of SpC and because the regression is used to predict rather than to simply

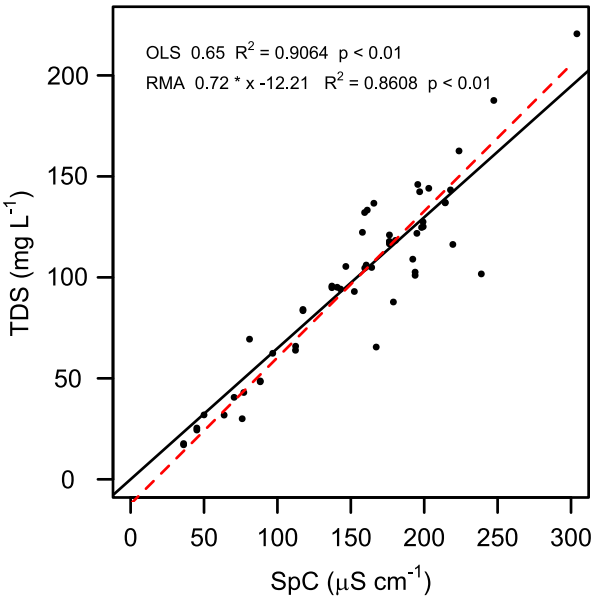

Figure 4.2. Relation between electrical conductivity and dissolved solid concentrations, with OLS (black line) and RMA (red dashed line) regressions.

correlate the variables.

Suspended sediment and dissolved solids yields were calculated by:

$$Yield_{SS/DS} = \frac{\sum_{i=1}^{T/\delta t} \cdot C_i \cdot Q_i \cdot \delta t}{A} \tag{4.4}$$

where C_i is the concentration, Q_i is discharge δt is time between measurements, T is time and A is the watershed area (Ferguson, 1987).

4.2.3. Slope morphology

Slope profiles were created upslope from each seep where discharge was measured. Each profile followed the flow path upslope from the seep using a Trimble VX spatial station (Trimble, Sunnyvale, USA). A measurement point was taken every meter up to the nearest snowdrift, and the slope was averaged every 2 m. Surface features were systematically noted during the survey. They were based on a combination of soil organisation (small scale landform identification) and type of deposit, which gave one of the following features: blockstream, colluviums (coarse, washed out surficial deposits), patterned ground (sorted appearance), vegetated patterned ground (non-sorted appearance), hybrid patterned ground (patchy vegetation), solifluction lobe, surface flow, channelled surface flow, stony vegetated water track and vegetated water track. These profiles were used as the baseline to delineate the watershed of all seeps up to the first snowdrift, with support from interpretation of satellite imagery (Geo-Eye 2, August 2011, 0.5 m resolution). Except for seep A which was estimated at 85 048 m^2, the uncertainty associated with subsurface flow pathways prevented an exact delineation of single watersheds. Instead, the outline of the combined watersheds was defined, and the total area of this basin was divided by the number of seeps in the area to provide an average watersheds size of 6052 m^2.

4.3. RESULTS

4.3.1. Slopewash

Discharge began on 10 June 2016, a few days after snowmelt had begun, and seeps showed clear diurnal oscillations (Figure 4.3). An interruption of discharge occurred between 20-25 June, as air temperatures dropped below 0 °C and a blizzard left an uneven blanket of fresh snow (0-40 + cm). Complete analysis of seep hydrological behavior can be found in Paquette et al. (2018). In seeps A, B, and D6, DSC showed daily variations, with peak discharges corresponding to lowest DSC values. Seep A exhibited highest DSC early in the season, with initial values up to 142 mg L^{-1}, but these values rapidly diminished when the hydrograph rose (Figure 4.3c). DSC were dropping overall during the high discharge period prior to the blizzard, and subsequently rose after that event. Seep B DSC rose and fell rapidly at the onset of snowmelt, with values oscillating between 60 to 157 mg L^{-1} (Figure 4.3d). This variation then diminished, and settled around 86 to 115 mg L^{-1}. These values rose again to $>$ 125 mg L^{-1} during a cold spell, as discharge shrank to low levels prior to the snowstorm. As water began flowing again, diurnal oscillations remained above 100 mg L^{-1}, and DSC kept rising steadily until water levels returned to baseflow conditions. During this period of low flow, DSC values were continually rising, reaching upwards of 200 mg L^{-1} at the end of the monitoring period. Seep D6 was not monitored from the beginning of snowmelt, and showed tamed daily DSC oscillations between 90 to 110 mg L^{-1} (Figure 4.3f). Low flow levels late in the season also coincided with increased DSC up to 163 mg L^{-1}. Punctual measurement in other seeps are presented in Figure 4.4. Discharge values remained similar between seeps D3 and D4. Seep D7 began the season with lower discharge values, but as the season went on it surpassed other seeps, even recording greater discharge than seep B near the end. DSC remained between 77 and 128 mg L^{-1}, and was similar in D3, D4 and D6, but slightly lower in D7 (Figure 4.4a. SSC went from undetected levels to a maximum of 103 mg L^{-1} after the snowfall (Figure 4.4b). D3 and D4 usually carried similar concentrations, which, at means of 23.5 and 20.1 mg L^{-1} respectively, were the highest of all the seeps.

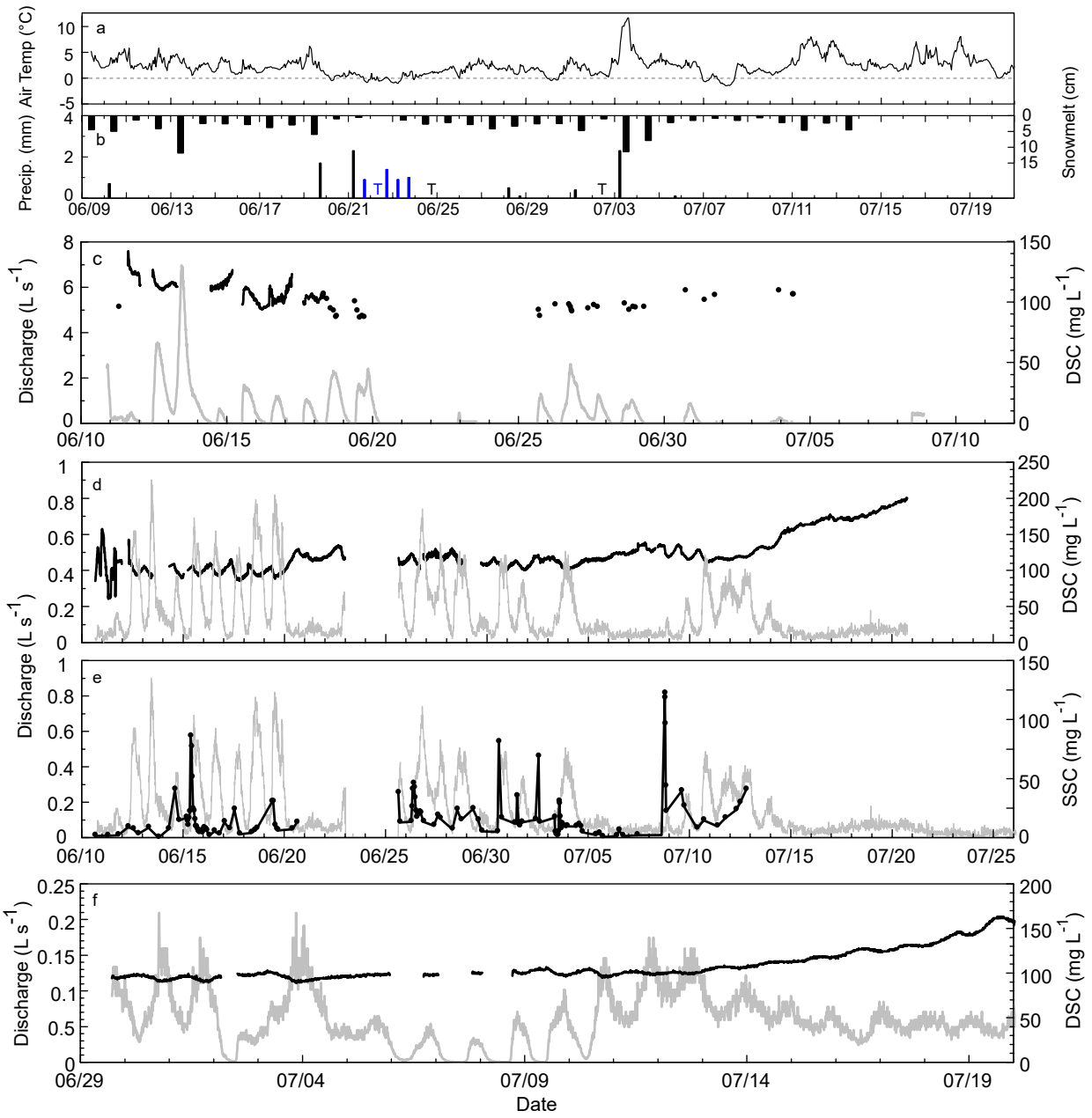

Figure 4.3. Figure 3: Meteorological and runoff data for 2016.(a) Air temperature; (b) Precipitation and snowmelt (blue = snow, T = trace); (c) Discharge (grey line) and dissolved solids concentration (DSC) at seep A; (d) Discharge (grey line) and DSC at seep B; (e) Discharge (grey line) and suspended sediments concentration (SSC) at seep B; (f) Discharge (grey line) and DSC at seep D6.

Dissolved loads mainly consisted of bicarbonates and calcium ions (Table 4.3.1, Figure 4.6), reflecting the local carbonate lithology. The pH was over 8.3 and concentrations of other weathering products such as Mg^{2+}, K^{+} and SO_4^{2-} remained low. In comparison, permafrost ice had much higher DSC, with 2 to 3 orders of magnitude increase in Na^{+}, Cl^{-}, SO_4^{2-}, Mg^{2+} and

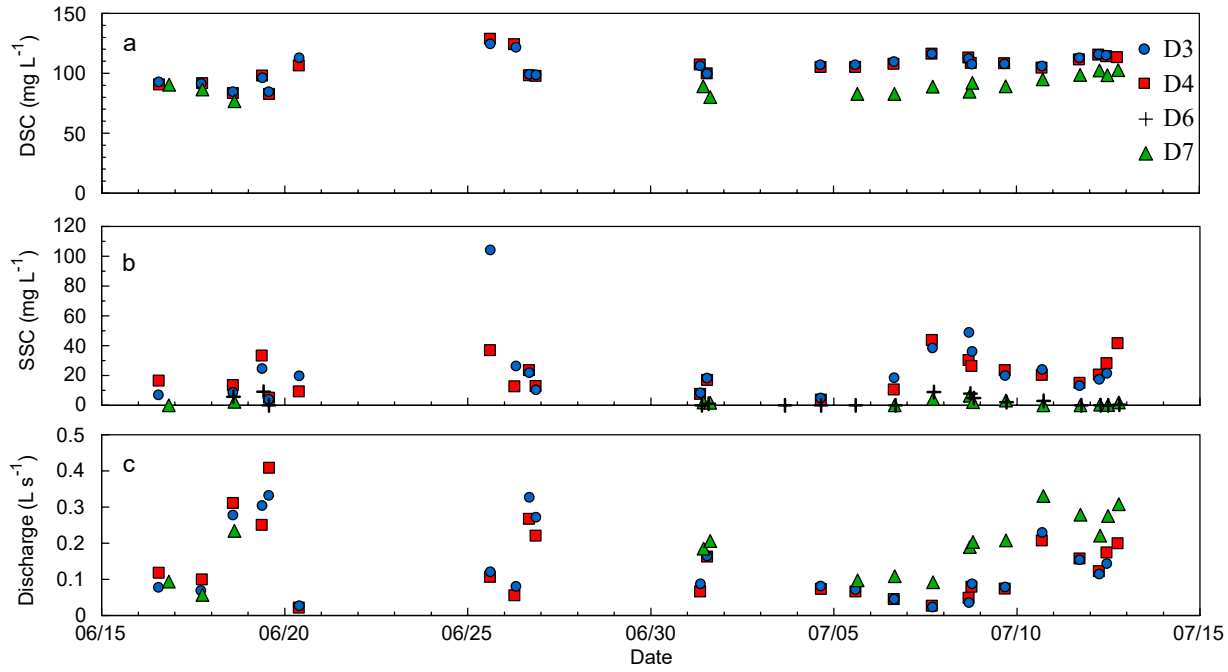

Figure 4.4. (a) DSC; (b) SSC and (c) discharge measured in seeps D3, D4, D6 and D7.

K^+ (Table 4.3.1). The amount of bicarbonates and Ca^2+ did not increase as much in permafrost, a bit more than doubling the surface water values. Composition of the samples also changed in August in all seeps; Na^+ and Cl^- concentrations sharply rose, followed by other weathering by-products, showing a load less typical of a carbonate setting and closer to the concentrations found in permafrost. Water temperatures in seep A greatly surpassed other seeps, averaging 9 °C in June and reaching a maximum of 12.9 °C on 18 June. In comparison, other seeps never exceeded 5.6 °C and averaged at best 2.8 °C. Figure 4.5 presents the time series of major ions concentrations in seep B in 2016. It is punctuated by short increases in Na^+ and Cl^- concentrations during the season, to values greater than background levels by 1 to 1.3 orders of magnitude. The 2 greatest peaks correspond to the onset of snowmelt and to a $<$ 1 mm precipitation event. Other peaks occurred after small ($<$ 1mm total) rainfall events, but not all precipitation were met with such increases. The small drop in concentration on 03 July corresponds to the warmest day of the summer, where snowmelt reached its peak just after a 2 mm rain event.

Table 4. I. Geochemistry of seeps by month, all years combined (2013, 2015 and 2016). Values are means, with standard deviations in parentheses. "Other seeps" refer to measurements made in nearby seepage sites in 2015, when no snow was left upstream. "Permafrost" samples were collected at depths between 54 and 252 cm.

		SpC			Concentration (mg L^{-1})							
Site	*n*	(µS cm^{-1})	pH	T °C	HCO_3^-	Cl^-	SO_4^{2-}	NO_3^-	Ca^{2+}	K^+	Mg^{2+}	Na^+
Seep A												
June	5	198 (23.2)	8.6 (0.2)	9 (2.9)	124.4 (5.1)	4.7 (3.1)	1.8 (0.8)	0.5 (0.0)	34 (2.1)	0.3 (0.03)	3.5 (0.3)	4.8 (0.8)
July	4	191 (28.5)	8.3 (0.02)	6.6 (1.7)	101.6 (12.7)	3 (1.2)	1.2 (0.3)	0.1 (0.05)	28.3 (4.1)	0.3 (0.03)	3.1 (0.4)	2.4 (0.4)
Seep B												
June	22	174 (21.5)	8.6 (0.1)	1.7 (1.1)	99.1 (13.9)	4.4 (8.6)	1.3 (1.1)	0.2 (0.2)	28.8 (3.6)	0.3 (0.2)	1.9 (0.6)	4 (5.4)
July	16	192 (51.6)	8.5 (0.2)	2.2 (1.1)	107.6 (18.8)	0.7 (0.3)	0.9 (0.2)	0.2 (0.2)	30.5 (3.5)	0.3 (0.2)	1.7 (0.5)	2.0 (0.8)
August	2	359 (2.1)	8.5 (0.0)	2.8 (1.6)	146.6 (0.1)	28.2 (5.2)	15.6 (2.3)	4.2 (0.5)	37.3 (0.9)	3.9 (0.3)	6.7 (0.3)	24.7 (2.8)
Other seeps												
August	7	309 (59.7)	8.5 (0.1)	1.9 (1.1)	140.5 (8.6)	16.8 (12.4)	9.9 (3.2)	3.7 (0.7)	37.5 (1.7)	2.5 (0.6)	5.5 (1.0)	15.1 (8.9)
Permafrost	6	6977 (4528)	8.1 (0.3)	-	250 (107)	1630 (1247)	644 (399)	0.1 (0.3)	82 (59)	93 (61)	104 (82)	1113 (726)

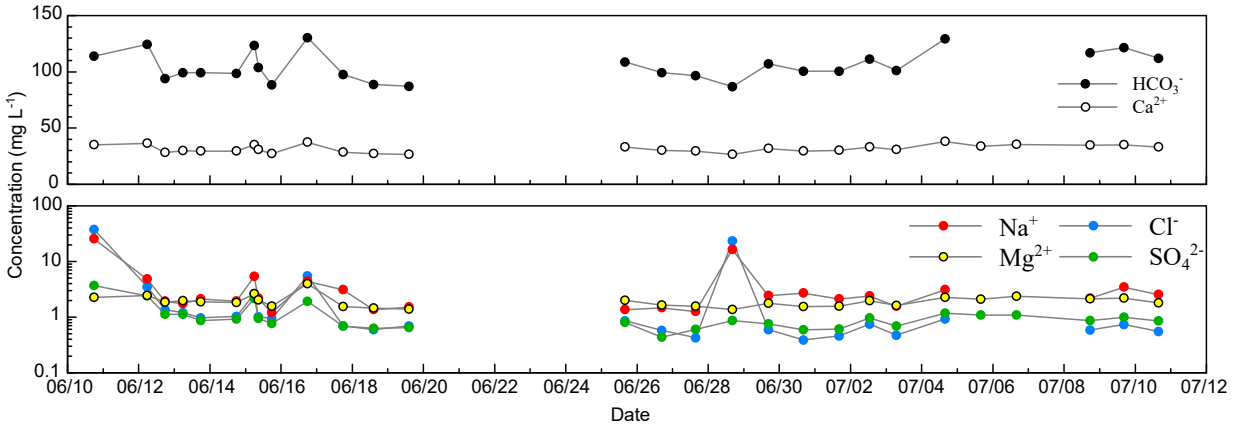

Figure 4.5. Seasonal changes in major ions concentrations in seep B. Concentrations are expressed on a linear y-axis in the upper plot, and on a log-scale on the bottom plot. The late June interruption was caused by the absence of flow during the blizzard.

SSC remained below detection limits in seep A for the entire season. In seep B, SSC were typically below 20 mg L^{-1}, but would rise sharply in the morning, up to an order of magnitude during the rise of the hydrograph, rapidly falling afterwards (Figure 4.3e). They peaked at 86 mg L^{-1} during the first portion of the snowmelt period, following a relatively small peak discharge on the previous day. They peaked again at 81, 69 and 122 mg L^{-1} in late June and early July, with the greatest peak occurring after 4 days of baseflow. D6 and D7 remained poor in SSC, often being under the detection limit (Figure 4.4b). Linear correlation of normalized seep B SSC showed a significant ($p < 0.001$) correlation with normalized D3 and D4 SSC ($R^2 = 0.44$ and 0.40 respectively). Correlation were not significant with other seeps.

Daily variations in DSC and SSC were examined using hysteresis curves (Figure 4.7). Clockwise hysteresis was measured for DSC and SSC at seep B and for DSC at seep D6 (Figure 4.7d, e & f). DSC hysteresis was typically "flatter" and varied by $<$ 20 mg L^{-1}, but SSC at seep B rose sharply from below 20 to 86 mg L^{-1}, with slow recession to levels around 20 mg L^{-1} during the remainder of the rise of the hydrograph. A second peak in discharge was muted in terms of SSC, which kept diminishing to levels $<$ 10 mg L^{-1}. Seep A behaved differently as the season progressed. Early melt (11 June to 13 June) hysteresis curves were clockwise, but became counter-clockwise from 13 June onward (Figure 4.7a,b & c). The counter-clockwise hysteresis on 15 June (and 14 June) began with a rising concentration during the rise of the

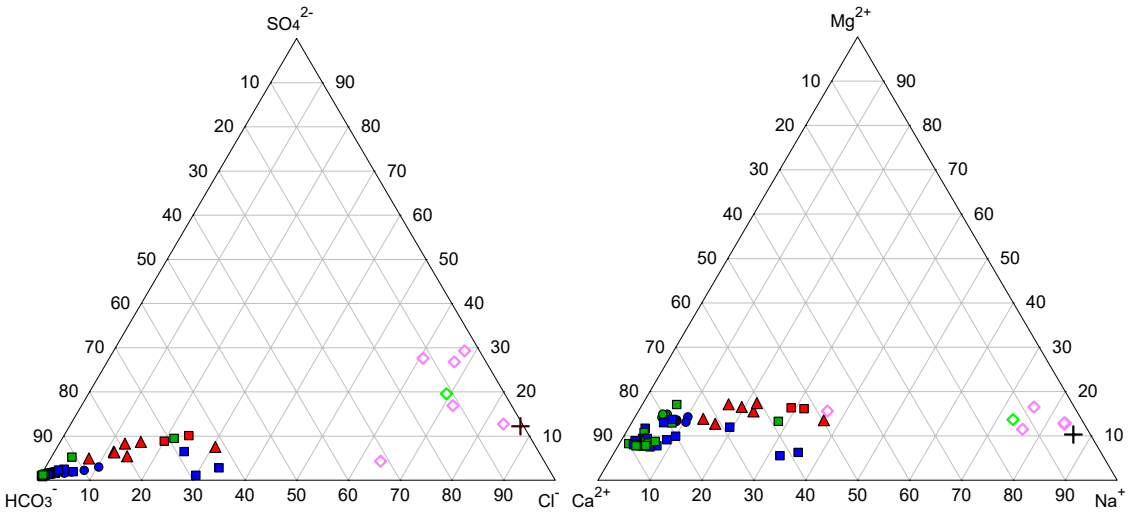

Figure 4.6. Ternary diagrams showing anions and cations percentages in samples. Colors represent the sampling month. Blue : June; Green : July; Red : August. Symbols shapes are sampling locations. Round : A; Square : B; Triangle : Others. Pink diamonds are permafrost samples (the green diamond is the mean), and the black cross is seawater composition.

hydrograph, followed by a drop during the recession. The event of 17 June (and 16 June) also had a counter-clockwise hysteresis, but accompanied with an initial drop in DSC and a fairly even DSC during the recession. As is the case in other sites, concentrations typically varied by < 20 mg L^{-1}.

Total fluxes varied between sites, mostly because of differences in total runoff (Table 4. II). Seep A carried more than 90 kg of dissolved solids during its short but intense activity period. Less water flowed from seep B but fluxes were compensated by continuous discharge, such that dissolved solids were carried with greater concentrations during low flows and totaled nearly 53 kg. Other seeps showed less solution transport, with D6 transporting only 11.6 kg during its monitored period. Suspended fluxes were less dependant on discharge. Seeps B, D3 and D4 maintained relatively high SSC values, and fluxes in them exceeded fluxes in D6 and D7 by an order of magnitude, while seep A had undetectable SSC. In every seep, however, total dissolved solids (TDS) largely exceeded total suspended sediments (TSS). Yields varied by an order of magnitude between sites, ranging between 1.1 and 10.2 t km^{-2}. Highest yields were recorded in seep B, which combined both the highest dissolved and suspended yields. Lowest yields were found in seep A and D6, as suspended sediments remained almost undetectable in both locations.

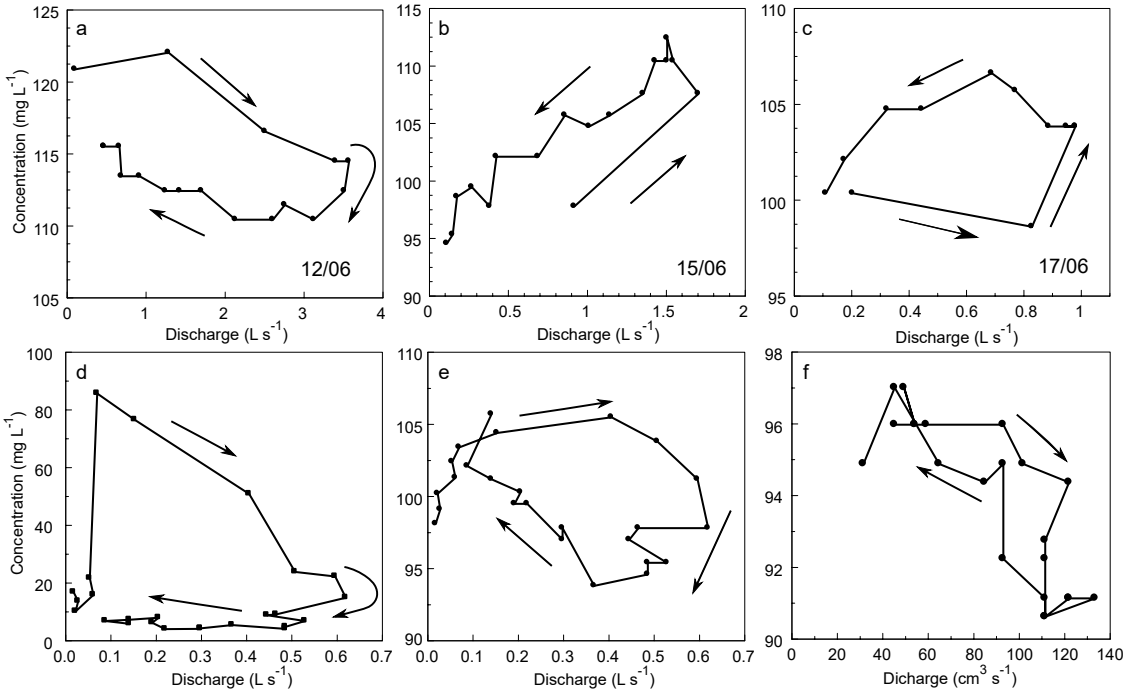

Figure 4.7. Daily discharge-sediments hysteresis curves. The top plots represent DSC hysteresis curves in seep A for (a)12 June; (b) 15 June; (c) 17 June; (d) SSC hysteresis in seep B on 15 June; (e) DSC hysteresis in seep B on 15 June; (f) DSC hysteresis in seep D6 on 30 June.

Seeps D3, D4 and D7 had similar yields, but D7 loads consisted essentially of solutes. Assuming the recorded measurements cover the essential of the runoff season, an absence of inputs, and a mean dry density of 1.97 t m^{-3} for mineral soil (Paquette et al., 2017), denudation rates were established in the range of 0.6 to 5.2 mm ky^{-1}.

Table 4. II. Sediment fluxes and yields for the seeps in 2016

	Dissolved solids				Suspended sediments				Total	
Seep	Conc. mg L^{-1}	Flux kg	Yield t km^{-2}	Yield kg km^{-2} d^{-1}	Conc. mg L^{-1}	Flux kg	Yield t km^{-2}	Yield kg km^{-2} d^{-1}	Yield t km^{-2}	Yield kg km^{-2} d^{-1}
A	105	90.1	1.06	44.2	0	0	0	-	1.1	44.2
B	124	53.0	8.76	199.0	14.7	8.5	1.41	32.1	10.2	231.1
D3	107.2	32.3	5.33	222.2	23.5	7.1	1.17	48.7	6.5	270.9
D4	106.8	31.1	5.14	214.0	20.1	5.9	0.97	40.3	6.1	254.3
D6	109.7	11.6	1.92	91.5	2.4	0.3	0.04	2	2.0	93.5
D7	90	39.2	6.47	269.5	1.7	0.7	0.12	5.1	6.6	274.6

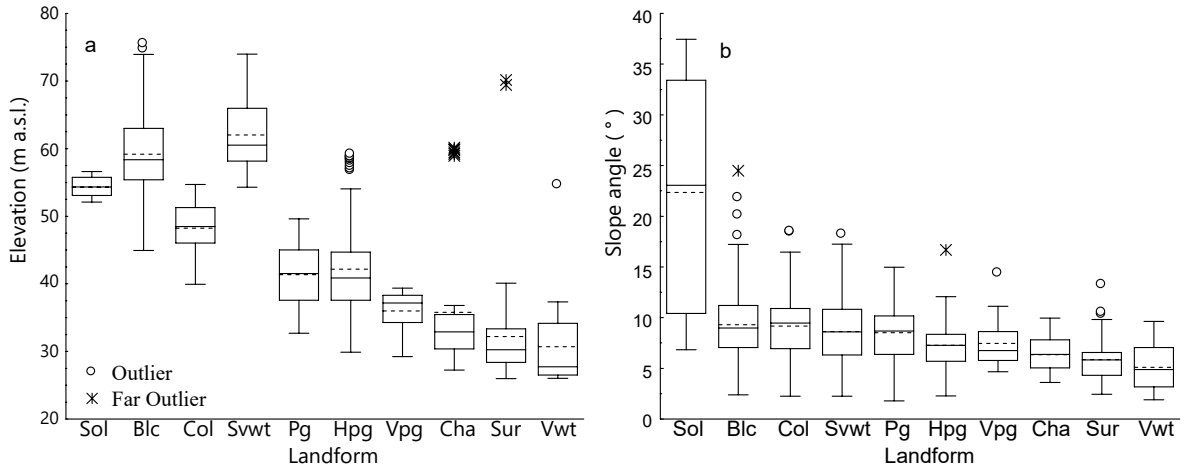

Figure 4.8. (a) Elevation and (b) slope angle where landforms develop. Sol: Solifluction lobe; Blc: Blockstream; Col: Colluvium deposits; Svwt: Stony and vegetated water track; Pg: Patterned ground; Hpg: Hybrid patterned ground (partly vegetated); Vpg: Vegetated patterned ground; Cha: Channeled surface runoff (seepage); Sur: Unchanneled surface runoff; Vwt: Vegetated water track (non-sorted stripes). Far outliers for Cha and Sur in (a) were located at the front of snowdrifts, while outliers for Hpg were on top of solifluction lobes.

4.3.2. Flow paths

Water seeping at the measurement points had to travel between 211 to 272 m from the lower elevation snowdrift to the monitoring sites. This flow occurred across a variety of small landforms and soil patterns, which were a by-product of the slow evolution of deposits by means of freeze-thaw sorting and mass wasting, depending on the slope angle and the amount of humidity in the soil. Each landform would generally be observed between a distinct range of elevation and along a range of slope angles (Figure 4.8). Beginning at the front of a row of large snowdrifts, which laid at about 70 m a.s.l., water typically either flowed on the surface for a few meters before infiltrating into blockstreams or stony and vegetated water tracks. Water tracks ended by feeding into solifluction lobes, which were widespread between 52 m and 57 m a.s.l, while blockstreams bypassed the lobes by flowing around them. Solifluction lobes advanced over colluvium or coarse slope deposits, with few instances of patterned ground over short distances at the toe of the lobes. At 45 m, most of the flow passed through patterned ground, which became vegetated as flow rose closer to the surface, until it seeped into channeled flow, where discharge was measured. Channelled flow then gave way to unchanneled surface flow, which infiltrated the ground into

vegetated water tracks ending into the lake.

The previous description portrayed a general flowpath taken between snowdrifts and seeps, but every site possessed a different arrangement of flow paths (Figure 4.9). Seep B showed a flowpath dominated by water tracks (38%), blockstreams (31%) and patterned ground (24%), while D6 was mostly a mix of patterned ground (40%), colluvium/coarse slope deposits (29%) and water tracks (23%). D3 was clearly dominated by patterned ground (60%) and colluvium/coarse slope deposits (24%), the latter also constituting the greater part of flowpaths upstream from D4 (46%), followed by patterned ground (21%) and water tracks (16%). D4 also had 17% of its length going through a blockstream. Blockstreams were the dominant flowpath in D7 with 78% of the length, the rest being mostly occupied by patterned ground (17%). The exercise was not performed for seep A, but it drains a large, flat area of patterned ground. Upslope from that area, multiple seeps were observed, each with their own flow path (Figure 4.1).

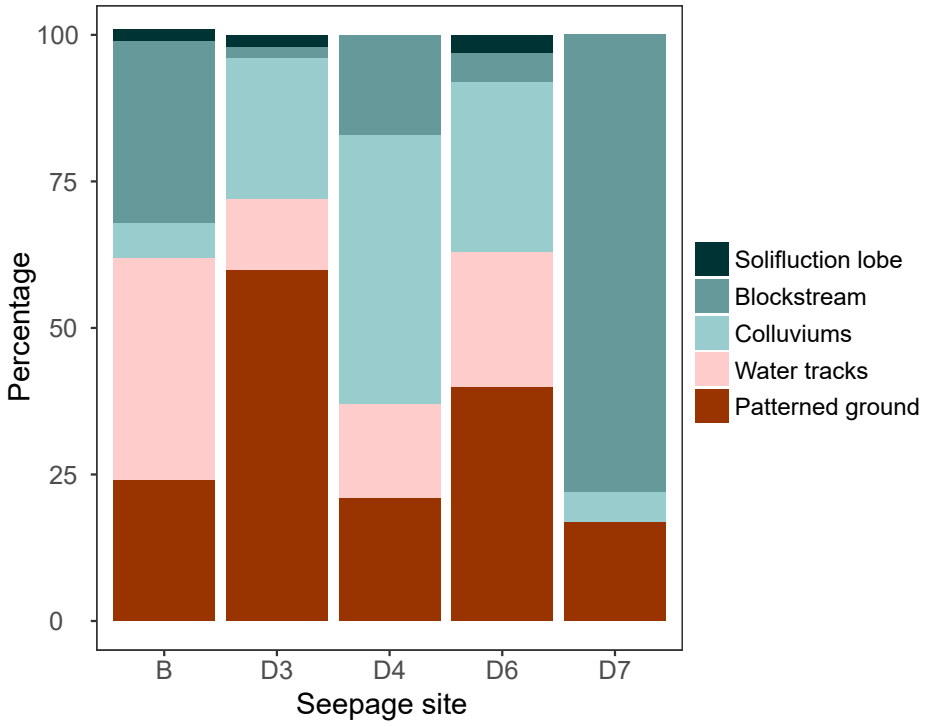

Figure 4.9. Relative distribution of landforms along respective flow paths of seepage sites. See figure 4.1 for sites locations.

4.4. DISCUSSION

4.4.1. Water tracks and slope wash processes

The relation between DSC and discharge gives further insight on the runoff generating processes established in Paquette et al. (2018), namely throughflow in water tracks, and saturation overland flow downstream from flat areas. Solute concentrations reacted similarly in all seeps, except in A, reflecting the daily input of snow meltwater governing the hydrograph. Higher concentrations found during low flow dropped as the hydrograph rose, only to increase again after the hydrograph peaked. This is well shown in the hysteresis curves of seep B and D6 (Figure 4.7e & f), which demonstrated a depleting supply as the hydrograph reached its peak. The hydrograph recession was accompanied by increased solute concentrations, as water travelling more slowly through the system was evacuated. Paquette et al. (2017) have shown that water flowed through the patterned ground in a wedge of gravel and cobble where grain size diminished with depth. Large discharge events in these pathways could therefore activate flow in the coarser, more conductive upper layers, limiting both contact time with sediments and groundwater mixing. Recession flow drained the less conductive parts of the flow paths, where sediment contact time and solute loads were greater. This is in accordance with the throughflow runoff generating process determined for the water track seeps in Paquette et al. (2018). In addition to a daily variation, DSC also showed a slowly rising trend during the melting season. This seasonal trend is concordant with the diminution of direct freshwater inputs from snowmelt and the increase in the relative contribution of soil water as measured with stable isotopes in Paquette et al. (2018).

Seep A DSC behaved uniquely, exposing a transition in flow dynamics during the summer. Hysteresis curves show the first two days of discharge produced clockwise hysteresis (Figure 4.7a). At this point, the runoff generating process is probably troughflow, similar to B and D6. The next four events, however, produced counter-clockwise hysteresis, with opposite DSC behavior during the rise of the hydrograph. The event of 15 June saw a rise in DSC during the rise of the hydrograph (Figure 4.7b), while the event of 17 June showed an initial drop in DSC and a fairly even DSC during the recession (Figure 4.7c). Following the guidelines of Nistor and Church (2005) for

the interpretation of hysteresis curves, this suggests at least three processes of runoff generation possible for this seepage site:

1. Throughflow early in the season, similarly to other seeps
2. Saturation overland flow
3. Throughflow quickly followed by saturation flow through patterned ground

Throughflow (1), as explained above, is caused by preferential flow through coarse sections of patterned ground which are similar to the polygonal and stripe network pictured in Ballantyne (2001). The event of 12 June occurred with relatively shallow active layer development (20 to 40 cm) and therefore little groundwater to evacuate. Much of the water must have flowed through the wedge-shaped coarse sediments of the sorted polygon field just upstream, with little interaction with fine areas of the patterned ground. Saturation overlands flow (2) in turn created return flow conditions where the upstream flat area became flooded, flushing previous event water as discharge rose. Most flow transited on the soil surface and through the coarse area of patterned ground. On 15 June, the active layer was already $>$ 40 cm deep, and the flow event was sufficient to connect both the coarse and the fine portions of the ground. Throughflow followed by saturation flow (3) occured during the event of 17 June (Figure 4.7c) and is schematized in Figure 4.10. It began with a rapid increase in flow through the coarse areas of patterned ground. This caused a (slower) rise in groundwater levels in the fine portions, which then drained more slowly when snowmelt inputs diminished. This process explains why highest DSC occured as discharge diminished, as pore water in the fine section had more time to equilibrate with soil conditions. The low-sloping morphology and mostly subsurface flowpaths also explain the high temperatures in seep A, as soils are left to heat up under the dark biological crust surface, which are known to increase soil temperatures (Gold, 1998). Patterned ground morphology, along with active layer thawing conditions therefore strongly influence flow generation and water properties in this site.

Solute concentrations, dominated by carbonate weathering products early in the season, reflected the lithology of Walker Hill. Daily composition were punctuated by short increases in solute concentrations, which were synchronous to increased ground water contributions as

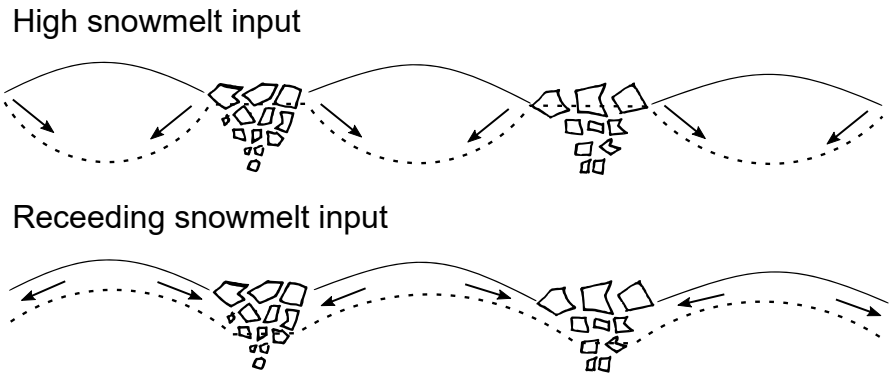

Figure 4.10. Flow dynamics at seep A, showing water table (dashed line) relative to discharge from snowmelt. When snowmelt peaks, water levels are higher in coarse areas of patterned grounds. As snowmelt inputs diminish, water is drained from the surrounding soils through the coarse areas. The bottom situation does not occur in other seeps.

measured by isotopic signature in Paquette et al. (2018). In contrast, permafrost ice possessed much greater solute concentrations. This is often the case in cold permafrost (Kokelj and Burn, 2003, Kokelj and Burn, 2005), as gravity is enough to prevent salt expulsion during upward freezing from the base of the active layer (Baker and Osterkamp, 1989). In this case, however, the ionic ratios and high concentrations suggest a marine influence on solute composition. Seepage sites are all below 40 m. a.s.l., well under the estimated marine transgression limit located $\geq$ 62 m a.s.l. (Lemmen, 1989). Permafrost up to the marine transgression limit therefore contains salt-rich ice that could be inherited from the most recent marine transgression and regression event. The cryosphere has been steadily decaying in the area (Jeffries and Serson, 1983, Mueller et al., 2003, Braun et al., 2004, Antoniades et al., 2005, Paquette et al., 2015), and the activation of seeps in August 2015 showed that the increased summer lengths and warmer temperatures are affecting permafrost. In this context, thawing of the transient layer (Shur et al., 2005) of permafrost during warm summers and of the transition zone in general during warm periods increases salt concentrations in the flowing waters. Similar finding by Roberts et al. (2017) have demonstrated that thermal perturbations in a High Arctic catchment has resulted in up to 500% increases in weathering ion abundance in downstream lakes. These perturbations caused increased soil water contribution to discharge, allowing ionic-rich waters from the top of permafrost to reach surface drainage systems (Lamhonwah et al., 2017). Local disturbances can also increase salinization in dry areas where permafrost was formed under marine conditions

(Kokelj and Lewkowicz, 1999). On Ward Hunt Island, more of this salt-rich permafrost could be found higher in the slope, as evidence suggest drift deposits on Walker Hill date from a more extensive glaciation (Lemmen and England, 1992), which would be associated with greater marine transgressions. With projected increases in temperatures and precipitation in the High Arctic (Bintanja and Andry, 2017), areas where permafrost contains ice formed under marine regressions could see intensifying changes in geochemistry of flowing waters, especially late in the season, with cascading effects on soil geochemistry, lake chemistry, and freshwater ecosystems.

SSC varied largely between seepage sites. Seeps B, D3 and D4 had higher concentrations, while they were low to often non-detectable in seeps A, D6 and D7. At seep B, hysteresis curve of SSC in relation to discharge demonstrated that an initial, very small daily rise in discharge was met with a disproportional increase in SSC, and the clockwise hysteresis suggests a supply-limited delivery system. Nearby seeps D3 and D4 behave similarly with B, as indicated by the significant linear correlation. D6 and D7 had smaller SSC by an order of magnitude, while seep A did not carry a significant amount of sediment. This cannot be linked to flow transport capacity alone, as D7 at times possessed the largest discharge of all seeps, and seep A registered the maximum discharge of all sites. Instead, sediment concentration and yield were influenced by the morphology of the flow paths. In particular, the presence of surface flow and flat areas upslope from A and D6, as well as the dominant flow through a blockstream at D7, likely explain the low SSC. Reports of seepage sites on gravelly terrain in permafrost areas have previously shown they can cause the deposition of fine sediments. Woo and Xia (1995) identified such process on the surface of wetlands at the bottom of a slope near Resolute Bay, Nunavut, at a site that was presented as having a similar drainage system to Ward Hunt Island (Paquette et al. 2017). Fine deposition also typically occurs at the front of snowdrifts in zones of "rillwash" (Ballantyne, 1978, Woo and Steer, 1986, Wilkinson and Bunting, 1975). Our data indicates these flat wetlands are efficient fine sediment sinks, disconnecting the fluxes of sediment from the bottom of the slopes. It therefore appears that on this coarse sediment slope, surface flow occurrence (as in seeps A and D6) inhibits the downslope transfer of sediments, while flow that remains in underground

pathways (seeps B, D3 and D4) favors sediment transfer and slope denudation. This is dependant on local slope morphology, i.e. the presence of a break of slope, of flat areas or of concave-up areas, where seepage can develop. In the case of D7, where subsurface flow is maintained, the low amount of sediments can be explained by the dominant blockstream flow path, which is nowadays mostly devoid of fine sediment. It appears clearly that the aforementioned deduction of Tricart (1967) on the effectiveness of subsurface slopewash is a fundamental aspect of periglacial denudation, and should have been the subject of investigation before this day.

4.4.2. Sediment yield vs other environments

Yield values from studied seepage sites are compared to other studies of permafrost environment in Figure 4.11 (Supporting informations Table 4.I). Total yields are on the low end of the overall scope, while suspended sediment yields sit among the lower half of the range of slope sections at other sites. The denudation rates are 2 to 5 times higher than measured on sandstone slopes of the dry valleys, Antarctica (Summerfield et al., 1999), but in the same range as polar outcrops from a compilation by Portenga and Bierman (2011). Those values are low for sedimentary outcrops, especially for carbonates which should yield more dissolved solids. While the polar desert climate can diminish water inputs and limit yield, it is important to note that some of the studies in this compilation were also performed in polar deserts. Low yields could, to a certain point, be attributed to errors on the watershed size, but even a 50 % increase or decrease of the size of the watersheds would barely move the position of the points on the logarithmic scale. A possible explanation for these low yields is the flow path morphology, which favor rapid transfer of snow meltwater and reduces the contact time needed for chemical weathering and mineral dissolution. Rivers and slope sections with surface runoff will always carry a certain proportion of groundwater, usually below 60 % (Taylor et al., 2002, Boucher and Carey, 2010) which maintains contact with sediments for longer periods and can therefore contribute to the total yield. In this case, however, the nival regime, the efficient transfer of water through the system and the lack of post-snowmelt return flow events caused by rainfall limits the total amount of solutes reaching the

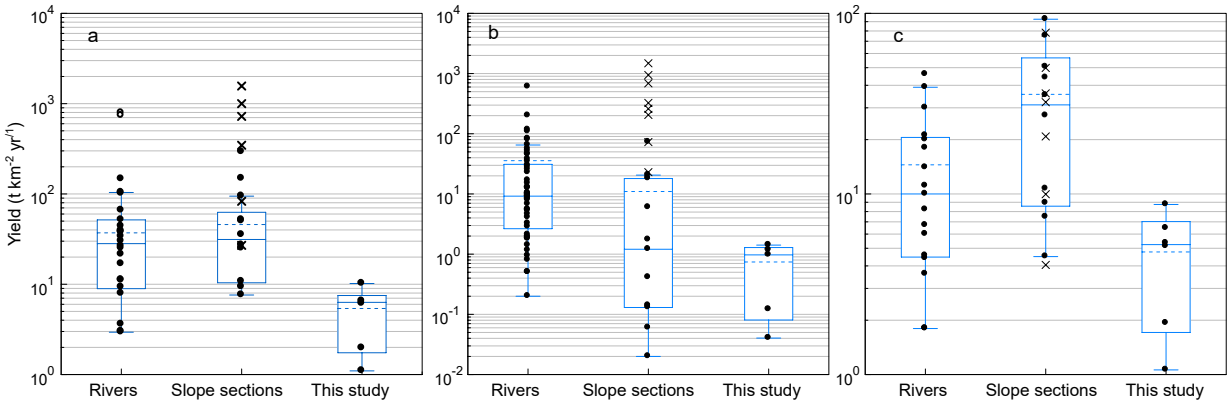

Figure 4.11. Yields from periglacial areas, as reported in the literature. The type of data is separated depending if the research was performed at the plot scale (Slope sections) or in an entire watershed (Rivers). Open circles show values from a paraglacial environment, and x marks show values from disturbed areas; (a): total yield; (b): suspended sediments; (c): dissolved solids. Data and references are available as supporting information Table 4.I.

preferential channels.

It has been established that most of the removal of material occurs by solute transport. The measurement of high turbidity events in the seeps however confirms that the major flow paths such as blockstreams and patterned ground were created by a mix of cryoturbation and leaching of fine sediments (Paquette et al., 2017). This underscores the importance of mechanical, subsurface wash for landform evolution on these slopes. These suspended sediments however only moved for short distances before being re-deposited as surface flow occurred.

The conceptual model of Peltier (1950) presented the periglacial landscapes as dominated by freeze-thaw processes and as areas in which only weak chemical weathering occurs. This model has weakened over the years, after being regularly challenged by field evidence of chemical transport surpassing mechanical wash (Rapp, 1960, Beylich et al., 2005, Milliman and Farnsworth, 2011, Dixon, 2016, Lewkowicz, 1981). Carbonate catchments, such as the one studied here, are especially expected to evolve through dissolution because of the high solubility of carbonates, even considering their high frost susceptibility. While sediment transfers to lakes in streams of a higher order are often considered to be dominated by suspended sediments even in high latitudes (Braun et al., 2000), in this case the occurrence of surface flow on the low slopes effectively

disconnected suspended sediment delivery, essentially making solutes the only inputs into the lake.

4.4.3. Significance for the evolution of Ward Hunt landscape

The characteristics of the sediment system suggest the slope is well adapted to its nival regime. The relatively smooth concave slope, limited amount of suspended sediments, and the well developed, subsurface drainage system are all indicators of a system close to maturity, where the sediment delivery is in equilibrium to periglacial and nival conditions. In this case, solute supplies is dependant on the connectivity of subsurface and surface, while suspended sediment supplies likely depends on weathering rates or on periglacial processes such as cryoturbation in order to disturb local armouring, as recently suggested by Berthling and Etzelmüller (2016). In the most active denudation sites, nivation benches are well entrenched, the backwalls exposing weathered bedrock in some instances. The landscape has therefore exhausted excess paraglacial sediment supplies available at deglaciation, in this case the till veneer. This is expected of small headwater systems, as they tend to re-adjust more rapidly than large ones (Ballantyne, 2002).

This observation is an important one for headwater catchments in this region, as time since deglaciation plays an important role in sediment transport. Ward Hunt Island possesses an uncertain glacial and post-glacial history, limiting our interpretations on own long it took to develop the landscape. Ice retreat begun at least 9.5 ka BP (Lemmen and England, 1992), but the effects of the last glaciation are unknown. According to Lyons and Mielke (1973), glaciers up to 600 m thick covered Ward Hunt Island during the Pleistocene, extending 16 km north of the island into the Arctic Ocean. Further investigation by Lemmen (1989) identified landforms pre-dating Wisconsinian glacial events, and insisted that signs of an extensive glaciation can only be found outside the limit of the last glacial extent. According to this model, the fjords of Northern Ellesmere Island were mostly free of ice, and ice tongues only occupied major valleys on the mainland, limited by aridity and calving. A previous, more extensive glaciation coming from the Grant Land Mountains would have covered Ward Hunt Island, as erratics from that region can be found up to the top of Walker Hill. According to amino acid analysis, this extensive

glaciation occurred at least > 400 000 BP (Lemmen and England, 1992). It is not excluded that very local ice was present on Ward Hunt Island, as is still the case with the adjacent ice rise, but the extent to which these masses could have re-shaped the landscape remains uncertain. The gelifract mantled upper slopes suggest a classic periglacial landscape as envisioned by Łoziński (1909, cited in French (2000)), and probably pre-date Wisconsinian glaciations, but the lower elevations could have been submitted to local ice movement and marine transgressions, leaving behind the discontinuous till veneer found on the slopes. This landscape has therefore reached an advanced state of evolution while adapting to strong nival and periglacial action. Yet, even in a desertic frost-rubble zone such as this, water flow seems to be the principal denudation agent of this slope, constrained by the redistribution of snow cover.

4.4.4. Landform assemblage model

Data from Figures 4.8 and 4.9 was used to establish a conceptual model of nivation slope morphology. In this model, schematized in figure 4.12, denudation mainly occurs below ground, and surface flow is associated with sediment deposition rather than erosion. In the upper sections, snowdrifts provide the bulk of the meltwater, eroding their backslope while channelling water to surface flow in rills. Sediments are deposited as surface flow occurs, and rills become water tracks when water infiltrates the surface to flow between stones, under a moss and algae cover. This part of the model is similar to the model of Ballantyne (1978, 1985) of slopes on Ellesmere island, and of Wilkinson and Bunting (1975) from Cornwallis and Devon Islands. Fine redistribution as surface flow occurs is similar to the process exposed in Thorn (1979). From there however, the subsurface flow can take two pathways. It can follow the path suggested by Verpaelst et al. (2017), where the deposition of fine sediment has created suitable conditions for the formation of solifluction lobes, which diffuses the water thtrough its ridges into a colluvium slope. It can also evolve into a blockstream, which maintains rapid flow because of its large pore sizes. Further downslope, as the soil becomes more frost susceptible, patterned ground begin to appear, at first showing their sorted structure, then increasingly covered by vegetation. This occurs as water is funneled, as pathways merge into stripes. Seepage then occurs as surface flow in rills, which are

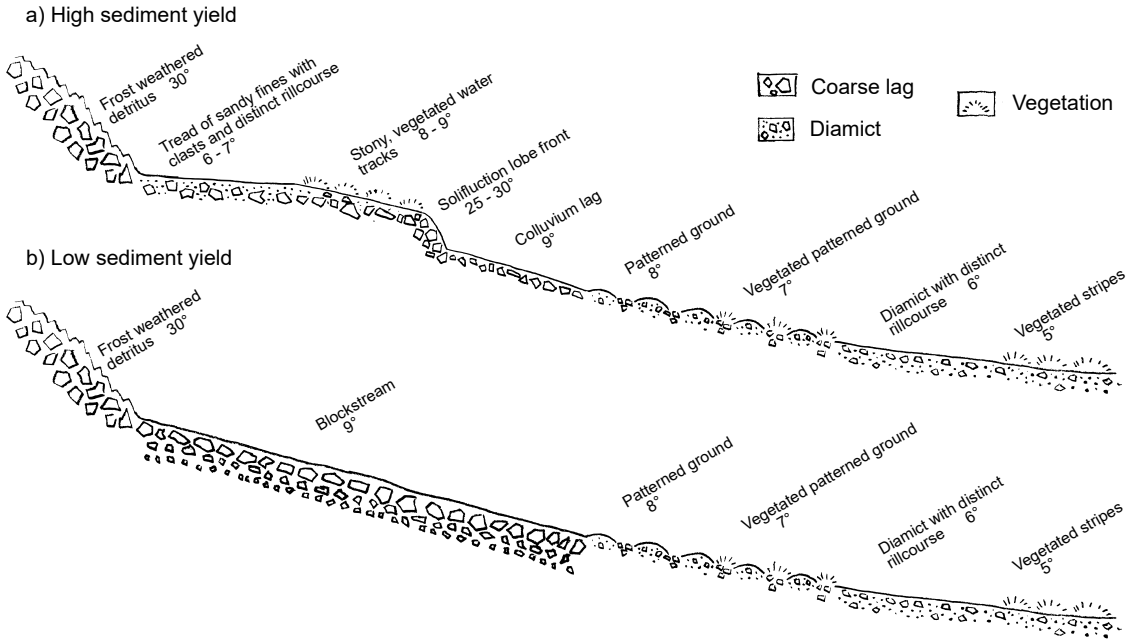

Figure 4.12. Slope profiles showing landform assemblages for seeps with a) high sediment yield (B, D3, D4) and b) low sediment yield (D7). The assemblage in (a) is found in its entirety upslope from the wetland from which seep A emerges. The occurrence of surface flow before the wetland therefore eliminates suspended sediment transport to seep A.

carved in the surface material over a short distance. As surface flow is lost through infiltration, the channels are less incised, fine materials accumulates and vegetation colonize the channel. The soil is then rearranged as non-sorted stripes, through which water flows in gravel conduits as shown in Paquette et al. (2017) until it reaches the lake downslope.

This model shows the sequence of flowpath morphology on a nival polar desert slope, and could be extended to other sites. It is complementary to the polar desert soil wetness classification model created by Woo and Young (2003), which was based on the location of wetlands in the landscape. According to this work, the upper sequence of the model suits a "wetland below a snowbank", and the lower sequence resembles "ground-water-fed wetlands", except for the presence of a lake instead of a pond. The classification as wetlands, in these cases, relates to the abundance of vegetation compared to the deserted surroundings, and in our case is not based on water levels measurements at the site. Also, the appellation of "ground-water-fed wetland" is a bit misleading, as it is also mostly fed by snowmelt from late-lying snowdrifts, but only after the

water has infiltrated and exfiltrated the ground. Both locations possess coarse grained carbonate deposits, and it is possible that this form of slope evolution is partly dependant on lithological controls.

Our measurements add to the examples of features owed to nivation. It is clear that the presence of nivation niches accentuates the development of solifluction lobes in their vicinity, and this is likely caused both by an increase water supply and by fine enrichment as water infiltrates the ground a few meters from the snowdrifts. This suits nivation wash dynamics described by Ballantyne (1985), the conceptual model of Christiansen (1998) and detailed investigation of a solifluction lobe on an adjacent slope (Verpaelst et al., 2017). However, since we lack clear measurements of nivation processes, we cannot state with exactitude its effect on the transport of sediments, other than providing the meltwater necessary for transport.

4.5. Conclusion

This study investigated the potential of preferential flow paths such as water tracks for subsurface wash on a polar desert slope, evaluating the role of this process in slope evolution and matter transfer to downstream systems. Results indicated preferential subsurface flow paths can be important pathways both for suspended and solute transport. Dissolved transport is limited by the short interactions between snowmelt water and soils, while suspended sediment transport is limited by supply and by the flow path morphology. By relating sediment yields with landform occurrence, we established that sediment transport on coarse nival polar desert slopes are mainly caused by subsurface processes, and that surface flow is synonym with sediment deposition and weakened connection between upstream sources and downstream water bodies.

These findings were used to upgrade existing conceptual models of nival slope morphology. Using this model, it is possible to quickly determine locations of sediment supply and deposition in other polar desert areas. Overall, the studied slope showed an advanced state of evolution, and

an adaptation to periglacial and nival conditions which include large local variations in water inputs. Increases in active layer depths and in summer precipitation are expected to occur as climate changes continue in the High Arctic. The occurrence of late-season discharge events during a warm summer showed this system is also adapted to drain water issued from permafrost thaw. However, the modification of water input locations caused by increased rainfall could greatly affect these types of slopes, which are tailored to a completely different precipitation regime. This could involve the development of a new drainage system customized for more widespread inputs, which would include increased erosion as the slope respond to new flow path formation.

4.6. ACKNOWLEDGEMENTS

This research was conducted with the financial support of the Natural Sciences and Engineering Research Council of Canada (NSERC), including the Discovery Frontiers project Arctic Development and Adaptation to Permafrost in Transition (ADAPT); the Networks of Centres of Excellence program ArcticNet; the Canada Research Chair program; the Northern Scientific Training Program; the Canadian Foundation for Innovation: Canadian Northern Studies Trust; Centre d'études nordiques (CEN); and Fond de Recherche du Québec-Nature et Technologie (FRQNT). Logistical support was provided by the Polar Continental Shelf Program (PCSP) and Parks Canada graciously granted us the use of their facility. The authors would like to thank I. de Grandpré, M. Verpaelst, P. Bégin, G. Davesne, A. Veillette and D. Sarrazin for their field assistance.

4.7. SUPPORTING INFORMATIONS

Supporting information Table 4.I. Measurements of catchment exports in permafrost environments, extracted from published sources

Yield (t km^{-2} year^{-1})			Location	Reference
Total	Suspended	Dissolved		
146.0	116.0	30.0	Colville Alaska	Arnborg et al., 1967
44.0	30.0	14.0	Beinbekken North Spitsberg	Barsch et al., 1994
66.0	46.0	20.0	Beinbekken North Spitsberg	Barsch et al., 1994
74.1	19.3	28.9	Hrafndalur, iceland	Beylich and Kneisel, 2009
52.0	42.1	7.8	Austdalur, Iceland	Beylich and Kneisel, 2009
7.3	2.4	4.9	Latnjavagge	Beylich, 2012
3.4	0.3	3.1	Kidisjoki	Beylich, 2012
-	5.5	-	Lena River	Bobrovitskaya and Zubkova, 1998
-	9.9	-	Lena River	Bobrovitskaya and Zubkova, 1998
-	9.0	-	Lena River	Bobrovitskaya and Zubkova, 1998
-	8.4	-	Lena River	Bobrovitskaya and Zubkova, 1998
-	8.2	-	Lena River	Bobrovitskaya and Zubkova, 1998
-	4.1	-	Lena River	Bobrovitskaya and Zubkova, 1998
-	5.3	-	Lena River	Bobrovitskaya and Zubkova, 1998
-	9.8	-	Lena River	Bobrovitskaya and Zubkova, 1998
-	4.6	-	Lena River	Bobrovitskaya and Zubkova, 1998
-	2.1	-	Lena River	Bobrovitskaya and Zubkova, 1998
-	12.7	-	Lena River	Bobrovitskaya and Zubkova, 1998
-	6.7	-	Lena River	Bobrovitskaya and Zubkova, 1998
-	9.1	-	Lena River	Bobrovitskaya and Zubkova, 1998
-	2.0	-	Lena River	Bobrovitskaya and Zubkova, 1998
-	0.9	-	Lena River	Bobrovitskaya and Zubkova, 1998
-	3.2	-	Lena River	Bobrovitskaya and Zubkova, 1998
-	5.3	-	Ob' River	Bobrovitskaya et al., 1996
-	5.4	-	Yenisey	Bobrovitskaya et al., 1996
-	82.0	-	Londonelva Ny-Alesund	Bogen and Bønsnes, 2003
790.0	-	-	Baffin	Church and Ryder, 1972
735.0	-	-	Baffin	Church and Ryder, 1972
16.8	16.8	-	Melville Island	Cockburn and Lamoureux, 2008
51.6	51.6	-	Melville Island	Cockburn and Lamoureux, 2008
7.9	7.9	-	Melville Island	Cockburn and Lamoureux, 2008
37.7	37.7	-	Melville Island	Cockburn and Lamoureux, 2008
9.3	9.3	-	Melville Island	Cockburn and Lamoureux, 2008
33.8	12.7	21.1	Mecham River, Cornwallis Island	Cogley, 1975
101.0	45.0	46.0	Kärkevagge	Dixon, 2016
-	1.8	-	Lord Lindsay River, Boothia Pen.	Forbes and Lamoureux 2005

Yield (t km^{-2} year^{-1})			Location	Reference
Total	Suspended	Dissolved		
-	0.5	-	Lord Lindsay River, Boothia Pen.	Forbes and Lamoureux 2005
-	1.9	-	East Tributary, Boothia Peninsula	Forbes and Lamoureux 2005
-	0.5	-	East Tributary, Boothia Peninsula	Forbes and Lamoureux 2005
-	0.2	-	West Tributary, Boothia Peninsula	Forbes and Lamoureux 2005
-	12.4	-	Lake C2, Ellesmere Island	Hardy, 1996
-	1.4	-	Greenland	Hasholt, 1996
-	56.0	-	Greenland	Hasholt, 1996
11.2	0.8	6.7	Greenland	Hasholt, 2016
-	-	6.0	Greenland	Hasholt, 2016
-	-	18.0	Greenland	Hasholt, 2016
-	15.0	-	Spitsberg	Jahn, 1961
-	18.0	-	Spitsberg snowdrift	Jahn, 1961
37.9	27.9	10.0	Dynamiskbekken West Spitsberg	Kostrzewski et al., 1989
-	109.8	-	Nicolay Lake, Cornwallis Island	Lamoureux, 2000
50.0	6.0	44.0	Ellesmere Island (Eureka)	Lewkowicz and Kokelj, 2002
25.0	20.5	4.5	Ellesmere Island (Eureka)	Lewkowicz and Kokelj, 2002
-	205.0	-	Ellesmere Island (Eureka)	Lewkowicz and Kokelj, 2002
998.0	948.1	49.9	Ellesmere Island (Eureka)	Lewkowicz and Kokelj, 2002
1564.0	1485.8	78.2	Ellesmere Island (Eureka)	Lewkowicz and Kokelj, 2002
347.0	326.2	20.8	Ellesmere Island (Eureka)	Lewkowicz and Kokelj, 2002
27.0	23.0	4.1	Ellesmere Island (Eureka)	Lewkowicz and Kokelj, 2002
83.0	73.0	10.0	Ellesmere Island (Eureka)	Lewkowicz and Kokelj, 2002
721.0	685.0	36.1	Ellesmere Island (Eureka)	Lewkowicz and Kokelj, 2002
293.0	260.8	32.2	Ellesmere Island (Eureka)	Lewkowicz and Kokelj, 2002
39.2	34.6	4.6	Hot weather creek	Lewkowicz and Wolfe, 1994
3.6	1.8	1.8	Hot weather creek	Lewkowicz and Wolfe, 1994
3.0	1.2	1.8	Heather Creek	Lewkowicz and Wolfe, 1994
7.6	0.1	7.5	Banks Island	Lewkowicz, 1981
9.3	0.4	8.9	Banks Island	Lewkowicz, 1981
35.3	0.1	35.2	Banks Island	Lewkowicz, 1981
27.2	0.1	27.1	Banks Island	Lewkowicz, 1981
10.7	0.0	10.7	Banks Island	Lewkowicz, 1981
94.6	1.7	92.9	Banks Island	Lewkowicz, 1981
51.7	1.2	50.5	Banks Island	Lewkowicz, 1981
-	5.4	-	Yenisey	Lisitsyna, 1974
3.0	-	-		Lisitsyna and Alexandrova, 1972
25.0	-	-		Lisitsyna and Alexandrova, 1972
-	605.0	-	Consett Head River, Melville Island	McLaren, 1981
148.0	72.6	75.2	Spitsberg	Mercier et al. 1998
104.0	65.0	39.0	Mackenzie River	Meybeck, 1988

Yield (t km^{-2} year^{-1})			Location	Reference
Total	Suspended	Dissolved		
-	80.0	-	Colville Alaska	Ritchie and Walker, 1974
11.0	2.8	8.2	Graviyka River Siberia 2013	Tananaev
21.5	10.4	11.1	Graviyka River Siberia 2014	Tananaev
1.1	-	1.1		This study
10.2	1.4	8.8	Ward Hunt Island	This study
6.5	1.2	5.3	Ward Hunt Island	This study
6.1	1.0	5.1	Ward Hunt Island	This study
2.0	0.0	1.9	Ward Hunt Island	This study
6.6	0.1	6.5	Ward Hunt Island	This study
-	10.0	-	Iceland	Thomasson 1990, 1991
-	200.0	-	Iceland	Thomasson 1990, 1991
30.0	25.6	4.4	Snowbird Creek, Bathurst Island	Wedel et al., 1997
26.4	22.8	3.6	Whitebear Creek, Bathurst Island	Wedel et al., 1997

Chapitre 5

RAPID DISAPPEARANCE OF PERENNIAL ICE ON CANADA'S MOST NORTHERN LAKE

Abstract

Field records, aerial photographs, and satellite imagery show that the perennial ice cover on Ward Hunt Lake at Canada's northern coast experienced rapid contraction and thinning after at least 50 years of relative stability. On all dates of sampling from 1953 to 2007, 3.5 to 4.3 m of perennial ice covered 65-85 % of the lake surface in summer. The ice cover thinned from 2008 onward, and the lake became ice free in 2011, an event followed by 26 days of open water conditions in 2012. This rapid ice loss corresponded to a significant increase in melting degree days (MDD), from a mean (±SD) of 80.4 (±36.5) MDD (1996-2007) to 136.2 (±16.4) MDD (2008-2012). The shallow bathymetry combined with heat advection by warm inflows caused feedback effects that accelerated the ice decay. These observations show how changes across a critical threshold can result in the rapid disappearance of thick perennial ice.

5.1. INTRODUCTION

1. Introduction The northern cryosphere is experiencing rapid contraction, with pronounced, ongoing losses of ice shelves, sea ice, lake ice, glaciers, ground ice, and summer snow cover

Paquette, M., Fortier, D., Mueller, D. R., Sarrazin, D. et Vincent, W. F. (2015). Rapid disappearance of perennial ice on Canada's most northern lake. *Geophysical Research Letters, 42*(5), 1433-1440. doi: 10.1002/2014GL062960

(Derksen et al., 2012). In the Arctic and elsewhere, the phenology of lake ice cover has been identified as a sensitive indicator of climate change (Magnuson et al., 2000, Duguay et al., 2006). For example, radar satellite imagery of several hundred tundra lakes at Barrow, Alaska, has shown that over a 20 year period (1991-2011) the number of lakes freezing completely to the bottom in winter decreased substantially (Surdu et al., 2014). Polar lakes have long been recognized as sentinels of global climate change (Vincent et al., 1998, Adrian et al., 2009), and the regime shift from perennial (persistence over decades or longer) to multi-year (persistence for $>$ 1 year but rarely $>$ 5 years) to seasonal (annual melt out) ice cover has wide-ranging implications for limnological conditions such as lake temperature, light penetration, primary production, oxygen and nutrient availability, water column mixing, and transport pathways (Veillette et al., 2010). Limnological changes can have cascading effects on biological communities, with a gradual or rapid shift from ecosystems dominated by shallow benthic/pelagic communities to the prevalence of deeper water, planktonic communities (Smol et al., 2005, Quayle et al., 2002).

Several larger lakes in the northern Ellesmere Island region have lost their perennial ice cover in the past decade (Veillette et al., 2010, Mueller et al., 2009), but Ward Hunt Lake (WHL), located at the northern limit of this region, has been consistently reported as having perennial ice cover about 4 m thick, even in late July, beginning with measurements in the early 1950s (Hattersley-Smith et al., 1955). Our objectives in the present study were to bring together and analyze all available data on ice extent and thickness over WHL during the last half of the twentieth century (since 1953), to include our own observations between 2000 and 2014, and to evaluate the factors contributing to the recent disappearance of this perennial ice cover. We compiled all previous records, undertook temperature measurements in the lake and the inflowing waters, produced a detailed bathymetric map and obtained new ice thickness measurements and imagery throughout the year, including by automated camera. As the northernmost lake in Canada, WHL is a latitudinal end-member of interest for examining how polar lakes can undergo regime shifts in ice cover.

5.2. STUDY SITE AND METHODS

WHL (83°03'07"N, 74°10'30"W; Figure 5.1) is located 26 m above sea level on Ward Hunt Island (WHI), off the north coast of Ellesmere Island, Nunavut (supporting information Figure 5.1). This area has a cold, dry climate, with a mean annual air temperature of 18.0 °C, an average air temperature of 33.5 °C in February and +1.5 °C in July (CEN, 2014) , and precipitation of 154 mm yr^{-1}, as measured at Alert, 170 km to the east (Canada, 2014) . Until 2008, WHI was entirely surrounded by thick glacial and marine ice, but recent break-up and disintegration of the Ward Hunt Ice Shelf, have left WHI partially exposed to the Arctic Ocean and Disraeli Bay (Vincent et al., 2011).

WHL is a 0.35 km^2 snow-fed, ultra-oligotrophic lake, with a pH between 7.6 and 8.2 (Villeneuve et al., 2001). WHL ice cover extent had not been surveyed prior to this study, but paleolimnological studies of diatom assemblages and pigment concentrations suggested that the lake likely remained permanently frozen over in summer until at least the nineteenth century (Antoniades et al., 2007). Historical variations in ice cover were estimated using aerial photographs from the Canadian National Air Photo Library (2), oblique photos from previous field expeditions (7), and Radarsat-1 and Radarsat-2 Synthetic Aperture Radar (SAR) imagery (25). Since the backscatter of perennial ice is much higher than first year ice (Mueller et al., 2009), the extent of different ice types was manually digitized from each mid-winter SAR image, with validation from other visual sources when available. Ice thickness was assessed by drilling through the ice cover and measuring with a metal tape from the lower ice surface. We measured water temperature and conductivity (fine structure at centimeter-scale intervals) from 2010 onward, with all temperature measurements performed between 27 June and 1 July. Temperature and conductivity were also measured in water track inflows to the lake in 2011, and discharge was measured in 2013. Air temperature, snow depth, wind conditions, and incoming solar radiation measurements were provided by Parks Canada and by the Centre for Northern Studies (Centre d'études nordiques; CEN) from a weather station located on the northern shore of WHI, 1 km from the lake (CEN,

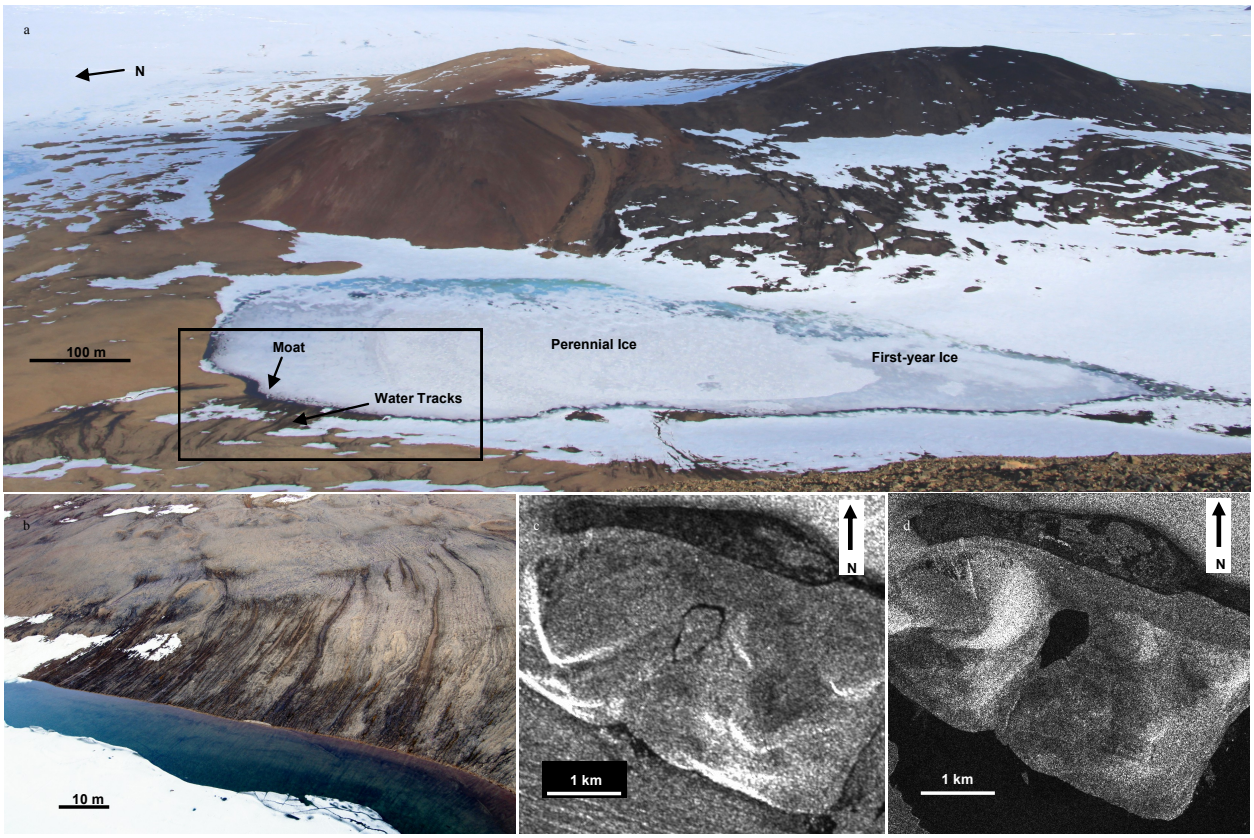

Figure 5.1. Ward Hunt Lake, Nunavut, Canada. a) Photograph from Walker Hill, looking eastwards, 5 July 2009. The first-year ice can be distinguished from the central perennial ice pan that detached from the shore of the lake in summer 2008. Snowmelt had barely begun at the time of the picture and only a small moat created by water flowing from the water tracks (bottom left) had formed. b) Enlarged view of the water tracks and of the inshore moat. c) RADARSAT image of WHL on 9 September 2003, showing the extensive coverage by perennial ice, except around the edges of the lake. d) RADARSAT image on 26 August 2011, showing the complete loss of ice cover over WHL and also the complete loss of the thick ice shelf ice around the southern side of Ward Hunt Island. RADARSAT Data and Products © MacDonald, Dettwiler and Associates Ltd – All Rights Reserved.

2014).

In order to estimate grounded ice area and lake volume, the bathymetry of WHL was measured with Ground Penetrating Radar (GPR) surveys using 50 MHz antennas over the ice cover in early June 2013. Signals were calibrated on three auger holes in the ice and with a common mid-point survey (Jol and Bristow, 2003). Measurements from a total of 14 transects were then spline interpolated to produce a digital elevation model of the lake bottom.

5.3. RESULTS

5.3.1. Ice cover history

Throughout all years of field observations, WHL remained fully ice covered for at least 9.5 months each year, with a moat of open water forming in late June along the northern, western, and southern shores, where slope runoff and near-surface inflows through water tracks spaced about 1 m apart were widespread (Figure 5.1a,b). At other parts of the shoreline, snowdrifts extended from the hillslopes onto the lake, strongly impeding the input of runoff and nearshore melting of lake ice for most of the melting season.

The percentage of ice cover remaining at the end of summer provides a measure corresponding to the perennial ice cover at the beginning of the next year (Figure 5.2a). While WHL was visited almost yearly from 1998 onward, there was no evidence suggesting extensive areas of open water prior to 2008, with perennial ice fluctuating around a mean of 74.8% of lake area as measured prior to that date. The lake ice cover percentage in summer months showed that there was $> 90\%$ ice cover in July and $> 70\%$ in August during much of the record (Figure 5.2b). The year with observations in both July and August (2000) showed only a slight decrease, from 79% to 72% over the 24 day period between 25 July and 18 August.

In 2008 and until 2010, there was a reduction to less than 50% perennial ice, followed by its complete melt out in summer 2011. This warm summer was also the time of extensive break out of the thick land-fast ice of the Ward Hunt Ice Shelf, resulting in open seas around much of WHI for the first time in recorded history (Figure 5.1c versus 5.1d). Images from the automated camera installed on the western lake shore in 2012 revealed a second year of full melt out, with an absence of ice cover for 26 days, from 11 August to 5 September (supporting information Figure 5.2). In contrast, 2013 saw the return of an ice cover lasting through the summer and of multiyear ice conditions.

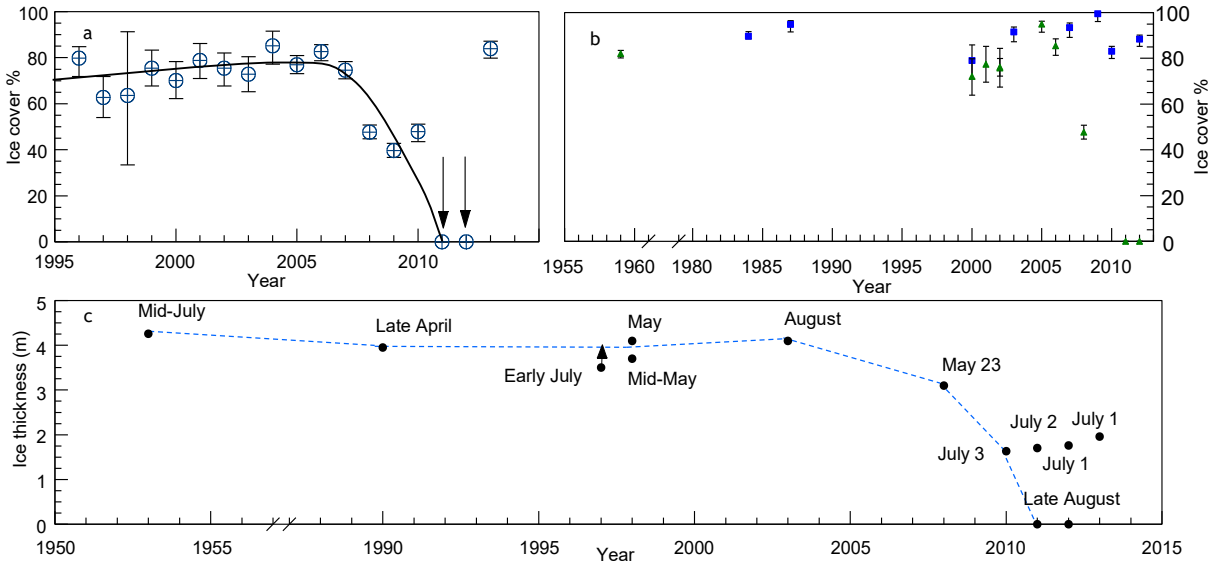

Figure 5.2. Ice over Ward Hunt Lake. a) Ice cover extent at the end of each season; the arrows point to dates of complete disappearance. The values correspond to the "multi year ice" type presented in Supporting Table 1. The curve was fitted visually to the data. b) Lake ice cover phenology during July and August; note the break in the x-axis due to absence of data. Blue squares are July measurements and green triangles are August measurements. The values used correspond to the "summer ice" type as presented in Supporting Table 1. c) Lake ice thickness, annotated with the date of measurement. Note the break in the x-axis due to a lack of data; data for b and c includes unpublished and published data from Antoniades et al. (2007), Hattersley-Smith et al. (1955), King, L., E. Schmidt, and S. Becker (Unpublished Data, 1990), Lemmen, D. S. (Personal communication, 1987); Wharton, R. A., D. T. Andersen, C. Cockell, R. Costello and P. T. Doran (Unpublished data, 1997).

The ice thickness records followed a similar trend to that of ice cover extent. For the decades following the first measurement in 1953, midsummer ice thickness varied between 3.7 and 4.26 m (Figure 5.2c). However, the records since 2008 showed thinning to values of 3.1 m, 1.63 m in 2010, and 1.76 m in 2011, until complete disappearance in August 2011. The ice thickness on 1 July was 1.88 m in 2012 and 1.99 m in 2013. Our measurements at three sampling sites in June 2013 (before the onset of melt) gave a mean thickness of 1.96 m. Ice was thinner (1.53 m) under a 0.55 m thick snow cover, consistent with the low 2010 thickness taken near that location, and thicker (2.30 m) where snow was absent.

5.3.2. Lake and watershed characteristics

Photo interpretation of the watershed of WHL provided an area estimate of 1.82 km^2 and a watershed to lake area ratio of 5.2:1. Snow banks in the watershed are the main water sources for the lake. Water flow paths include surface flow through overland flow and short rills ($<$ 30 m), and near-surface flow through snowmelt-fed water tracks up to a few hundred meters long (Figure 5.1). The lake drains to the sea through a channel 10 to 15 m wide and up to 0.1 m deep located at its southern shore.

The survey of WHL bathymetry (supporting information Figure S3) shows that the deepest part of the lake is on the northeastern side, with a maximum depth of 9.7 m, while the southeastern and western portions have extended shallows less than 3 m deep and a small ridge in the middle of the lake rises to less than 3 m depth. The hypsographic curve for the lake underscores the predominance of shallow waters (supporting information Figure 5.3); water volumes above the 4 and 2 m isobaths, corresponding to the thickness of perennial and seasonal ice respectively, represent 82% and 49% of total lake volume. A 4 m thick perennial ice cover on the lake results in ice being grounded and frozen to the bottom over 55% of the surface area of the lake, a value dropping to 21% under conditions of 2 m thick seasonal ice.

The lake temperature profiles showed large interannual variation (Figure 5.3a). All profiles were taken during a similar time period in late June to early July and, while the 2011 profile had temperatures up to 6 °C, lake temperatures were usually less than 4 °C in other years. Lake water temperatures were coldest in 2013, with a maximum of 2.8 °C near the bottom, reflecting the low-cumulative melting degree days (MDD, the sum of daily mean air temperature above 0 °C) at that moment in the season. Conductivity showed little variation throughout the water column of the lake, with values within the range 200 to 275 µS cm-1 (Figure 3b).

Temperatures in the inflowing water tracks in 2011 reached up to 8.8 °C, with a mean of 6.3 °C (Figure 5.3a), and conductivities from 113 to 196 µS cm^{-1}, with a mean of 140 µS cm^{-1}

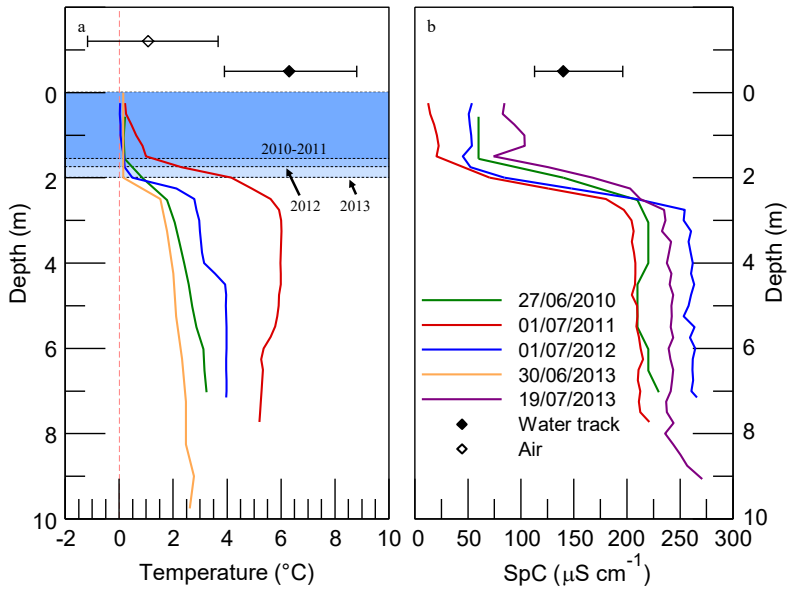

Figure 5.3. Water column profiles in WHL, in late summer 2010 to 2013. Blue areas show ice thickness at time of measurements. a) Water temperature, blue bars represent ice thickness in 2010-11, 2012 and 2013 in order from dark to pale. b) Specific conductivity. Also shown are the temperature and specific conductivity of an inflowing water track, with maximum and minimum values (black diamonds and bars), and the corresponding air temperature range (open diamond and bars). The conductivity profile from 30/06/2013 could not be performed and was replaced by a profile from 19/07/2013.

(Figure 5.3b). These temperatures exceeded air temperatures, which averaged 1.1 °C during the same measurement period and never exceeded 3.6 °C. In 2013, discharge measurements showed a median discharge of 8.18 (± 0.52) x 10^{-5} m^3 s^{-1} (peak discharge of 3.71 (± 0.10) x 10^{-4} m^3 s^{-1}) in a water track over a 22 day period.

The air temperature data from WHI also showed a large amount of interannual variability: MDD varied by up to a factor of 3 between recorded years (Table 1). The MDD values were particularly high in 2003 and in all years from 2008 to 2012. Warm episodes occurred in the month of June in 2008, 2011, and 2012, with maximum air temperatures $>$ 10 °C in each of these years. In comparison, the amount of freezing degree days (the sum of daily mean air temperature below 0 °C) varied between 5992 and 7175, with a mean of 6600, and reached lows in the winters of 2010 and 2011. Incoming solar radiation showed some year to year variability, with a mean of 1758 MW m-2 per summer, ranging between extreme values of 1542 and 1973 MW m-2 in 2012 and 2009, respectively. The amount of MDD did not covary significantly with incoming solar

Table 5. I. Air temperature in degree days and incoming solar radiation in summer at Ward Hunt Island, Nunavut.

	1996	1997	1999	2001	2003	2004	2005	2006	2007	2008	2009	2010	2011	2012	2013	2014	Mean
Month	*Melting degree days*[a]																
June	9.2	1.2	13.7	24.8	15.2	5.5	2.3	13.7	22.8	**56.5**	14.2	28.4	**56.7**	**46.8**	10	10.2	20.7
July	31.4	42	48.5	41.3	**91.3**	30	39	52.9	31	56.3	**69.8**	**77.5**	43.7	**72.8**	34.2	34.2	49.7
August	7	-	-	20.6	**48.2**	21.7	10.9	15.3	28.9	34.7	36.5	13.7	36.5	37.2	11	-	24.8
Total	47.6	-	-	86.7	**154.7**	57.2	52.2	81.9	82.7	147.5	120.5	119.5	136.9	**156.8**	55.2	-	100.0
	Freezing degree days[b]																
Total	6954	6779	6526	7175	6524	7040	6828	6316	6392	6769	6721	**5992**	**6083**	6647	6548	6308	
	Summer Incoming Solar Radiation (MW m^{-2})[c]																
Total	-	-	-	-	-	-	-	1617	1754	1859	**1973**	1696	1862	**1542**	-		1758

[a] **Bold** values exceed the mean by more than one standard deviation. [b] Totals are from the completed winter of that year. **Bold** values are below the mean by more than one standard deviation. [c] **Bold** values exceed the range of one standard deviation from the mean. Missing years had incomplete data and dashes indicate that no data are available.

radiation on a daily, monthly, or yearly basis. A return to cold conditions in summer 2013 (55.2 MDD) resulted in an ice thickness of 2.1 m on 17 July. Incomplete measurements (40.9 MDD on 08 August 2014) suggest that the 2014 summer should allow the 2.05 m thick ice cover to be maintained.

5.4. DISCUSSION

The complete loss of perennial ice from WHL appears to be unprecedented for at least 60 years, but is consistent with other major changes that have recently taken place throughout the Arctic cryosphere. For example, record minimum extent of sea ice over the Arctic Ocean was observed in late summer 2012 (Parkinson and Comiso, 2013), which was also the time of prolonged ice-free conditions on WHL. Large expanses of open water were observed along the northern edge of High Arctic Canada in 2008, along with the collapse of certain ice shelves (Mueller et al., 2009). This was also the year that the WHL ice cover detached from the eastern shore of the lake and then persisted during late summer as a floating ice pan of substantially reduced thickness relative to previous years (Figure 5.2).

The cooler summers at WHI had similar MDD values to certain summers of substantial perennial lake ice ablation in the McMurdo Dry Valleys, Antarctica ; for example, in 2001 and

2002, above-average MDD were recorded at Lake Fryxell, Lake Hoare, and Lake Bonney: 53.9, 57.4, and 99.4 MDD (Doran et al., 2008), with ice cover ablation of 0.67 m, 1.62 m, and 0.59 m, respectively (Dugan et al., 2013). WHI experienced a warm summer in 2003 but there was no apparent change in lake ice thickness. The large variability among these polar lakes and lack of correspondence with MDD values imply other factors in addition to air temperature are likely important in controlling ice melt. Among these factors are the timing of warm events and the repetition of warm summers. In contrast to 2003, the summers of 2008 and 2011 at WHI each began with warm episodes in June (max temperature > 5 °C), while 2012 had 10 days of unusual warming in early to mid-July, in which the maximum temperature reached 18 °C. Such events corresponded to large reductions in measured ice cover. The combination of early summer warm events and a continuous sequence of warm summers is likely to have been pivotal in the WHL regime shift from perennial ice and limited moat development to seasonal ice and full open water conditions in summer. The effects of this combination are likely to result in increased surface ablation by sensible heat influx and increased melt at the ice-water interface due to warmer lake temperatures. Two factors that may influence the increase in lake temperatures other than variation in meteorological forcing are the bathymetry of the lake and its effect on the extent of grounded ice and the timing of moat development as controlled by the input of snowmelt water from the water tracks.

Adams et al. (1989), in a study of Colour Lake on Axel Heiberg Island, argued that similar to ice sheets, lake ice melts from the surface downward, and similarly Dugan et al. (2013) assumed bottom melt to be negligible when evaluating Antarctic lake ice reduction processes, an assumption also made in recent modeling of lake ice phenology and multiyear ice formation (Nolan, 2013). Most of the melting of WHL ice cover likely occurs by surface ablation, and the absence of a clear link between ice melt and incoming solar radiation identifies atmospheric sensible heat flux (rather than radiative heating) as the dominant process in melting the ice cover.

Heron and Woo (1994) demonstrated through measurements and modeling of Small Lake (Cornwallis Island) that about 25% of melting occurred at the ice-water interface, and that the thermal gradient at this interface increased by an order of magnitude during the season, thereby accelerating the bottom melt process. In early July 2011 at WHL, much of the water column under the ice had already warmed to $>$ 5 oC (Figure 5.3a), a temperature similar to those recorded in the water tracks. The temperature gradient at the ice-water interface (upper 0.05 m of the water column) at that time was 60.4 °C m^{-1}. This value is similar to the highest values recorded in Small Lake, when bottom melt accounted for more than 1 cm d^{-1} of melt; applying this loss rate to WHL implies that at least 24% of the ice was lost by underice melting during the remaining 41 days of ice cover. At WHL, and possibly other extreme polar lakes with low air temperatures in summer, a substantial fraction of the ice melting likely occurs at the ice-water interface.

The bathymetric survey of WHL showed that 82% of the lake volume was at depths less than 4 m. This predominance of shallows means that much of the lake ice was grounded in the past, inhibiting bottom water circulation and melting. The extensive grounded ice combined with the cooler early summer temperatures likely explains why WHL has maintained such a thick ice cover prior to 2008. The thinning of the ice from 4 m to 2 m exposed large areas of previously grounded ice cover to heat transfer from the lake water while also uncovering and exposing areas of the littoral zone to heating via direct solar radiation.

The rate at which air temperatures rise above freezing in early summer controls the timing and extent of moat development, which affect lake water temperature by allowing prolonged direct solar warming of the lake water, additional ice melt, and increased open water conditions. This explains the pronounced difference in water temperature between 2011 and 2012. An additional factor that may affect moat development is the advection of heat from the catchment via the numerous shallow water inflows (rills and water tracks), which flow across dark, sunlight-absorbing soil crusts (Steven et al., 2013). The water track thermal record (Figure 3) showed temperatures that were well above air and lake values, and greatest moat development in the lake occurred in the areas adjacent to these inflows. For a water track discharge of 8.2 x 10^{-5} m^3 s^{-1} and a maximum

recorded water temperature in a flowing track of 8.8 °C (4 July 2011), the heat advection to the lake is:

$$q = Q \cdot \rho \cdot C_p \cdot \Delta T \tag{5.1}$$

where q is heat flux (W), Q is discharge (m^3 s^{-1}), ρ is water density (kg m^3), C_p is the heat capacity of water (J kg^{-1} $°C^{-1}$) and ΔT is the difference in temperature (°C). Assuming a lake temperature of 0 °C, the maximum heat flux to the lake from a single water track is equal to 3.05 ± 0.19 kW. This is an order of magnitude higher than the maximum daily average incoming solar radiation flux per m^2 measured at Ward Hunt Island during these 4 days (0.376 kW). Heat advection has been recognized elsewhere as an important factor for ice decay (Williams, 1965, Brown and Duguay, 2010) and this calculation indicates the potential importance of water tracks for the inshore heat budget of the lake, particularly given their abundance along the western shore.

The transition from thick perennial ice to a regime of thin seasonal ice cover with prolonged open water conditions will have many effects on the biophysical and biogeochemical properties of WHL, including greater light availability for primary production and increased nutrient entrainment from deeper waters by wind-induced mixing (Veillette et al., 2010). The seasonal loss of ice cover will also lead to increased water temperatures and evaporation, which could result in the lake level falling below the shallow outflow sill and closure of the lake in late summer when inputs are limited.

The rapid disappearance of lake ice on WHL also raises questions about the fate of perennial ice elsewhere in polar regions. Some lakes in Greenland retain their ice throughout the year (Perren et al., 2012), and many Antarctic lakes, such as those in the McMurdo Dry Valleys, have thick perennial ice (Chinn, 1993, Doran et al., 1994). Our observations from WHL at the northern terrestrial limit of the Canadian High Arctic show the precarious nature of perennial ice and its vulnerability to rapid disappearance through multiple feedback effects once air temperatures begin to warm. This effect may be reversible when summer conditions return to colder temperatures, as

was observed at WHL in 2013, but the accumulation to ice thicknesses $\geq$ 4 m is unlikely under the current and projected regime of long-term warming.

5.5. CONCLUSIONS

WHL maintained a 4 m thick, perennial ice cover from at least the 1950s to the early 21st century. Rapid thinning was observed from 2008 onward, culminating in the complete disappearance of ice cover in the summers of 2011 and 2012. This was associated with recurring warm summer temperatures, elevated early summer air temperatures, warming of the water column beneath the ice, and warm water inflows from the watershed slopes. The shallow bathymetry of the lake results in a large change in area of ice freezing to the bottom of the lake and extensive open water shallows that likely accelerated ice melt. Most of the ice cover is now in contact with liquid water throughout the year and as a result may be more sensitive to interannual variations in climate. These observations underscore the vulnerability of thick perennial ice to rapid thinning and disappearance during periods of warming.

5.6. ACKNOWLEDGEMENTS

Radarsat-1 imagery was provided courtesy of the Alaska Satellite Facility, and Radarsat-2 imagery courtesy of the Canadian Ice Service and the Canadian Space Agency (SOAR program). RADARSAT is an official mark of the Canadian Space Agency. Other data used in this study are available in the Polar Data Catalogue (www.polardata.ca). This research was funded by Natural Sciences and Engineering Research Council of Canada (NSERC), the Networks of Centres of Excellence Program ArcticNet, the Canada Research Chair program, the Northern Scientific Training Program, the Canadian Foundation for Innovation, Canadian Northern Studies Trust, Centre d'études nordiques (CEN) and Fonds de recherche du Québec - Nature et technologies (FRQNT). We also thank the Polar Continental Shelf Program (PCSP) for logistical support, Parks Canada for the use of facilities, and D. Antoniades and two anonymous reviewers for insightful

comments on the manuscript.

5.7. SUPPORTING INFORMATIONS

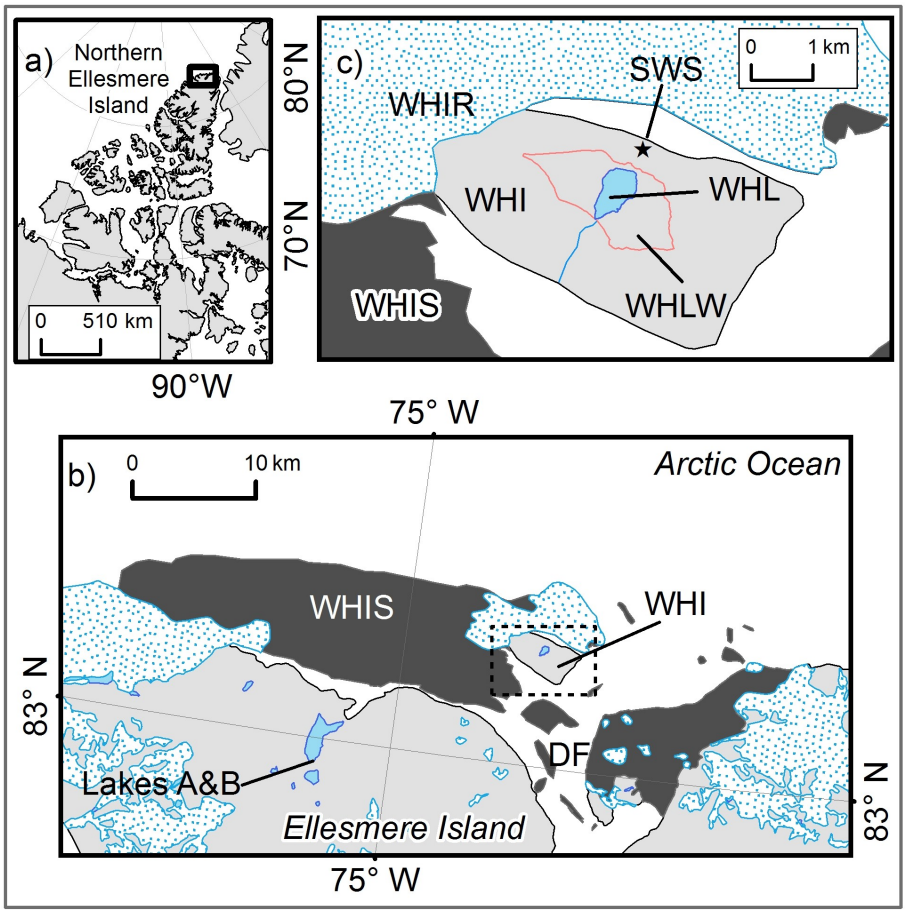

Supporting information figure 5.1. Map of the Ward Hunt Island area. DF: Disraeli Fjord; SWS: CEN weather station (SILA Network); WHI : Ward Hunt Island; WHIR : Ward Hunt Ice Rise; WHIS : Ward Hunt Ice Shelf (extent at the end of summer 2012); WHL: Ward Hunt Lake; WHLW: Ward Hunt Lake watershed.

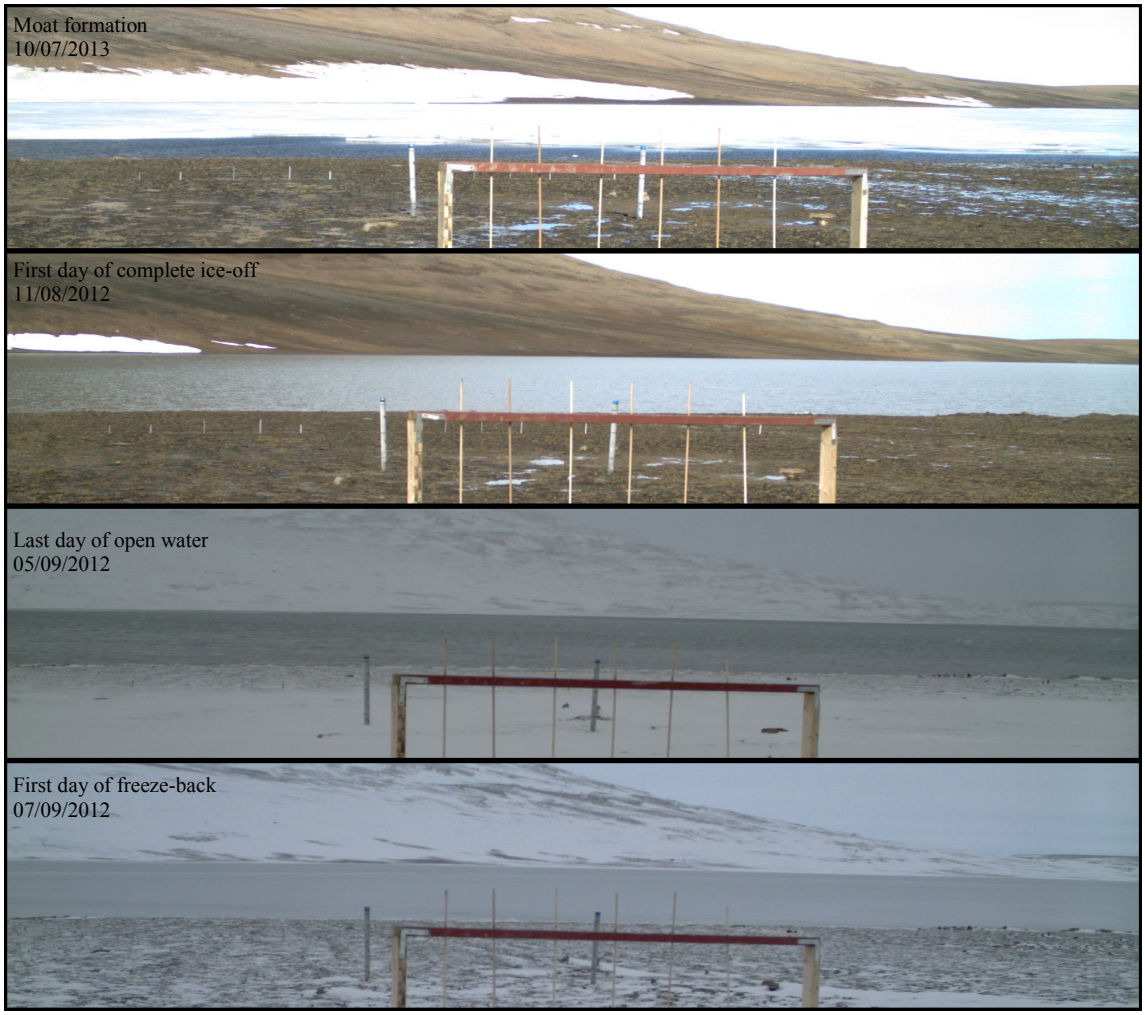

Supporting information figure 5.2. Photographs from a northwest-facing automated camera showing the period of extensive open water conditions in Ward Hunt Lake in late summer 2012. The camera was installed on 10 July, ice-off was complete on 11 August and freeze-up began on 6 September.

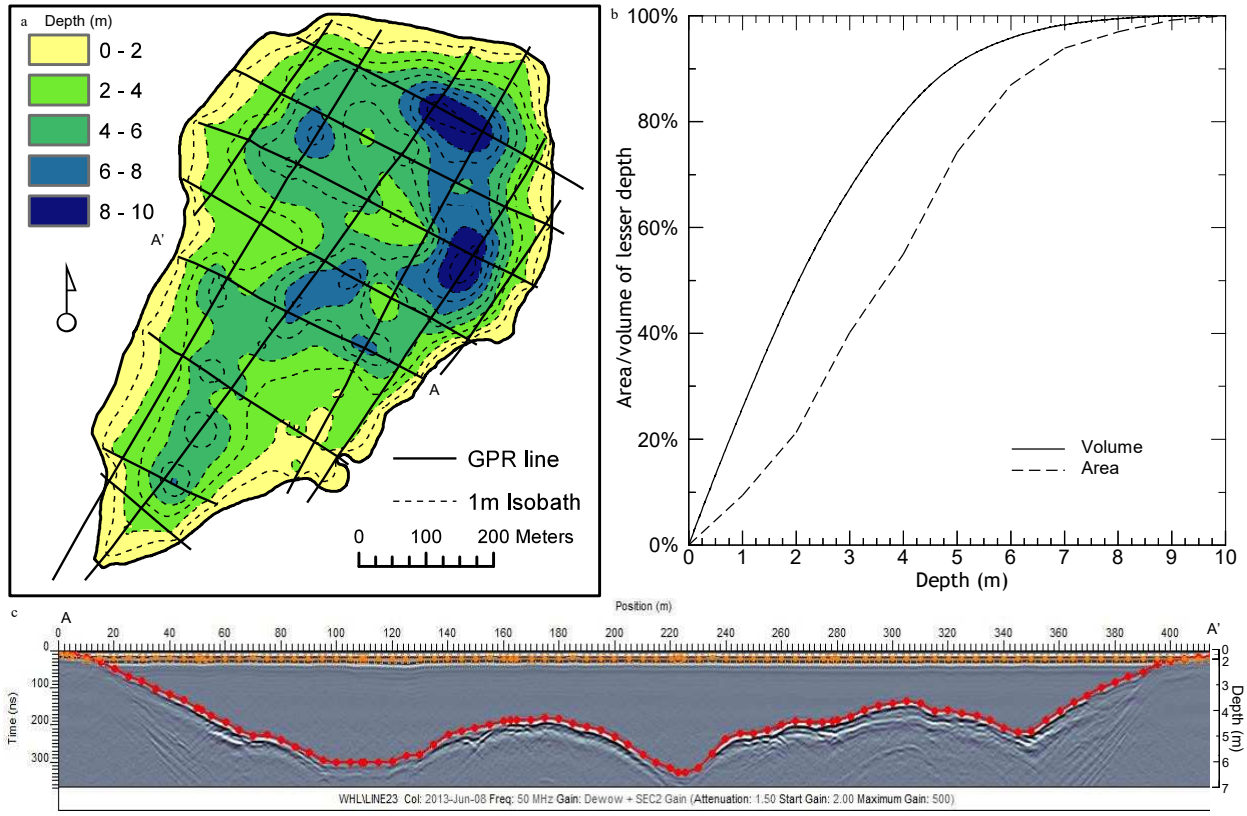

Supporting information figure 5.3. Bathymetric data for Ward Hunt Lake. a) DEM showing the extent of the < 2 m and < 4 m depth zones. b) Hypsographic curves in terms of lake area and volume. (c) An illustrative GPR profile across the lake without topographic corrections, with the colored lines representing the lake bottom (red) and ice/water interface (orange).

Chapitre 6

CONCLUSION

Le terme « périglaciaire », lorsque utilisé en tant que descriptif du paysage, engendre interrogations et remises en question depuis au moins le début des années 1990 (Barsch, 1993 ; Berthling et Etzelmüller, 2011 ; French, 2000 ; French et Thorn, 2006 ; Pissart, 2005). Ces questionnements sont surtout issus de la dérive du terme depuis son utilisation initiale par Łoziński (1909, cité dans Tricart, 1967) afin de désigner des zones de gélifracts créés par l'action intense du gel. Lorsque de nombreux processus et formes dont l'intensité et le développement sont propres au domaine périglaciaire furent ensuite découverts, ils donnèrent naissance à une théorisation de l'évolution du paysage issu de la dominance de ces processus (Peltier, 1950 ; Demek, 1969 ; Selby, 1971). Ces théories négligent cependant l'importance prouvée des processus azonaux, qu'il s'agisse du ruissellement de surface (Ballantyne, 1985 ; Lewkowicz, 1981 ; Mercier, Marlin et Laffly, 1998), de la météorisation chimique (Darmody, Thorn, Harder, Schlyter et Dixon, 2000 ; Rapp, 1960) ou de l'action éolienne (Murton et al., 2015 ; Seppälä, 2004). L'ubiquité de ces processus vient sans doute expliquer l'absence de paysages purement périglaciaires (French 2000 ; 2015), soulevant des questions sur la recevabilité de certains termes associés au périglaciaire, par exemple la nivation (Thorn 1988 ; Thorn et Hall, 2002), et poussant certains à simplement rejetter les processus liés au gel comme agent efficaces de transformation du paysage (André 1999).

L'identification du rôle relatif des processus périglaciaires dans la dynamique d'évolution des paysages est désormais une question à laquelle les géomorphologues des régions froides

doivent faire face. Cette thèse s'attarde ainsi à l'effet de la combinaison des formes périglaciaires avec le processus azonal de ruissellement, ainsi qu'aux fonctions géomorphologiques, hydrologiques, physico-chimiques et thermiques issues de cette évolution du paysage. Le premier chapitre présente quelques notions d'hydrologie périglaciaire, en s'attardant surtout aux chemins d'écoulement préférentiels nommés *water tracks*, ainsi qu'à leur signification pour les transferts de matière. Le second chapitre présente le site d'étude et s'attarde à la morphologie, aux caractéristiques physico-chimiques et à la signification environnementale des *water tracks* pour les déserts polaires. Il réfère à la faible étendue géographique des connaissances sur les *water tracks* présentées au chapitre 1. Le troisième chapitre s'intéresse aux comportements hydrologiques des sources provenant de chemins d'écoulements préférentiels. Il s'attarde à leur régime hydrologique journalier et à leur évolution saisonnière, ainsi qu'aux sources des eaux s'y écoulant. Il démontre ainsi de manière générale les liens entre le régime hydrologique spécifique et les formes de paysage. Le quatrième chapitre concerne les liens entre les formes, les chemins d'écoulements préférentiels et la qualité des eaux qui s'y écoule. On s'y attarde au contenu sédimentaire dissous et en suspension, ainsi qu'à la morphologie de la pente obtenue à travers les relations entre les processus périglaciaires et l'érosion. Ce chapitre lie notamment l'écoulement préférentiel à la présence de formes périglaciaire et à des notions d'évolution de la pente. Il s'inscrit ainsi comme le lien conceptuel entre le sujet spécifique de la thèse et les théories de cryo-conditionnement du paysage vues en introduction. Le cinquième chapitre fait état d'un rôle que joue les chemins d'écoulement préférentiels dans le système limnologique du bassin versant du lac Ward Hunt. Il s'appuie sur la disparition rapide du couvert de glace du lac afin de démontrer le rôle énergétique que peuvent jouer les *water tracks* dans un système comme celui-ci.

De manière générale, la thèse s'attaque autant à la notion de gel/dégel comme butoir de la géomorphologie périglaciaire qu'à l'abandon de la prise en compte des processus périglaciaires lors de l'investigation des paysages froids. Elle ajoute à la pertinence d'une conception des paysages périglaciaires issue de l'interaction des processus périglaciaires et des processus azonaux, surtout en ce qui concerne l'établissement de réseaux de drainages. Les formes

issues du triage ou de la solifluxion peuvent exercer un certain contrôle dans l'établissement du réseau de drainage d'une pente périglaciaire (ch. 2). Il s'ensuit un réseau hydrologique fortement influencé par les conditions climatiques, autant à travers le remodelage des dépôts par l'action périglaciaire intensive (ch. 2) qu'à travers le régime nival dominé par la radiation solaire, rappelant un régime hydrologique glaciaire (ch. 3). La présence de zones d'écoulement préférentiels modifie les propriétés du sol, et peuvent même réduire la profondeur de la couche active en réduisant la température de la surface du sol (ch. 2). Les écoulements souterrains se rapprochent davantage de ceux des *water tracks* d'Alaska que de l'Antarctique (ch.1 et 2), et sont présent à plusieurs autres sites dans l'Arctique (ch. 2). Ce type de réseau est très efficace pour évacuer les eaux de fonte de la neige (ch.3), transportant des sédiments en suspension et des solides dissous de manière comparable aux écoulements de surface mesurés sur d'autres sites possédant du pergélisol (ch. 4). Les liens présentés contredisent les affirmations de Slaymaker (2009) et d'André (1999), qui contestent la fonctionnalité des formes périglaciaires à établir des liens significatifs pour l'évolution du paysage (ch. 4). Le dégel du pergélisol est par ailleurs enregistré dans la signature isotopique (ch. 3), ainsi que géochimique des eaux d'écoulement, indiquant une possible hausse future des transports d'éléments en solution suite aux changements climatiques et à l'approfondissement de la couche active en résultant (ch. 4). Le lien entre les conditions d'écoulement et les conditions limnologiques est également démontré par la formation rapide d'une zone dégelée sur les berges où les écoulements des *water tracks* pénètrent le lac, accélérant le dégel du couvert de glace en modifiant la luminosité et la température des eaux (ch. 5).

Les conclusions de cette thèse sont importantes pour la poursuite de la recherche arctique, surtout en ce qui a trait à l'hydrologie et au transport sédimentaire, mais également lors de la considération des liens entre les écosystèmes et des contrôles de la géomorphologie sur ceux-ci. Au niveau local, la présence de tapis microbiens est surtout relevée dans la zone des *water tracks*, et il apparait désormais clair que leur développement est lié au développement de ces formes. Ces liens pourraient être développés davantage en étudiant les transports de nutriments vers le lac, notamment en mesurant les taux d'oxygénation, la température et autres facteurs régulant

les transports d'azote et de phosphore. De telles recherches permettraient de mesurer de manière tangible le rôle que peut avoir la géomorphologie sur les conditions limnologiques. D'un point de vue plus régional, la présence de chemins d'écoulements préférentiels liant combes à neige et cours d'eau fut relevée un peu partout dans l'Arctique (ch. 2), en plus de nombreux autres sites aperçus lors des transports par avions vers le site d'étude. Il semble donc que ce type de formation est omniprésent comme mode de drainage des combes à neige. Leur efficacité à évacuer de grandes quantités d'eau de fonte de neige a été bien démontré (ch. 3), cependant leur réaction aux événements de pluies, qui répartissent également les précipitations sur l'ensemble du territoire, demeure peu connu. Étant donné les prévisions d'augmentation des pluies intenses dans les déserts polaires au cours du 21e siècle (Bintanja et Andry, 2017), il serait essentiel de voir si ces chemins d'écoulement préférentiels permettront toujours un drainage des pentes efficace lors de ces événements. Dans le cas contraire, l'établissement de nouveaux chemins d'écoulements risquerait d'augmenter l'érosion lors de leur formation.

D'un point de vue plus théorique, cette étude détaillée ne soutient pas la vision d'une géomorphologie périglaciaire uniquement modelée par les effets du gel/dégel sur les sols. Les rôles de la redistribution de la neige et des eaux de ruissellement demeurent essentiels dans ces paysages arides, et sont les facteurs clés pour le transport du matériel. Par contre, l'abandon de la prise en compte des conditions périglaciaires est également à proscrire, car il néglige les processus de triage et de solifluxion permettant d'établir les réseaux de drainage. Elle encourage toutefois l'utilisation du concept de cryo-conditionnement afin d'expliquer ce paysage qui doit son modelé à son histoire glaciaire, post-glaciaire et aux conditions particulièrement froides et arides qui y règnent.

Finalement, il m'apparait important de saisir l'opportunité de mettre en garde contre l'utilisation du terme *water track* en recherche polaire. Les éléments de littérature présentés au chapitre 1 ne font que légèrement état de la confusion qui règne chez les utilisateurs du terme. Cette confusion reflète une désignation de *water tracks* basée en partie sur la forme, en partie sur un

processus particulier et en partie sur la fonction. Du fait de sa naissance en dehors des conditions périglaciaires, son adaptation au domaine périglaciaire s'apparente à une dérive utilitariste possiblement issue de l'impression d'exceptionnalité que posent les conditions périglaciaires. Il apparait clair que ce qui est désigné par *water track* possède en fait une variété inconnue de caractéristiques morphologiques ainsi que de nombreuses fonctionnalités, et les ch. 1 et 2 soulèvent l'absence relative d'élément unificateur pour les définir. Ainsi, les *water tracks* des vallées sèches n'ont pratiquement rien à voir avec celles de Ward Hunt ou de la toundra arctique, et vice-versa. D'un point de vue hydrologique, il conviendrait plutôt d'utiliser le terme existant de « zone d'écoulement préférentiel » ou de « chemin d'écoulement préférentiel » (preferential flow path où preferential flow pathways). Ceux-ci évitent toute référence à une forme, ne sous-entendant aucune contrainte morphologique, et ne laissant que peu de place à l'interprétation. L'acceptation de cette suggestion ne ferait qu'enrichir la recherche sur les zones d'écoulement préférentiels, qui demeurent un aspect fondamental de l'hydrologie, et ce non seulement en milieu périglaciaire.

BIBLIOGRAPHIE

Adams, W., Doran, P., Ecclestone, M., Kingsbury, C. et Allan, C. (1989). A rare second year-lake ice cover in the Canadian High Arctic. *Arctic, 42*(4), 299-306. doi : 10.14430/arctic1670

Adrian, R., O'Reilly, C. M., Zagarese, H., Baines, S. B., Hessen, D. O., Keller, W., . . .Winder, M. (2009). Lakes as sentinels of climate change. *Limnology and Oceanography, 54*(6), 2283-2297. doi : 10.4319/lo.2009.54.6_part_2.2283

André, M.-F. (1999). La livrée périglaciaire des paysages polaires : l'arbre qui cache la forêt ? *Géomorphologie : relief, processus, environnement, 5*(3), 231-251. doi : 10.3406/morfo.1999.990

André, M.-F. (2003). Do periglacial landscapes evolve under periglacial conditions ? *Geomorphology, 52*(1–2), 149-164. doi : 10.1016/S0169-555X(02)00255-6

Antoniades, D., Crawley, C., Douglas, M. S. V., Pienitz, R., Andersen, D., Doran, P. T., . . .Vincent, W. F. (2007). Abrupt environmental change in Canada's northernmost lake inferred from fossil diatom and pigment stratigraphy. *Geophysical Research Letters, 34*(18), L18708. doi : 10.1029/2007gl030947

Antoniades, D., Douglas, M. S. V. et Smol, J. P. (2005). Quantitative estimates of recent environmental changes in the Canadian High Arctic inferred from diatoms in lake and pond sediments. *Journal of Paleolimnology, 33*(3), 349-360. doi : 10.1007/s10933-004-6611-3

Baker, G. C. et Osterkamp, T. E. (1989). Salt redistribution during freezing of saline sand columns at constant rates. *Water Resources Research, 25*(8), 1825-1831. doi : 10.1029/WR025i008p01825

Ball, B. A., Barrett, J. E., Gooseff, M. N., Virginia, R. A. et Wall, D. H. (2011). Implications of meltwater pulse events for soil biology and biogeochemical cycling in a polar desert. *Polar Research, 30*(1), 14555. doi : 10.3402/polar.v30i0.14555

Ballantyne, C. K. (1978). The hydrologic significance of nivation features in permafrost areas. *Geografiska Annaler. Series A, Physical Geography, 60*(1/2), 51-54. doi : 10.2307/520965

Ballantyne, C. K. (1985). Nivation landforms and snowpatch erosion on two massifs in the Northern Highlands of Scotland. *Scottish Geographical Magazine, 101*(1), 40-49. doi : 10.1080/00369228518736611

Ballantyne, C. K. (2001). The sorted stone stripes of Tingo Hill. *Scottish Geographical Journal, 117*(4), 313-324. doi : 10.1080/00369220118737131

Ballantyne, C. K. (2002). Paraglacial geomorphology. *Quaternary Science Reviews, 21*(18–19), 1935-2017. doi : 10.1016/S0277-3791(02)00005-7

Barsch, D. (1993). Periglacial geomorphology in the 21st century. *Geomorphology, 7*(1), 141-163. doi : 10.1016/0169-555X(93)90015-T

Berrisford, M. S. (1991). Evidence for enhanced mechanical weathering associated with seasonally late-lying and perennial snow patches, Jotunheimen, Norway. *Permafrost and Periglacial Processes, 2*(4), 331-340. doi : 10.1002/ppp.3430020408

Berthling, I. et Etzelmüller, B. (2011). The concept of cryo-conditioning in landscape evolution. *Quaternary Research, 75*(2), 378-384. doi : 10.1016/j.yqres.2010.12.011

Berthling, I. et Etzelmüller, B. (2016). The changing cryosphere – implications for solute and sedimentary fluxes in cold climate environments. Dans A. A. Beylich, J. C. Dixon & Z. Zwoliński (dir.), *Source-to-Sink Fluxes in Undisturbed Cold Environments* (p. 11-12). Cambridge : Cambridge University Press.

Beylich, A., Molau, U., Luthbom, K. et Gintz, D. (2005). Rates of chemical and mechanical fluvial denudation in an arctic oceanic periglacial environment, Latnjavagge drainage basin, northernmost Swedish Lapland. *Arctic, Antarctic, and Alpine Research, 37*(1), 75-87. doi :

10.1657/1523-0430(2005)037[0075 :rocamf]2.0.co ;2

Beylich, A. et Warburton, J. (2007). Analysis of source-to-sink-fluxes and sediment budgets in changing high-latitude and high-altitude cold environments. *Sediflux manual (1st ed.), NGU Report*.

Beylich, A. A., Kolstrup, E., Thyrsted, T., Linde, N., Pedersen, L. B. et Dynesius, L. (2004). Chemical denudation in arctic-alpine Latnjavagge (Swedish Lapland) in relation to regolith as assessed by radio magnetotelluric-geophysical profiles. *Geomorphology, 57*(3–4), 303-319. doi : 10.1016/s0169-555x(03)00162-4

Bintanja, R. et Andry, O. (2017). Towards a rain-dominated Arctic. *Nature Climate Change, 7*(4), 263-267. doi : 10.1038/nclimate3240

Blaen, P. J., Hannah, D. M., Brown, L. E. et Milner, A. M. (2014). Water source dynamics of high Arctic river basins. *Hydrological Processes, 28*(10), 3521-3538. doi : 10.1002/hyp.9891

Bockheim, J. G. et Tarnocai, C. (1998). Recognition of cryoturbation for classifying permafrost-affected soils. *Geoderma, 81*(3–4), 281-293. doi : 10.1016/S0016-7061(97)00115-8

Bonilla, S., Villeneuve, V. et Vincent, W. F. (2005). Benthic and planktonic algal communities in a high arctic lake : Pigment structure and contrasting responses to nutrient enrichment1. *Journal of Phycology, 41*(6), 1120-1130. doi : 10.1111/j.1529-8817.2005.00154.x

Boucher, J. L. et Carey, S. K. G. (2010). Exploring runoff processes using chemical, isotopic and hydrometric data in a discontinuous permafrost catchment. *Hydrology Research, 41*(6), 508-519. doi : 10.2166/nh.2010.146

Bowden, W. B., Gooseff, M. N., Balser, A., Green, A., Peterson, B. J. et Bradford, J. (2008). Sediment and nutrient delivery from thermokarst features in the foothills of the North Slope, Alaska : Potential impacts on headwater stream ecosystems. *Journal of Geophysical Research, 113*(G2), G02026. doi : 10.1029/2007jg000470

Bracken, L. J. et Croke, J. (2007). The concept of hydrological connectivity and its contribution to understanding runoff-dominated geomorphic systems. *Hydrological Processes, 21*(13),

1749-1763. doi : 10.1002/hyp.6313

Bracken, L. J., Wainwright, J., Ali, G., Tetzlaff, D., Smith, M., Reaney, S. et Roy, A. (2013). Concepts of hydrological connectivity : Research approaches, pathways and future agendas. *Earth-Science Reviews*, (119), 17-34. doi : 10.1016/j.earscirev.2013.02.001

Braun, C., Hardy, D. R., Bradley, R. S. et Retelle, M. J. (2000). Streamflow and suspended sediment transfer to Lake Sophia, Cornwallis Island, Nunavut, Canada. *Arctic, Antarctic, and Alpine Research, 32*(4) 456-465. doi : 10.2307/1552395

Braun, C., Hardy, D. R., Bradley, R. S. et Sahanatien, V. (2004). Surface mass balance of the Ward Hunt Ice Rise and Ward Hunt Ice Shelf, Ellesmere Island, Nunavut, Canada. *Journal of Geophysical Research : Atmospheres, 109*(D22), D22110. doi : 10.1029/2004JD004560

Brown, L. C. et Duguay, C. R. (2010). The response and role of ice cover in lake-climate interactions. *Progress in Physical Geography, 34*(5), 671-704. doi : 10.1177/0309133310375653

Bunting, B. T. (1961). The role of seepage moisture in soil formation, slope development, and stream initiation. *American Journal of Science, 259*(7), 503-518. doi : 10.2475/ajs.259.7.503

Burn, C. R. et Lewkowicz, A. G. (1990). Canadian landform examples - 17 retrogressive thaw slumps. *Canadian Geographer / Géographe Canadien, 34*(3), 273-276. doi : 10.1111/j.1541-0064.1990.tb01092.x

Caine, T. N. (1963). The origin of sorted stripes in the Lake District. northern England. *Geografiska Annaler, 45*(2/3), 172-179. doi : 10.2307/520392

Carey, S. K. (2003). Dissolved organic carbon fluxes in a discontinuous permafrost subarctic alpine catchment. *Permafrost and Periglacial Processes, 14*(2), 161-171. doi : 10.1002/ppp.444

Carey, S. K. et Quinton, W. L. (2005). Evaluating runoff generation during summer using hydrometric, stable isotope and hydrochemical methods in a discontinuous permafrost alpine catchment. *Hydrological Processes, 19*(1), 95-114. doi : 10.1002/hyp.5764

Carey, S. K., Tetzlaff, D., Seibert, J., Soulsby, C., Buttle, J., Laudon, H., . . .Pomeroy, J. W. (2010). Inter-comparison of hydro-climatic regimes across northern catchments : synchronicity, resistance and resilience. *Hydrological Processes, 24*(24), 3591-3602. doi : 10.1002/hyp.7880

Carey, S. K. et Woo, M.-K. (1999). Hydrology of two slopes in subarctic Yukon, Canada. *Hydrological Processes, 13*(16), 2549-2562. doi : 10.1002/(sici)1099-1085(199911)13 :16<2549 : :aid-hyp938>3.0.co ;2-h

Carey, S. K. et Woo, M.-K. (2000). The role of soil pipes as a slope runoff mechanism, subarctic Yukon, Canada. *Journal of Hydrology, 233*(1), 206-222.

Carey, S. K. et Woo, M.-k. (2001). Slope runoff processes and flow generation in a subarctic, subalpine catchment. *Journal of Hydrology, 253*(1-4), 110-129. doi : 10.1016/s0022-1694(01)00478-4

Carey, S. K. et Woo, M.-k. (2002). Hydrogeomorphic relations among soil pipes, flow pathways, and soil detachments within a permafrost hillslope. *Physical Geography, 23*(2), 95-114. doi : 10.2747/0272-3646.23.2.95

CEN. (2016). Climate station data from Northern Ellesmere Island in Nunavut, Canada, Nordicana D, doi : 10.5885/44985SL-8F203FD3ACCD4138, Repéré à http ://www.cen.ulaval.ca/nordicanad

Chapin, F. S. I., Fetcher, N., Kielland, K., Everett, K. R. et Linkins, A. E. (1988). Productivity and nutrient cycling of alaskan tundra : Enhancement by flowing soil water. *Ecology, 69*(3), 693-702. doi : 10.2307/1941017

Cheng, W. X., Virginia, R. A., Oberbauer, S. F., Gillespie, C. T., Reynolds, J. F. et Tenhunen, J. D. (1998). Soil nitrogen, microbial biomass, and respiration along an arctic toposequence. *Soil Science Society of America Journal, 62*(3), 654-662. doi : 10.2136/sssaj1998.03615995006200030016x

Chinn, T. (1993). Physical hydrology of the dry valley lakes. *Antarctic Research Series, 59*, 1-51. doi : 10.1029/AR059p0001

Christiansen, H. H. (1996). Effects of nivation on periglacial landscape evolution in western Jutland, Denmark. *Permafrost and Periglacial Processes, 7*(2), 111-138.

Christiansen, H. H. (1996). *Nivation forms, processes and sediments in recent and former periglacial areas* (Thèse de doctorat, University of Copenhagen). Repéré à https ://www.researchgate.net/publication/293613705

Christiansen, H. H. (1998). Nivation forms and processes in unconsolidated sediments, NE Greenland. *Earth Surface Processes and Landforms, 23*(8), 751-760.

Church, M. (1974). Hydrology and permafrost with reference to northern North America. *Permafrost hydrology : Proceedings of a Workshop Seminar*, 7-20. Ottawa, Ontario, Canada

Cooper, L. W., Solis, C., Kane, D. L. et Hinzman, L. D. (1993). Application of oxygen-18 tracer techniques to arctic hydrological processes. *Arctic and Alpine Research, 25*(3), 247-255. doi : 10.2307/1551821

Craig, H. (1961). Isotopic variations in meteoric waters. *Science, 133*(3465), 1702-1703. doi : 10.1126/science.133.3465.1702

Curasi, S. R., Loranty, M. M. et Natali, S. M. (2016). Water track distribution and effects on carbon dioxide flux in an eastern Siberian upland tundra landscape. *Environmental Research Letters, 11*(4), 045002. doi : 10.1088/1748-9326/11/4/045002

Dagesse, D. F. (2013). Freezing cycle effects on water stability of soil aggregates. *Canadian Journal of Soil Science, 93*(4), 473-483. doi : doi :10.4141/cjss2012-046

Darmody, R. G., Thorn, C. E., Harder, R. L., Schlyter, J. P. L. et Dixon, J. C. (2000). Weathering implications of water chemistry in an arctic–alpine environment, northern Sweden. *Geomorphology, 34*(1–2), 89-100. doi : 10.1016/S0169-555X(00)00002-7

de Grandpré, I., Fortier, D. et Stephani, E. (2012). Degradation of permafrost beneath a road embankment enhanced by heat advected in groundwater. *Canadian Journal of Earth Sciences, 49*(8), 953-962. doi :10.1139/e2012-018

Dean Jr, W. E. (1974). Determination of carbonate and organic matter in calcareous sediments and sedimentary rocks by loss on ignition : comparison with other methods. *Journal of Sedimentary Research, 44*(1), p. 242-248. doi : 10.1306/74D729D2-2B21-11D7-8648000102C1865D

Demek, J. (1969). Cryoplanation terraces, their geographical distribution, genesis and development. *Praha : Academia nakladatelství ceskoslovenské akademie ved, 79*(4) : 80.

Derksen, C., Smith, S., Sharp, M., Brown, L., Howell, S., Copland, L., ...Tivy, A. (2012). Variability and change in the Canadian cryosphere. *Climatic change, 115*(1), 59-88.

Dixon, J. C. (2016). Contemporary solute and sedimentary fluxes in Arctic and subarctic environments : current knowledge. Dans A. A. Beylich, J. C. Dixon & Z. Zwoliński (dir.), *Source-to-Sink Fluxes in Undisturbed Cold Environments* (p. 39-51). Cambridge, Angleterre : Cambridge University Press.

Dixon, J. C. et Thorn, C. E. (2005). Chemical weathering and landscape development in mid-latitude alpine environments. *Geomorphology, 67*(1–2), 127-145. doi : 10.1016/j.geomorph.2004.07.009

Dixon, J. C., Thorn, C. E. et Darmody, R. G. (1984). Chemical weathering processes on the Vantage peak nunatak, Juneau icefield, southern Alaska. *Physical Geography, 5*(2), 111-131. doi : 10.1080/02723646.1984.10642247

Doran, P. T., McKay, C. P., Fountain, A. G., Nylen, T., McKnight, D. M., Jaros, C. et Barrett, J. E. (2008). Hydrologic response to extreme warm and cold summers in the McMurdo Dry Valleys, East Antarctica. *Antarctic Science, 20*(05), 499-509. doi : doi :10.1017/S0954102008001272

Doran, P. T., Wharton Jr, R. A. et Lyons, W. B. (1994). Paleolimnology of the McMurdo dry valleys, Antarctica. *Journal of Paleolimnology, 10*(2), 85-114. doi : 10.1007/BF00682507

Dugan, H. A., Obryk, M. K. et Doran, P. T. (2013). Lake ice ablation rates from permanently ice-covered Antarctic lakes. *Journal of Glaciology, 59*(215), 491. doi : 10.3189/2013JoG12J080

Duguay, C. R., Prowse, T. D., Bonsal, B. R., Brown, R. D., Lacroix, M. P. et Ménard, P. (2006). Recent trends in Canadian lake ice cover. *Hydrological Processes, 20*(4), 781-801. doi : 10.1002/hyp.6131

Dunn, A. J. et Mehuys, G. R. (1984). Relationship between gravel content of soils and saturated hydraulic conductivity in laboratory tests. Dans J. D. Nichols, P. L. Brown & W. J. Grant (dir.), *Erosion and Productivity of Soils Containing Rock Fragments* (p. 55-63). Madison, É-U : Soil Science Society of America

Dunne, T. et Black, R. D. (1971). Runoff processes during snowmelt. *Water Resources Research, 7*(5), 1160-1172. doi : 10.1029/WR007i005p01160

Dunne, T., Moore, T. R. et Taylor, C. H. (1975). Recognition and prediction of runoff-producing zones in humid regions. *Hydrological Sciences Bulletin, 3*(9), 305-327. Repéré à http ://hydrologie.org/hsj/203/203003.pdf

Dunne, T., Price, A. G. et Colbeck, S. C. (1976). The generation of runoff from subarctic snowpacks. *Water Resources Research, 12*(4), 677-685. doi : 10.1029/WR012i004p00677

Dyke, L. et Egginton, P. (1988). Till behavior and its relationship to active layer hydrology, District of Keewatin, Northwest Territories. *Canadian Geotechnical Journal, 25*(1), 167-172. doi : doi :10.1139/t88-018

Dylik, J. (1968). The significance of the slope in geomorphology. *Bulletin de la société des sciences et des lettres de Łódź, 19*(3), 1-19.

Environment Canada. (2014). Canadian climate normals 1971-2000 station data. Repéré à http ://www.climate.weatheroffice.gc.ca

Environment Canada. (2016). Canadian climate normals 1981-2010 station data. Repéré à http ://www.climate.weatheroffice.gc.ca

Farouki, O. T. (1981). *Thermal properties of soils* (U.S. Army Cold Regions Research Engineering Laboratory Monograph 81-1). Repéré sur le site du Defense Technical Information Center : www.dtic.mil/dtic/tr/fulltext/u2/a111734.pdf

Ferguson, R. I., (1987). Accuracy and precision of methods for estimating river loads. *Earth Surface Processes and Landforms, 12*(1), 95–104. doi : 10.1002/esp.3290120111

Fetter, C. W. (1980). *Applied hydrogeology* (4e éd.). New Jersey, É-U : Prentice Hall.

Fortier, D., Allard, M. et Pivot, F. (2006). A late-Holocene record of loess deposition in ice-wedge polygons reflecting wind activity and ground moisture conditions, Bylot Island, eastern Canadian Arctic. *The Holocene, 16*(5), 635-646. doi : 10.1191/0959683606hl960rp

Fortier, D., Allard, M. et Shur, Y. (2007). Observation of rapid drainage system development by thermal erosion of ice wedges on Bylot Island, Canadian Arctic Archipelago. *Permafrost Periglacial Processes, 18*(3), 229-243. doi : 10.1002/ppp.595

French, H. M. (1987). Periglacial geomorphology in North America : current research and future trends. *Ecological Bulletins*, (38), 5-16. Repéré à http ://www.jstor.org/stable/20112968

French, H. M. (1997). *The Periglacial Environment* (2e éd.). Londres, Angleterre : Longman.

French, H. M. (2000). Does Lozinski's periglacial realm exist today ? A discussion relevant to modern usage of the term 'periglacial'. *Permafrost and Periglacial Processes, 11*(1), 35-42. doi : 10.1002/(SICI)1099-1530(200001/03)11 :1<35 : :AID-PPP334>3.0.CO ;2-6

French, H. M. (2007). *The Periglacial Environment* (3e éd.). Londres, Angleterre : Wiley.

French, H. M. (2015). Do periglacial landscapes exist ? A discussion of the upland landscapes of Northern Interior Yukon, Canada. *Permafrost and Periglacial Processes, 27*(2). doi : 10.1002/ppp.1866

French, H. M. et Thorn, C. E. (2006). The changing nature of periglacial geomorphology. *Géomorphologie : relief, processus, environnement, 12*(3), 165-174. doi : 10.4000/geomorphologie.119

Fryirs, K. (2013). (Dis)Connectivity in catchment sediment cascades : a fresh look at the sediment delivery problem. *Earth Surface Processes and Landforms, 38*(1), 30-46. doi : 10.1002/esp.3242

Genereux, D. (1998). Quantifying uncertainty in tracer-based hydrograph separations. *Water Resources Research, 34*(4), 915-919. doi : 10.1029/98WR00010

Gerke, H. H. (2006). Preferential flow descriptions for structured soils. *Journal of Plant Nutrition and Soil Science, 169*(3), 382-400. doi : 10.1002/jpln.200521955

Glaser, P. H. (1987). The development of streamlined bog islands in the continental interior of North America. *Arctic and Alpine Research, 19*(4), 402-413. doi : 10.2307/1551405

Glaser, P. H., Wheeler, G. A., Gorham, E. et Wright, H. E., Jr. (1981). The patterned mires of the Red Lake peatland, northern Minnesota : Vegetation, water chemistry and landforms. *Journal of Ecology, 69*(2), 575-599. doi : 10.2307/2259685

Goldthwait, R. P. (1976). Frost sorted patterned ground : A review. *Quaternary Research, 6*(1), 27-35. doi : 10.1016/0033-5894(76)90038-7

Gooseff, M. N., Barrett, J. E. et Levy, J. S. (2013). Shallow groundwater systems in a polar desert, McMurdo Dry Valleys, Antarctica. *Hydrogeology Journal, 21*(1), 171-183. doi : 10.1007/s10040-012-0926-3

Gooseff, M. N., McKnight, D. M., Runkel, R. L. et Vaughn, B. H. (2003). Determining long time-scale hyporheic zone flow paths in Antarctic streams. *Hydrological Processes, 17*(9), 1691-1710. doi : 10.1002/hyp.1210

Graf, W. L. (1977). The rate law in fluvial geomorphology. *American Journal of Science, 277*(2), 178-191. doi : 10.2475/ajs.277.2.178

Grosse, G., Schirrmeister, L., Siegert, C., Kunitsky, V. V., Slagoda, E. A., Andreev, A. A. et Dereviagyn, A. Y. (2007). Geological and geomorphological evolution of a sedimentary periglacial landscape in Northeast Siberia during the Late Quaternary. *Geomorphology, 86*(1–2), 25-51.

doi : 10.1016/j.geomorph.2006.08.005

Hall, K., Thorn, C. E., Matsuoka, N. et Prick, A. (2002). Weathering in cold regions : some thoughts and perspectives. *Progress in Physical Geography, 26*(4), 577-603. doi : 10.1191/0309133302pp353ra

Hamlin, L., Pietroniro, A., Prowse, T., Soulis, R. et Kouwen, N. (1998). Application of indexed snowmelt algorithms in a northern wetland regime. *Hydrological Processes, 12*(10-11), 1641-1657. doi : 10.1002/(sici)1099-1085(199808/09)12 :10/11<1641 : :aid-hyp686>3.0.co ;2-w

Hardy, D. R. (1996). Climatic influences on streamflow and sediment flux into Lake C2, northern Ellesmere Island, Canada. *Journal of Paleolimnology, 16*(2), 133-149. doi : 10.1007/BF00176932

Harris, C., Luetschg, M., Davies, M. C. R., Smith, F., Christiansen, H. H. et Isaksen, K. (2007). Field instrumentation for real-time monitoring of periglacial solifluction. *Permafrost and Periglacial Processes, 18*(1), 105-114. doi : 10.1002/ppp.573

Harris, S. A., French, H. M., Heginbottom, J. A., Johnston, G. H., Ladanyi, B., Sego, D. C. et van Everdingen, R. O. (1988). *Glossary of permafrost and selected ground-ice terms* (Mémoire technique No. ACGR-TM-142). Repéré sur le site du Conseil National de la Recherche du Canada http ://nparc.nrc-cnrc.gc.ca/eng/view/fulltext/ ?id=69fb8993-1baa-4225-b33a-6a02341d383d

Hastings, S. J., Luchessa, S. A., Oechel, W. C. et Tenhunen, J. D. (1989). Standing biomass and production in water drainages of the foothills of the Philip Smith Mountains, Alaska. *Holarctic Ecology, 12*(3), 304-311. doi : 10.1111/j.1600-0587.1989.tb00850.x

Hattersley-Smith, G., Crary, A. P. et Christie, R. L. (1955). Northern Ellesmere Island 1953 and 1954. *Arctic, 8*(1), 1-36. doi : 10.14430/arctic3802

Heiri, O., Lotter, A. et Lemcke, G. (2001). Loss on ignition as a method for estimating organic and carbonate content in sediments : reproducibility and comparability of results. *Journal of*

Paleolimnology, 25(1), 101-110. doi : 10.1023/A :1008119611481

Heron, R. et Woo, M.-K. (1994). Decay of a High Arctic lake-ice cover : observations and modelling. *Journal of Glaciology, 40*(135), 283-291. doi : 1994JGlac..40..283H

Hinzman, L. D., Kane, D. L. et Everett, K. R. (1993). Hillslope hydrology in an Arctic setting. *Proceedings of the Sixth International Conference on Permafrost, 1*, 267-271. Repéré à https ://ipa.arcticportal.org/meetings/international-conferences.

Hinzman, L. D., Kane, D. L., Gieck, R. E. et Everett, K. R. (1991). Hydrologic and thermal properties of the active layer in the Alaskan Arctic. *Cold Regions Science and Technology, 19*(2), 95-110. doi : 10.1016/0165-232X(91)90001-W

Hodgson, R. et Young, K. L. (2001). Preferential groundwater flow through a sorted net landscape, Arctic Canada. *Earth Surface Processes and Landforms, 26*(3), 319-328. doi : 10.1002/1096-9837(200103)26 :3<319 : :AID-ESP176>3.0.CO ;2-1

Hoffman, M. J., Fountain, A. G. et Liston, G. E. (2014). Near-surface internal melting : a substantial mass loss on Antarctic Dry Valley glaciers. *Journal of Glaciology, 60*(220), 361-374. doi : 10.3189/2014JoG13J095

Hope, A. S., Kimball, J. S. et Stow, D. A. (1993). The relationship between tussock tundra spectral reflectance properties and biomass and vegetation composition. *International Journal of Remote Sensing, 14*(10), 1861-1874. doi : 10.1080/01431169308954008

Horwath, J. L., Sletten, R. S., Hagedorn, B. et Hallet, B. (2008). Spatial and temporal distribution of soil organic carbon in nonsorted striped patterned ground of the High Arctic. *Journal of Geophysical Research : Biogeosciences, 113*(G3), G03S07. doi : 10.1029/2007JG000511

IAEA/WMO. (2017). *Global Network of Isotopes in Precipitation. The GNIP Database*. Accessible dans The GNIP Database. Repéré à http ://www.iaea.org/water

Ingram, H. A. P. (1967). Problems of hydrology and plant distribution in mires. *Journal of Ecology, 55*(3), 711-724.

Jahn, A. (1961). Quantitative analysis of some periglacial processes in Spitsbergen. *Nauka O Ziemi II, seria B*(5), 3-34.

Jeffries, M. O. et Serson, H. (1983). Recent changes at the front of Ward Hunt Ice Shelf, Ellesmere Island, N.W.T. *Arctic, 36*(3), 289-290. doi : 10.14430/arctic2278

Jol, H. M. et Bristow, C. S. (2003). GPR in sediments : advice on data collection, basic processing and interpretation, a good practice guide. *Geological Society, London, Special Publications, 211*(1), 9-27. doi : 10.1144/gsl.sp.2001.211.01.02

Jones, A. (1971). Soil piping and stream channel initiation. *Water Ressources Research, 7*(3), 602-610. doi : 10.1029/WR007i003p00602

Jones, J. A. A. (1987). The effects of soil piping on contributing areas and erosion patterns. *Earth Surface Processes and Landforms, 12*(3), 229-248. doi : 10.1002/esp.3290120303

Jorgenson, M. T. (1984). The response of vegetation to landscape evolution on glacial till near Toolik Lake, Alaska. *Proceedings of the Society of American Forestry Regional Technical Conference*, 134-141.

Jorgenson, M. T., Shur, Y. et Osterkamp, T. E. (2008). Thermokarst in Alaska. *Proceedings of the Ninth International Conference on Permafrost, 1*, 869-876. Repéré à https ://ipa.arcticportal.org/meetings/international-conferences.

Kane, D. L., Hinzman, L. D., Benson, C. S. et Liston, G. E. (1991). Snow hydrology of a headwater Arctic basin. 1. Physical measurements and process studies. *Water Resources Research, 27*,(6), 1099-1109. doi : 10.1029/91WR00262

Kanevskiy, M., Shur, Y., Strauss, J., Jorgenson, T., Fortier, D., Stephani, E. et Vasiliev, A. (2016). Patterns and rates of riverbank erosion involving ice-rich permafrost (yedoma) in northern Alaska. *Geomorphology, 253*, 370-384. doi : 10.1016/j.geomorph.2015.10.023

Kessler, M. A. et Werner, B. T. (2003). Self-organization of sorted patterned ground. *Science, 299*(5605), 380-383. doi : 10.1126/science.1077309

King, L., Schmidt, E. et Becker, S. (1990). *Ward Hunt Island logbook*. Document inédit.

Klatkowa, H. (1965). Niecki i doliny denudacyjne w okolicach Łodzi. *Acta Geographica Lodziensia, 19*, 141 p.

Kokelj, S. V. et Burn, C. R. (2003). Ground ice and soluble cations in near-surface permafrost, Inuvik, Northwest Territories, Canada. *Permafrost and Periglacial Processes, 14*(3), 275-289. doi : 10.1002/ppp.458

Kokelj, S. V. et Burn, C. R. (2005). Geochemistry of the active layer and near-surface permafrost, Mackenzie delta region, Northwest Territories, Canada. *Canadian Journal of Earth Sciences, 42*(1), 37-48. doi : doi :10.1139/e04-089

Kokelj, S. V. et Lewkowicz, A. G. (1999). Salinization of permafrost terrain due to natural geomorphic disturbance, Fosheim Peninsula, Ellesmere Island. *Arctic, 52*(4), 372-385. doi : 10.2307/40511752

Kokelj, S. V., Smith, C. A. S. et Burn, C. R. (2002). Physical and chemical characteristics of the active layer and permafrost, Herschel Island, western Arctic Coast, Canada. *Permafrost and Periglacial Processes, 13*(2), 171-185. doi : 10.1002/ppp.417

Kung, K. J. S. (1990). Preferential flow in a sandy vadose zone : 2. Mechanism and implications. *Geoderma, 46*(1), 59-71. doi : 10.1016/0016-7061(90)90007-V

Lacelle, D. (2011). On the δ^{18}O, δD and D-excess relations in meteoric precipitation and during equilibrium freezing : theoretical approach and field examples. *Permafrost and Periglacial Processes, 22(*1), 13-25. doi : 10.1002/ppp.712

Lamhonwah, D., Lafrenière, M. J., Lamoureux, S. F. et Wolfe, B. B. (2017). Evaluating the hydrological and hydrochemical responses of a High Arctic catchment during an exceptionally warm summer. *Hydrological Processes, 31*(12), 2296-2313. doi : 10.1002/hyp.11191

Lee, J., Feng, X., Posmentier, E. S., Faiia, A. M. et Taylor, S. (2009). Stable isotopic exchange rate constant between snow and liquid water. *Chemical Geology, 260*(1–2), 57-62. doi :

10.1016/j.chemgeo.2008.11.023

Lemmen, D. S. (1988). The glacial history of Marvin Peninsula, northern Ellesmere Island, and Ward Hunt Island, High Arctic Canada. (Thèse de doctorat, University of Alberta, Edmonton, Canada). Accessible par ProQuest Dissertations & Theses. (275653863)

Lemmen, D. S. (1989). The last glaciation of Marvin Peninsula, northern Ellesmere Island, High Arctic, Canada. *Canadian Journal of Earth Sciences, 26*(12), 2578-2590. doi : 10.1139/e89-220

Lemmen, D. S. et England, J. (1992). Multiple glaciations and sea level changes, northern Ellesmere Island, High Arctic Canada. *Boreas, 21*(2), 137-152. doi : 10.1111/j.1502-3885.1992.tb00021.x

Levy, J. S., Fountain, A. G., Gooseff, M. N., Barrett, J. E., Vantreese, R., Welch, K. A., . . .Wall, D. H. (2013). Water track modification of soil ecosystems in the Lake Hoare basin, Taylor Valley, Antarctica. *Antarctic Science, 26*(2), 1-10. doi : 10.1017/S095410201300045X

Levy, J. S., Fountain, A. G., Gooseff, M. N., Welch, K. A. et Lyons, W. B. (2011). Water tracks and permafrost in Taylor Valley, Antarctica : Extensive and shallow groundwater connectivity in a cold desert ecosystem. *Geological Society of America Bulletin, 123*(11-12), 2295-2311. doi : 10.1130/b30436.1

Levy, J. S. et Schmidt, L. M. (2016). Thermal properties of Antarctic soils : wetting controls subsurface thermal state. *Antarctic Science, 28*(5), 361-370. doi : 10.1017/S0954102016000201

Lewis, T., Lafrenière, M. J. et Lamoureux, S. F. (2012). Hydrochemical and sedimentary responses of paired High Arctic watersheds to unusual climate and permafrost disturbance, Cape Bounty, Melville Island, Canada. *Hydrological Processes, 26*(13), 2003-2018. doi : 10.1002/hyp.8335

Lewkowicz, A. G. (1981). *A study of slopewash processes in the continuous permafrost zone, Banks Island, Western Canadian Arctic* (Thèse de doctorat, University of Ottawa, Ottawa, Canada). Accessible par ProQuest Dissertations & Theses. (89240626)

Lewkowicz, A. G. et French, H. M. (1982). The hydrology of small runoff plots in an area of continuous permafrost, Banks Island, N.W.T. *Proceedings of the 4th Canadian Permafrost*

Conference, 151-162. Repéré à pubs.aina.ucalgary.ca/cpc/CPC4-151.pdf.

Lewkowicz, A. G. et Young, K. L. (1990a). Hydrological processes in a small catchment containing a perennial snowbank, Melville Island, N.W.T. *Northern Hydrology, Selected Perspectives, Proceedings of the NHRI Symposium No. 6*, 237–251.

Lewkowicz, A. G. et Young, K. L. (1990b). Hydrology of a perennial snowbank in the continuous permafrost zone, Melville Island, Canada. *Geografiska Annaler. Series A. Physical Geography, 72*(1), 13-21. doi : 10.2307/521234

Łoziński, W. V. (1912). Die periglaziale Fazies der mechanischen Verwitterung. *Comptes Rendus du XI Congrès International de Géologie*. 1039-1053.

Lyons, J. B. et Mielke, J. E. (1973). Holocene history of a portion of northernmost Ellesmere Island. *Arctic, 26*(4), 10. doi : 10.14430/arctic2930

Mackay, J. R. (1980). The origin of hummocks, western Arctic coast, Canada. *Canadian Journal of Earth Sciences, 17*(8), 996-1006. doi : 10.1139/e80-100

Mackay, J. R. (1984). The frost heave of stones in the active layer above permafrost with downward and upward freezing. *Arctic and Alpine Research, 16*(4), 439-446. doi : 10.2307/1550906

Magnuson, J. J., Robertson, D. M., Benson, B. J., Wynne, R. H., Livingstone, D. M., Arai, T., …Vuglinski, V. S. (2000). Historical trends in lake and river ice cover in the Northern Hemisphere. *Science, 289*(5485), 1743-1746. doi : 10.1126/science.289.5485.1743

Marsh, P. et Woo, M.-K. (1984). Wetting front advance and freezing of meltwater within a snow cover : 1. Observations in the Canadian Arctic. *Water Resources Research, 20*(12), 1853-1864. doi : 10.1029/WR020i012p01853

Matthes-Sears, U., Matthes-Sears, W. C., Hastings, S. J. et Oechel, W. C. (1988). The effects of topography and nutrient status on the biomass, vegetative characteristics, and gas exchange of two deciduous shrubs on an Arctic tundra slope. *Arctic and Alpine Research, 20*(3), 342-351. doi : 10.2307/1551266

McNamara, J. P., Kane, D. L. et Hinzman, L. D. (1997). Hydrograph separations in an arctic watershed using mixing model and graphical techniques. *Water Resources Research, 33*(7), 1707-1719. doi : 10.1029/97wr01033

McNamara, J. P., Kane, D. L. et Hinzman, L. D. (1998). An analysis of streamflow hydrology in the Kuparuk River Basin, Arctic Alaska : a nested watershed approach. *Journal of Hydrology, 206*(1–2), 39-57. doi : 10.1016/s0022-1694(98)00083-3

McNamara, J. P., Kane, D. L. et Hinzman, L. D. (1999). An analysis of an arctic channel network using a digital elevation model. *Geomorphology, 29*(3–4), 339-353. doi : 10.1016/s0169-555x(99)00017-3

McNamara, J. P., Kane, D. L., Hobbie, J. E. et Kling, G. W. (2008). Hydrologic and biogeochemical controls on the spatial and temporal patterns of nitrogen and phosphorus in the Kuparuk River, arctic Alaska. *Hydrological Processes, 22*(17), 3294-3309. doi : 10.1002/hyp.6920

Mercier, D., Marlin, C. et Laffly, D. (1998). Ruissellement et érosion en milieu polaire océanique : exemple du bassin-versant du Zeppelinfjellet, Presqu'île de Brøgger, Spitsberg nord-occidental (79°N). *Cahiers Nantais*(49), 159-179. Repéré à https ://www.researchgate.net/publication/278404054

Milliman, J. D. et Farnsworth, K. L. (2011). *River discharge to the coastal ocean : a global synthesis*. Cambridge, England : Cambridge University Press.

Morgenstern, A. (2012). *Thermokarst and thermal erosion : Degradation of Siberian ice-rich permafrost* (Thèse de doctorat, University of Potsdam, Potsdam, Allemagne). Repéré à https ://publishup.uni-potsdam.de/frontdoor/index/index/docId/5988

Mueller, D., Copland, L. et Jeffries, M. O. (2017). Changes in Canadian arctic ice shelf extent since 1906. Dans L. Copland & D. Mueller (dir.), *Arctic Ice Shelves and Ice Islands* (p. 109-148). Dordrecht, Pays-Bas : Springer Netherlands.

Mueller, D. R., Van Hove, P., Antoniades, D., Jeffries, M. O. et Vincent, W. F. (2009). High Arctic lakes as sentinel ecosystems : Cascading regime shifts in climate, ice cover, and mixing.

Limnology and Oceanography, 54(6), 2371-2385. doi : 10.4319/lo.2009.54.6_part_2.2371

Mueller, D. R., Vincent, W. F. et Jeffries, M. O. (2003). Break-up of the largest Arctic ice shelf and associated loss of an epishelf lake. *Geophysical Research Letters, 30*(20), 2031. doi : 10.1029/2003gl017931

Murton, J. B., Goslar, T., Edwards, M. E., Bateman, M. D., Danilov, P. P., Savvinov, G. N., . . . Wolfe, S. A. (2015). Palaeoenvironmental interpretation of yedoma silt (ice complex) deposition as cold-climate loess, Duvanny Yar, northeast Siberia. *Permafrost and Periglacial Processes, 26*(3), 208-288. doi : 10.1002/ppp.1843

Nelson, F. E. (1989). Cryoplanation terraces : Periglacial cirque analogs. *Geografiska Annaler. Series A, Physical Geography, 71*(1/2), 31-41. doi : 10.2307/521006

Nicholson, F. (1978). Permafrost distribution and characteristics near Schefferville, Quebec : Recent studies. *Proceedings of the 3rd International Conference on Permafrost*, 428-433. Repéré à https ://ipa.arcticportal.org/meetings/international-conferences.

Nicholson, F. H. (1976). Patterned ground formation and description as suggested by low arctic and subarctic examples. *Arctic and Alpine Research, 8*(4), 329-342. doi : 10.2307/1550437

Nistor, C. J. et Church, M. (2005). Suspended sediment transport regime in a debris-flow gully on Vancouver Island, British Columbia. *Hydrological Processes, 19*(4), 861-885. doi : 10.1002/hyp.5549

Nolan, M. (2013). Quantitative and qualitative constraints on hind-casting the formation of multiyear lake-ice covers at Lake El'gygytgyn. *Climate of the Past, 9*(3), 1253-1269. doi : 10.5194/cp-9-1253-2013

Oberbauer, S. F., Hastings, S. J., Beyers, J. L. et Oechel, W. C. (1989). Comparative effects of downslope water and nutrient movement on plant nutrition, photosynthesis, and growth in Alaskan tundra. *Holarctic Ecology, 12*(3), 324-334. doi : 10.1111/j.1600-0587.1989.tb00853.x

Oberbauer, S. F., Tenhunen, J. D. et Reynolds, J. F. (1991). Environmental effects on CO_2 efflux from water track and tussock tundra in arctic Alaska, U.S.A. *Arctic and Alpine Research, 23*(2),

162-169. doi : 10.2307/1551380

Obradovic, M. M. et Sklash, M. G. (1986). An isotopic and geochemical study of snowmelt runoff in a small arctic watershed. *Hydrological Processes, 1*(1), 15-30. doi : 10.1002/hyp.3360010104

O'Neil, J. R. (1968). Hydrogen and oxygen isotope fractionation between ice and water. *The Journal of Physical Chemistry, 72*(10), 3683-3684. doi : 10.1021/j100856a060

Osterkamp, T. E. (2005). The recent warming of permafrost in Alaska. *Global and Planetary Change, 49*(3–4), 187-202. doi : 10.1016/j.gloplacha.2005.09.001

Osterkamp, T. E. (2007). Characteristics of the recent warming of permafrost in Alaska. *Journal of Geophysical Research, 112*(F2), F02S02. doi : 10.1029/2006jf000578

Osterkamp, T. E., Jorgenson, M. T., Schuur, E. A. G., Shur, Y. L., Kanevskiy, M. Z., Vogel, J. G. et Tumskoy, V. E. (2009). Physical and ecological changes associated with warming permafrost and thermokarst in Interior Alaska. *Permafrost and Periglacial Processes, 20*(3), 235-256. doi : 10.1002/ppp.656

Paquette, M., Fortier, D., Mueller, D. R., Sarrazin, D. et Vincent, W. F. (2015). Rapid disappearance of perennial ice on Canada's most northern lake. *Geophysical Research Letters, 42*(5), 1433-1440. doi : 10.1002/2014GL062960

Paquette, M., Fortier, D. et Vincent, W. F. (2017). Water tracks in the High Arctic : a hydrological network dominated by rapid subsurface flow through patterned ground. *Arctic Science, 3*(2), 334-353. doi : 10.1139/as-2016-0014

Paquette, M., Fortier, D. et Vincent, W. F. (2018). Hillslope water tracks in the High Arctic : Seasonal flow dynamics with changing water sources in preferential flow paths. *Hydrological Processes, 32*(8), 1077-1089. doi : 10.1002/hyp.11483

Parkinson, C. L. et Comiso, J. C. (2013). On the 2012 record low Arctic sea ice cover : Combined impact of preconditioning and an August storm. *Geophysical Research Letters, 40*(7), 1356-1361. doi : 10.1002/grl.50349

Pecher, K. (1994). Hydrochemical analysis of spatial and temporal variations of solute composition in surface and subsurface waters of a high arctic [sic] catchment. *Catena, 21*(4), 305-327. doi : 10.1016/0341-8162(94)90043-4

Peltier, L. C. (1950). The geographic cycle in periglacial regions as it is related to climatic geomorphology. *Annals of the Association of American Geographers, 40*(3), 214-236. doi : 10.2307/2561059

Perren, B. B., Wolfe, A. P., Cooke, C. A., Kjær, K. H., Mazzucchi, D. et Steig, E. J. (2012). Twentieth-century warming revives the world's northernmost lake. *Geology, 40*(11), 1003-1006. doi : 10.1130/g33621.1

Petrone, K. C., Jones, J. B., Hinzman, L. D. et Boone, R. D. (2006). Seasonal export of carbon, nitrogen, and major solutes from Alaskan catchments with discontinuous permafrost. *Journal of Geophysical Research : Biogeosciences, 111*(G2), G02020. doi : 10.1029/2005JG000055

Pissart, A. (2005). Geomorphology. Dans D. J. A. Evans & H. M. French (dir.) *Critical concepts in geography* (Volume V : Periglacial geomorphology, p. 223-226). New York, É-U : Routledge, Taylor and Francis Group.

Portenga, E. et Bierman, P. (2011). Understanding Earth's eroding surface with 10Be. *GSA Today, 21*(8), 4-10. doi : doi : 10.1130/g111a.1

Quayle, W. C., Peck, L. S., Peat, H., Ellis-Evans, J. C. et Harrigan, P. R. (2002). Extreme responses to climate change in Antarctic lakes. *Science, 295*(5555), 645. doi : 10.1126/science.1064074

Quesada, A., Vincent, W. F., Kaup, E., Hobbie, J. E., Laurion, I., Pienitz, R., . . . Durán, J. J. (2006). Landscape control of high latitude lakes in a changing climate. Dans D. M. Bergstrom, P. Convey & A. H. L. Huiskes (dir.), *Trends in Antarctic Terrestrial and Limnetic Ecosystems* (p. 221-252). Dordrecht, Pays-Bas : Springer Netherlands. doi : 10.1007/1-4020-5277-4_11

Quinton, W. et Gray, D. (2003). Subsurface drainage from organic soils in permafrost terrain : the major factors to be represented in a runoff model. *Proceedings*

of the Eighth International Conference on Permafrost, 917-922. Repéré à http ://research.iarc.uaf.edu/NICOP/DVD/ICOP%202003%20Permafrost/Pdf/Chapter_161.pdf

Quinton, W. L., Carey, S. K. et Goeller, N. T. (2004). Snowmelt runoff from northern alpine tundra hillslopes : major processes and methods of simulation. *Hydrology and Earth System Sciences, 8*(5), 877-890. doi : 10.5194/hess-8-877-2004

Quinton, W. L., Gray, D. M. et Marsh, P. (2000). Subsurface drainage from hummock-covered hillslopes in the Arctic tundra. *Journal of Hydrology, 237*(1–2), 113-125. doi : 10.1016/S0022-1694(00)00304-8

Quinton, W. L. et Marsh, P. (1998). The influence of mineral earth hummocks on subsurface drainage in the continuous permafrost zone. *Permafrost and Periglacial Processes, 9*(3), 213-228. doi : 10.1002/(SICI)1099-1530(199807/09)9 :3<213 : :AID-PPP285>3.0.CO ;2-E

Quinton, W. L. et Marsh, P. (1999). A conceptual framework for runoff generation in a permafrost environment. *Hydrological Processes, 13*(16), 2563-2581. doi : 10.1002/(sici)1099-1085(199911)13 :16<2563 : :aid-hyp942>3.0.co ;2-d

R Core Team. 2014. R : a language and environment for statistical computing (3.1.1) [Logiciel]. Repéré à https ://www.R-project.org/

Rapp, A. (1960). Recent development of mountain slopes in Kärkevagge and surroundings, Northern Scandinavia. *Geografiska Annaler, 42*(2/3), 65-200. doi : 10.2307/520126

Roberts, K. E., Lamoureux, S. F., Kyser, T. K., Muir, D. C. G., Lafrenière, M. J., Iqaluk, D., . . .Normandeau, A. (2017). Climate and permafrost effects on the chemistry and ecosystems of High Arctic Lakes. *Scientific Reports, 7*(1), 13292. doi : 10.1038/s41598-017-13658-9

Roesch, A. et Schmidbauer, H. (2014) WaveletComp : Computational wavelet analysis (1.0) [Logiciel]. Repéré à http ://CRAN.R-project.org/package=WaveletComp

Rushlow, C. R. et Godsey, S. E. (2017). Rainfall-runoff responses on Arctic hillslopes underlain by continuous permafrost, North Slope, Alaska, USA. *Hydrological Processes, 31*(23),

4092-4106. doi : 10.1002/hyp.11294

Schmidt, L. M. et Levy, J. S. (2017). Hydraulic conductivity of active layer soils in the McMurdo Dry Valleys, Antarctica : Geological legacy controls modern hillslope connectivity. *Geomorphology, 283*, 61-71. doi : 10.1016/j.geomorph.2017.01.038

Schön, J. H. (2004). *Physical properties of rocks : Fundamentals and principles of petrophysics* (1ère ed. vol. 18). Tarrytown, É.-U. : Pergamon.

Schumm, S. et Rea, D. K. (1995). Sediment yield from disturbed earth systems. *Geology, 23*(5), 391-394. doi : 10.1130/0091-7613(1995)023<0391 :SYFDES>2.3.CO ;2

Selby, M. J. (1971). Slopes and their development in an ice-free, arid area of Antarctica. *Geografiska Annaler. Series A, Physical Geography, 53*(3/4), 235-245. doi : 10.2307/520793

Selby, M. J. (1974). Slope evolution in an Antarctic oasis. *New Zealand Geographer, 30*(1), 18-34. doi : 10.1111/j.1745-7939.1974.tb00753.x

Seppälä, M. (2004). *Wind as a geomorphic agent in cold climates*. Cambridge, Royaume-Uni : Cambridge University Press.

Shilts, W. W. (1978). Nature and genesis of mudboils, central Keewatin, Canada. *Canadian Journal of Earth Science, 15*(7), 1053-1068. doi : 10.1139/e78-113

Shur, Y. (1988). The upper horizon of permafrost soils. *Proceedings of the Fifth international conference on Permafrost, 1*,867-871. Repéré à https ://ipa.arcticportal.org/meetings/international-conferences

Shur, Y., Hinkel, K. M. et Nelson, F. E. (2005). The transient layer : implications for geocryology and climate-change science. *Permafrost and Periglacial Processes, 16*(1), 5-17. doi : 10.1002/ppp.518

Siddiqui, R., Lashari, B. et Skogerboe, G. V. (1996). *Converting a fabricated cutthroat flume into a discharge measuring instrument* (no T-5). Repéré sur le site de l'International Water

Management Institute à http ://publications.iwmi.org/pdf/H019735.pdf

Sklash, M. G. et Farvolden, R. N. (1979). The role of groundwater in storm runoff. *Journal of Hydrology, 12*, 45-65. doi : 10.1016/S0167-5648(09)70009-7

Slaymaker, O. (2009). Proglacial, periglacial or paraglacial ? *Geological Society, London, Special Publications, 320*(1), 71-84. doi : 10.1144/sp320.6

Smol, J. P., Wolfe, A. P., Birks, H. J. B., Douglas, M. S. V., Jones, V. J., Korhola, A., . . .Weckström, J. (2005). Climate-driven regime shifts in the biological communities of arctic lakes. *Proceedings of the National Academy of Sciences of the United States of America, 102*(12), 4397-4402. doi : 10.1073/pnas.0500245102

Steven, B., Lionard, M., Kuske, C. R. et Vincent, W. F. (2013). High bacterial diversity of biological soil crusts in water tracks over permafrost in the High Arctic polar desert. *PLoS ONE, 8*(8), e71489. doi : 10.1371/journal.pone.0071489

Stewart, K. A. et Lamoureux, S. F. (2011). Connections between river runoff and limnological conditions in adjacent High Arctic lakes : Cape Bounty, Melville Island, Nunavut. *Arctic, 64*(2), 169-182.

Stieglitz, M., Shaman, J., McNamara, J., Engel, V., Shanley, J. et Kling, G. W. (2003). An approach to understanding hydrologic connectivity on the hillslope and the implications for nutrient transport. *Global Biogeochemical Cycles, 17*(4), 1105. doi : 10.1029/2003gb002041

Strömquist, L. (1983). Gelifluction and surface wash, their importance and interaction on a periglacial slope. *Geografiska Annaler. Series A, Physical Geography, 65*(3), 245-254. doi : 10.2307/520589

Summerfield, M. A., Stuart, F. M., Cockburn, H. A. P., Sugden, D. E., Denton, G. H., Dunai, T. et Marchant, D. R. (1999). Long-term rates of denudation in the Dry Valleys, Transantarctic Mountains, southern Victoria Land, Antarctica based on in-situ-produced cosmogenic ^{2}1Ne. *Geomorphology, 27*(1), 113-129. doi : 10.1016/S0169-555X(98)00093-2

Surdu, C. M., Duguay, C. R., Brown, L. C. et Fernández Prieto, D. (2014). Response of ice cover on shallow lakes of the North Slope of Alaska to contemporary climate conditions (1950-2011) : radar remote-sensing and numerical modeling data analysis. *The Cryosphere, 8*(1), 167-180. doi : 10.5194/tc-8-167-2014

Taylor, S., Feng, X., Williams, M. et McNamara, J. (2002). How isotopic fractionation of snowmelt affects hydrograph separation. *Hydrological Processes, 16*(18), 3683-3690. doi : 10.1002/hyp.1232

Thorn, C. E. (1979). Ground temperatures and surficial transport in colluvium during snow-patch meltout ; Colorado Front Range. *Arctic and Alpine Research, 11*(1), 41-52. doi : 10.2307/1550458

Thorn, C. E. (1988). Nivation : a geomorphic Chimera. Dans M. J. Clark (dir.), *Advances in Periglacial Geomorphology* (p. 3-31). New York, É.-U. : Wiley.

Thorn, C. E., Darmody, R. G., Dixon, J. C. et Schlyter, P. (2001). The chemical weathering regime of Kärkevagge, arctic–alpine Sweden. *Geomorphology, 41*(1), 37-52. doi : 10.1016/S0169-555X(01)00102-7

Thorn, C. E. et Hall, K. (2002). Nivation and cryoplanation : the case for scrutiny and integration. *Progress in Physical Geography, 26*(4), 533-550. doi : 10.1191/0309133302pp351ra

Throckmorton, H. M., Newman, B. D., Heikoop, J. M., Perkins, G. B., Feng, X., Graham, D. E., …Wilson, C. J. (2016). Active layer hydrology in an arctic tundra ecosystem : quantifying water sources and cycling using water stable isotopes. *Hydrological Processes, 30*(26), 4972-4986. doi : 10.1002/hyp.10883

Tomkins, J. D., Lamoureux, S. F., Antoniades, D. et Vincent, W. F. (2010). Autumn snowfall and hydroclimatic variability during the past millennium inferred from the varved sediments of meromictic Lake A, northern Ellesmere Island, Canada. *Quaternary Research, 74*(2), 188-198. doi : 10.1016/j.yqres.2010.06.005

Trettin, H. P. (1991). *Geology of the Innuitian orogen and arctic platform of Canada and Greenland*. Ottawa, Canada : Geological Survey of Canada.

Tricart, J. (1967). *Le modelé des régions périglaciaires*. Paris, France : S.E.D.E.S.

Turnbull, L., Wainwright, J. et Brazier, R. E. (2008). A conceptual framework for understanding semi-arid land degradation : ecohydrological interactions across multiple-space and time scales. *Ecohydrology, 1*(1), 23-34. doi : 10.1002/eco.4

Uchida, T., Kosugi, K. et Mizuyama, T. (1999). Runoff characteristics of pipeflow and effects of pipeflow on rainfall-runoff phenomena in a mountainous watershed. *Journal of Hydrology, 222*(1–4), 18-36. doi : 10.1016/S0022-1694(99)00090-6

Uchida, T., Tromp-van Meerveld, I. et McDonnell, J. J. (2005). The role of lateral pipe flow in hillslope runoff response : an intercomparison of non-linear hillslope response. *Journal of Hydrology, 311*(1), 117-133. doi : 10.1016/j.jhydrol.2005.01.012

Van Everdingen, R. O. (2005). Multi-language glossary of permafrost and related ground-ice terms (p. 90) : Repéré sur le site de l'International Snow and Ice Data Center : http ://nsidc.org/fgdc/glossary .

Van Vliet-Lanoë, B. (1991). Differential frost heave, load casting and convection : Converging mechanisms ; a discussion of the origin of cryoturbations. *Permafrost and Periglacial Processes, 2*(2), 123-139. doi : 10.1002/ppp.3430020207

Veillette, J., Martineau, M.-J., Antoniades, D., Sarrazin, D. et Vincent, W. F. (2010). Effects of loss of perennial lake ice on mixing and phytoplankton dynamics : insights from High Arctic Canada. *Annals of Glaciology, 51*(56), 56-70. doi : 10.3189/172756411795931921

Veillette, J., Mueller, D. R., Antoniades, D. et Vincent, W. F. (2008). Arctic epishelf lakes as sentinel ecosystems : Past, present and future. *Journal of Geophysical Research, 113*(G4), G04014. doi : 10.1029/2008jg000730

Verachtert, E., Maetens, W., Van Den Eeckhaut, M., Poesen, J. et Deckers, J. (2011). Soil loss rates due to piping erosion. *Earth Surface Processes and Landforms, 36*(13), 1715-1725. doi :

10.1002/esp.2186

Verpaelst, M., Fortier, D., Kanevskiy, M., Paquette, M. et Shur, Y. (2017). Syngenetic dynamic of permafrost of a polar desert solifluction lobe, Ward Hunt Island, Nunavut. *Arctic Science, 3*(2), 301-319. doi : 10.1139/as-2016-0018

Veuille, S., Fortier, D., Verpaelst, M., Grandmont, K. et Charbonneau, S. (2015). Heat advection in the active layer of permafrost : Physical modelling to quantify the impact of subsurface flow on soil thawing. *Proceedings of the 7th Canadian Conference on Permafrost and 68th Canadian Conference on Geotechnic*.

Villeneuve, V., Vincent, W. et Komárek, J. (2001). Community structure and microhabitat characteristics of cyanobacterial mats in an extreme high Arctic environment : Ward Hunt Lake. *Nova Hedwigia Beiheft, 123*, 199-224.

Vincent, W. F., Fortier, D., Lévesque, E., Boulanger-Lapointe, N., Tremblay, B., Sarrazin, D., ...Mueller, D. R. (2011). Extreme ecosystems and geosystems in the canadian High Arctic : Ward Hunt Island and vicinity. *Ecoscience, 18*(3), 236-261. doi : 10.2980/18-3-3448

Vincent, W. F., Laurion, I. et Pienitz, R. (1998). Arctic and Antarctic lakes as optical indicators of global change. *Annals of Glaciology, 27*, 691-696. doi : 10.3189/1998AoG27-1-691-696

Walker, D. A. (1983). A hierarchical tundra vegetation classification especially designed for mapping in Northern Alaska. *Proceedings of the Fourth International Conference on Permafrost*, 1332-1337. Repéré à https ://ipa.arcticportal.org/meetings/international-conferences

Walker, D. A., Binnian, E., Evans, B. M., Lederer, N. D., Nordstrand, E. et Webber, P. J. (1989). Terrain, vegetation and landscape evolution of the R4D research site, Brooks Range Foothills, Alaska. *Ecography, 12*(3), 238-261. doi : 10.1111/j.1600-0587.1989.tb00844.x

Walker, D. A., Everett, K. R., Acevedo, W., Gaydos, J., Brown, J. et Webber, P. J. (1982). *Landsat-assisted environmental mapping in the Arctic National Wildlife Refuge, Alaska* (U.S. Army Cold Regions Research Engineering Laboratory Report 82-27). Repéré sur le site du

Defense Technical Information Center : www.dtic.mil/dtic/tr/fulltext/u2/a123440.pdf.

Walling, D. E. (1983). The sediment delivery problem. *Journal of Hydrology, 65*(1–3), 209-237. doi : 10.1016/0022-1694(83)90217-2

Washburn, A. L. (1956). Classification of patterned ground and review of suggested origins. *Geological Society of America Bulletin, 67*(7), 823-866. doi : 10.1130/0016-7606(1956)67[823 :copgar]2.0.co ;2

Washburn, A. L. (1979). Geocryology : a survey of periglacial processes and environments (2e éd.). Londres, Royaume-Uni : Arnold.

Watson, S. et Watson, E. (1971). Vertical stones and analogous structures. *Geografiska Annaler, 53*(2), 107-114. doi : 10.2307/520670

Wharton, R. A., Andersen, D. T., Cockell, C., Costello, R. et Doran, P. T. (1997). *Ward Hunt Island logbook*. Document inédit.

Whiting, P. J. (2005). Flow measurement and characterization. Dans G. M. Kondolf & H. Piégay (dir.), *Tools in Fluvial Geomorphology* (p. 323-346). Chichester, Royaume-Uni : John Wiley & Sons, Ltd.

Wilkinson, T. J. et Bunting, B. T. (1975). Overland transport of sediment by rill water in a periglacial environment in the canadian High Arctic. *Geografiska Annaler. Series A, Physical Geography, 57*(1), 105-116. doi : 10.2307/520531

Williams, G. P. (1965). Correlating freeze-up and break-up with weather conditions. *Canadian Geotechnical Journal, 2*(4), 313-326. doi : 10.1139/t65-047

Williams, M. W., Knauf, M., Caine, N., Liu, F. et Verplanck, P. L. (2006). Geochemistry and source waters of rock glacier outflow, Colorado Front Range. *Permafrost and Periglacial Processes, 17*(1), 13-33. doi : 10.1002/ppp.535

World Meteorological Organisation. (2012). *International Glossary of Hydrology*. Repéré à http ://library.wmo.int/pmb_ged/wmo_385-2012.pdf

Woo, M. K. (1983). Hydrology of a drainage basin in the canadian High Arctic. *Annals of the Association of American Geographers, 73*(4), 577-596. doi : 10.1111/j.1467-8306.1983.tb01860.x

Woo, M. K. (2012). *Permafrost Hydrology*. New York, É.-U. : Springer Berlin Heidelberg.

Woo, M. K. et Steer, P. (1982). Occurrence of surface flow on arctic slopes, southwestern Cornwallis Island. *Canadian Journal of Earth Sciences, 19*(12), 2368-2377. doi : 10.1139/e82-206

Woo, M. K. et Steer, P. (1983). Slope hydrology as influenced by thawing of the active layer, Resolute, N.W.T. *Canadian Journal of Earth Sciences, 20*(6), 978-986. doi : doi :10.1139/e83-087

Woo, M. K. et Steer, P. (1986). Runoff regime of slopes in continuous permafrost areas. *Canadian Water Resources Journal, 11*(1), 58-68. doi : 10.4296/cwrj1101058

Woo, M. K. et Xia, Z. (1995). Suprapermafrost groundwater seepage in gravelly terrain, Resolute, NWT, Canada. *Permafrost and Periglacial Processes, 6*(1), 57-72. doi : 10.1002/ppp.3430060107

Woo, M.-k., Heron, R. et Steer, P. (1981). Catchment hydrology of a High Arctic lake. *Cold Regions Science and Technology, 5*(1), 29-41. doi : 10.1016/0165-232x(81)90038-0

Woo, M.-K., Yang, D. et Young, K. L. (1999). Representativeness of arctic weather station data for the computation of snowmelt in a small area. *Hydrological Processes, 13*(12-13), 1859-1870. doi : 10.1002/(sici)1099-1085(199909)13 :12/13<1859 : :aid-hyp893>3.0.co ;2-d

Woo, M.-K., Yang, Z., Xia, Z. et Yang, D. (1994). Streamflow processes in an alpine permafrost catchment, tianshan, China. *Permafrost and Periglacial Processes, 5*(2), 71-85. doi : 10.1002/ppp.3430050202

Woo, M.-k. et Young, K. L. (2003). Hydrogeomorphology of patchy wetlands in the High Arctic, polar desert environment. *Wetlands, 23*(2), 291-309. doi : 10.1672/8-20

Young, K. L. et Lewkowicz, A. G. (1990). Surface energy balance of a perennial snowbank, Melville Island, Northwest Territories, Canada. *Arctic and Alpine Research, 22*(3), 290-301. doi : 10.2307/1551592

Young, K. L., Woo, M.-k. et Edlund, S. A. (1997). Influence of local topography, soils, and vegetation on microclimate and hydrology at a High Arctic site, Ellesmere Island, Canada. *Arctic and Alpine Research, 29*(3), 270-284. doi : 10.2307/1552141

Zhou, S., Nakawo, M., Hashimoto, S. et Sakai, A. (2008). The effect of refreezing on the isotopic composition of melting snowpack. *Hydrological Processes, 22*(6), 873-882. doi : 10.1002/hyp.6662

Zottola, J., Darrow, M., Daanen, R., Fortier, D. et De Grandpré, I. (2012). Investigating the effects of groundwater flow on the thermal stability of embankments over permafrost. *Proceedings of the 15th International Specialty Conference on Cold Regions Engineering*, 601-611. Repéré à http ://ascelibrary.org/doi/abs/10.1061/9780784412473.060